

UNIVERSITÀ DELLA CALABRIA



UNIVERSITÀ DELLA CALABRIA

Dipartimento di Farmacia e Scienza della Salute e della Nutrizione

**Dottorato di Ricerca in**

Medicina Traslationale

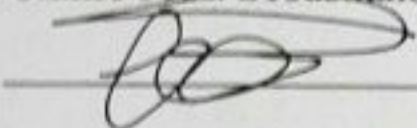
**CICLO**

XXIX

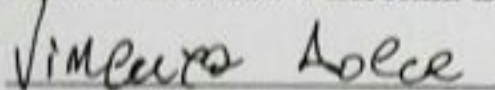
**IDENTIFICATION AND BIOCHEMICAL-MOLECULAR CHARACTERIZATION OF  
MITOCHONDRIAL CARRIER PROTEINS IN HUMAN AND MODEL ORGANISMS AND  
ASSOCIATED DISEASES**

**Settore Scientifico Disciplinare BIO/10**

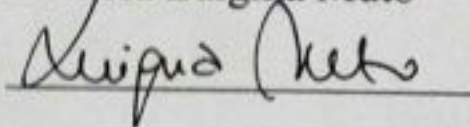
**Coordinatore:** Ch.mo Prof. Sebastiano Andò

  
\_\_\_\_\_

**Supervisore/Tutor:** Ch.ma Prof.ssa Vincenza Dolce

  
\_\_\_\_\_

**Dottorando:** Dott.ssa Luigina Muto

  
\_\_\_\_\_



## **Presentazione al Collegio dei docenti della Dott.ssa Luigina Muto per il conseguimento del titolo di “Dottore di Ricerca in Medicina Traslazionale” (XXIX ciclo)**

La Dott.ssa Luigina Muto ha svolto il corso di Dottorato di Ricerca in “Medicina Traslazionale” (XXIX ciclo) presso il Dipartimento di Farmacia e Scienze della Salute e della Nutrizione dell’Università della Calabria. Ha partecipato alle attività seminariali e didattico-formative organizzate dallo stesso Dipartimento.

Durante tale periodo la Dott.ssa Muto si è interessata principalmente allo studio delle caratteristiche biochimico-funzionali di alcuni trasportatori mitocondriali appartenenti alla Mitochondrial Carrier Family (MCF), proteine deputate a catalizzare il trasporto di soluti attraverso la membrana mitocondriale interna, allo scopo di accrescere le conoscenze sul loro ruolo fisiologico e patologico.

Nello specifico lo studio della Dott.ssa Muto è stato rivolto al carrier mitocondriale della glicina, importante nella sintesi dell’eme e nell’anemia sideroblastica congenita, al carrier mitocondriale del defosfocoenzima A, importante nella regolazione della compartimentalizzazione del CoA, il cui studio è cruciale per una migliore comprensione di alcune patologie neurodegenerative dipendenti dal biosintesi del CoA e al carrier mitocondriale del 2-oxoglutarato, di cui si sono voluti studiare i riarrangiamenti strutturali e funzionali necessari per il trasporto del substrato.

La strategia di ricerca adottata è basata sulla identificazione di proteine di membrana in banca dati, amplificazione mediante PCR e clonaggio in vettori di espressione, espressione in sistemi eterologhi, caratterizzazione funzionale dei prodotti proteici, analisi della distribuzione tissutale e localizzazione subcellulare.

Per quanto riguarda il trasportatore mitocondriale della glicina, gli studi sono stati concentrati sulla caratterizzazione biochimica e molecolare della proteina umana (SLC25A38) e sul suo omologo di lievito (Hem25p), scelto come organismo modello. In particolare, il primo obiettivo è stato quello di ottenere la proteina ricombinante Hem25 con caratteristiche strutturali e funzionali del tutto simili a quella nativa in modo da poterne studiare l’attività di trasporto.

Tale proteina è stata clonata in un sistema di espressione batterico, *Escherichia Coli* BL21, overespressa ad alti livelli come inclusion bodies, e purificata all’omogeneità, mediante cromatografia di affinità su colonna al Ni<sup>2+</sup>-NTA Agarosio.

Dopo che l’identità della proteina purificata è stata confermata tramite Western Blot, si è passati alla caratterizzazione funzionale della proteina. Hem25p è stata ricostituita in liposomi e la sua attività di trasporto di glicina (glicina/glicina) è stata osservata. Sono state calcolate le costanti



cinetiche ( $K_m$  e  $V_{max}$ ) e studiate le proprietà di trasporto (specificità di substrato e sensibilità agli inibitori) di Hem25p. Dagli studi di caratterizzazione cinetica è emerso che la proteina ricombinante catalizza il trasporto di glicina con una cinetica del primo ordine. I valori di  $K_m$  e  $V_{max}$  determinati sono stati rispettivamente  $0.75 \pm 0.084$  mM and  $169.8 \pm 13.7$  nmol/min per mg di proteina. Il *carrier* ha mostrato un'elevata efficienza di trasporto, oltre che di glicina, anche di sarcosina, L-alanina and N-methyl-L-alanina. Inoltre il trasporto del substrato è risultato quasi completamente inibito da acido tannico, piridossal-5'-fosfato (PLP) e batofenantrolina(BAT), così come p-idrossimercuribenzoato,  $HgCl_2$  e N-ethylmaleimide. Successivamente, altre prove di *uptake* di glicina sono state effettuate, andando a ricostituire in liposomi le proteine mitocondriali provenienti da ceppi di lievito Wild-Type, *hem25Δ* e *hem25Δ* trasformato con il plasmide *HEM25-pYES2*: un'attività di scambio glicina/glicina molto bassa è stata osservata nel delecto; un'attività di più del doppio è stata ottenuta con WT, mentre un'attività considerevolmente maggiore si è osservata nell'estratto mitocondriale proveniente dal *HEM25-pYES2*. Studi di localizzazione subcellulare, condotti mediante tecniche di microscopia a fluorescenza, hanno confermato la distribuzione mitocondriale della proteina. Sono stati inoltre studiati gli effetti della delezione del gene *HEM25* e l'inserzione dello stesso gene (*HEM25*) o del gene umano (*SLC25A38*) nelle cellule di lievito sulla crescita e sulla catena di trasporto degli elettroni e il consumo di ossigeno è stato analizzato attraverso prove di respirazione sui mitocondri intatti. È stata osservata la complementazione dovuta all'inserzione delle proteine sia umana sia di lievito. La conoscenza più dettagliata di questo trasportatore potrebbe essere utile per comprendere più a fondo l'anemia sideroblastica congenita, in quanto Hem25 è necessaria per l'*uptake* della glicina nella matrice mitocondriale, necessaria per la biosintesi dell'eme.

L'interesse scientifico della Dott.ssa Luigina Muto è stato anche rivolto allo studio di un altro *carrier* mitocondriale, il trasportatore del defosfocoenzima A. Nell'uomo il trasporto di Coenzima A (CoA) attraverso la membrana mitocondriale interna è stato attribuito a due differenti geni, *SLC25A16* e *SLC25A42*. Presunti ortologi di entrambi i geni sono presenti in molti genomi eucariotici, ma non in quello di *Drosophila melanogaster*, che contiene solo un gene, CG4241, filogeneticamente vicino a *SLC25A42*. CG4241 codifica per una isoforma lunga (dPCoAC1) e una corta (dPCoAC2) del *carrier* del dPCoA, derivante da un sito di start traduzionale alternativo.

Le due proteine, dPCoAC1 e dPCoAC2, così come nel caso del trasportatore della glicina, sono state clonate in un sistema di espressione batterico, *E. coli* C0214, overespresso ad alti livelli come inclusion bodies e ricostituite in proteoliposomi per caratterizzarle funzionalmente. dPCoAC1 è risultata catalizzare reazioni di scambio  $[^{14}C]ADP/ADP$ ,  $[^{14}C]AMP/AMP$ , e  $[^{14}C]ATP/ATP$ . La specificità di substrato è stata osservata misurando l'*uptake* di  $[^{14}C]ADP$  in proteoliposomi caricati con una varietà di potenziali substrati. Il maggiore *uptake* di  $[^{14}C]ADP$  si è ottenuto con dPCoA,



ADP, dADP, AMP e dAMP interni. L'effetto degli inibitori e le costanti cinetiche della proteina ricombinante dPCoAC1 sono state analizzate e calcolate. dPCoAC2 non ha mostrato alcuna attività di trasporto, probabilmente a causa di un errato avvolgimento della proteina ricombinante. La caratterizzazione funzionale del carrier del dPCoA di *D. melanogaster* risulta di particolare interesse in quanto è il primo trasportatore mitocondriale che mostra una particolare specificità di substrato per dPCoA e ADP. Nello scenario biochimico, dove la concentrazione di CoA della matrice è più di due volte superiore a quella del citosol, e i due pool sono mantenuti e adeguatamente costanti, un trasportatore come dPCoAC, che trasporta dPCoA dalla matrice al citosol in scambio con ADP, si adatta meglio rispetto ad uno che trasporta CoA.

Questo lavoro risulterà utile nel prossimo futuro per comprendere meglio il fenotipo PKAN (pantothenate kinase) umano, enzima coinvolto nella via biosintetica *de novo* del CoA, la cui deficienza è associata con un disturbo neurodegenerativo conosciuto come neurodegenerazione con accumulo di ferro celebrale (NBIA).

In ultimo, il lavoro della Dott.ssa Muto è stato anche volto ad analizzare le caratteristiche strutturali del carrier del 2-oxoglutarato (OGC), trasportatore ampiamente studiato di cui sono già note le caratteristiche di trasporto, e che svolge un ruolo chiave in importanti vie metaboliche.

Per comprendere i riarrangiamenti strutturali necessari per la traslocazione del substrato, è stata utilizzata la mutagenesi sito specifica, per sostituire la lisina 122 con un'arginina. Il mutante K122R è stato caratterizzato cinematicamente, esibendo una significativa riduzione della  $V_{max}$  rispetto al wild-type (WT) OGC, mentre il valore di  $K_m$  non ha subito variazioni, il che implica che questa sostituzione non interferisce con il sito di legame del 2-oxoglutarato. Inoltre, il mutante K122R era più inibito da diversi reagenti sulfidrilici rispetto al WT OGC, suggerendo che la reattività di alcuni residui di cisteina verso questi reagenti Cys specifici è aumentata nel mutante. Diversi reagenti sulfidrilici sono stati impiegati in saggi di trasporto per testare l'effetto delle modifiche cisteina su mutanti OGC single-Cys chiamati C184, C221, C224 (costruiti nel WT) e K122R/C184, K122R/C221, K122R/C224 (costruiti nel K122R). Le cisteine 221 e 224 sono state più profondamente influenzate da alcuni reagenti sulfidrilici quando i mutanti erano costruiti nel background del K122R. Inoltre, la presenza di 2-oxoglutarato ha notevolmente migliorato il grado d'inibizione della K122R/C221, K122R/C224, suggerendo che le cisteine 221 e 224, insieme con K122, prendono parte ai riarrangiamenti strutturali necessari per la transizione dallo stato c allo stato m durante la traslocazione del substrato.

Durante l'intero periodo del dottorato di ricerca la Dott.ssa Muto ha acquisito un'ottima padronanza delle tecniche laboratoristiche di biochimiche e di biologia molecolare, ed ha messo in luce una notevole capacità critica per la valutazione dei dati ottenuti. La Dott.ssa Muto ha inoltre mediante



assiduo studio della letteratura inerente al suo campo di studi acquisito un'eccellente formazione scientifica. L'esperienza maturata durante i tre anni di dottorato è stata accresciuta da un periodo di formazione di un anno svolto presso il Laboratorio di "Mitochondrial Physiology and Age-Related Diseases" dell'University of Texas at Austin (Austin, Texas, USA) diretto dal Dr. Edward M. Mills, e un breve soggiorno presso il Laboratorio di Biochimica e Biologia Molecolare del Dipartimento di Bioscienze, Biotecnologie e Biofarmaceutica, Università degli Studi di Bari "Aldo Moro", Bari, diretto dal Prof. Giuseppe Fiermonte. Il contributo scientifico della Dott.ssa Luigina Muto è dimostrato dai lavori pubblicati su riviste internazionali la cui rilevanza scientifica della collocazione editoriale è di ottimo livello quali Biochimica et Biophysica Acta (BBA), Journal of Biological Chemistry, The Journal of Physiology e Mini Reviews in Medicinal Chemistry.

L'esperienza maturata durante i tre anni di dottorato, ha favorito una crescita globale che allo stato si traduce in una concreta capacità a svolgere attività di ricerca in grande autonomia e con senso di responsabilità. Pertanto si esprime parere estremamente positivo sull'attività scientifica della Dott.ssa Luigina Muto.

Rende, 12 Maggio 2017

**Docente Tutor**

Prof.ssa Vincenza Dolce

Vincenza Dolce



---

# INDEX

---

|                                                                                                           |        |
|-----------------------------------------------------------------------------------------------------------|--------|
| <b>ABSTRACT</b>                                                                                           | pag.5  |
| <b>1 INTRODUCTION</b>                                                                                     | pag.9  |
| 1.1 Mitochondria – structure and function                                                                 | pag.9  |
| 1.2 Mitochondrial transport systems                                                                       | pag.12 |
| 1.3 Disorders related to mitochondrial carrier deficiency                                                 | pag.21 |
| <b>2 MATERIALS AND METHODS</b>                                                                            | pag.24 |
| 2.1 Construction of Expression Plasmids                                                                   | pag.24 |
| 2.1.1 Expression Plasmids for Glycine <i>Carrier</i>                                                      | pag.24 |
| 2.1.2 Expression Plasmids for dPCoA <i>Carriers</i>                                                       | pag.25 |
| 2.1.3 Expression Plasmids for OGC <i>Carrier</i> and site direct mutagenesis                              | pag.25 |
| 2.2 Bacterial expression and purification of recombinant proteins                                         | pag.26 |
| 2.3 Reconstitution of recombinant proteins into liposomes and transport measurements                      | pag.26 |
| 2.4 Overexpression in <i>Saccharomyces cerevisiae</i> of recombinant proteins and mitochondrial isolation | pag.30 |
| 2.5 Subcellular localization of recombinant proteins                                                      | pag.31 |
| 2.6 Sample preparation for yeast metabolite analysis                                                      | pag.32 |
| 2.7 Glycine and ALA analysis by gas chromatography coupled to tandem mass spectrometry (GC-MS/MS)         | pag.33 |
| 2.8 Determination of mitochondrial heme and cytochrome content                                            | pag.34 |
| 2.9 Mitochondrial respiration efficiency                                                                  | pag.35 |
| 2.10 Comparative modelling and docking investigations                                                     | pag.35 |
| 2.10.1 Comparative modelling and docking investigations of dPCoAC                                         | pag.36 |
| 2.10.2 Comparative modelling and docking investigations of BtOGC mutants                                  | pag.36 |
| 2.11 Molecular evolution analysis                                                                         | pag.37 |

|            |                                                                                            |        |
|------------|--------------------------------------------------------------------------------------------|--------|
| <b>3</b>   | <b>CHARACTERIZATION OF MITOCHONDRIAL GLYCINE CARRIER</b>                                   | pag.38 |
| <b>3.1</b> | <b>INTRODUCTION</b>                                                                        | pag.38 |
|            | <i>Glycine carrier</i> and associated diseases                                             |        |
| <b>3.2</b> | <b>RESULTS</b>                                                                             | pag.41 |
|            | <b>3.2.1 Bacterial expression of Hem25p</b>                                                | pag.41 |
|            | <b>3.2.2 Functional characterization of recombinant Hem25p</b>                             | pag.42 |
|            | <b>3.2.3 Impaired glycine uptake in mitochondria lacking Hem25p</b>                        | pag.45 |
|            | <b>3.2.4 Subcellular localization of Hem25p</b>                                            | pag.45 |
|            | <b>3.2.5 Growth characteristics of wild-type and hem25<math>\Delta</math></b>              | pag.47 |
|            | <b>3.2.6 Hem25p is required for the entry of glycine into mitochondria</b>                 | pag.50 |
|            | <b>3.2.7 Hem25p and GlyC deficiency cause defects in respiratory chain components</b>      | pag.51 |
|            | <b>3.2.8 Respiratory analysis of isolated mitochondria</b>                                 | pag.55 |
| <b>3.3</b> | <b>DISCUSSION</b>                                                                          | pag.57 |
| <br>       |                                                                                            |        |
| <b>4</b>   | <b>CHARACTERIZATION OF MITOCHONDRIAL DEPHOSPHOCOENZYME-A CARRIER</b>                       | pag.61 |
| <b>4.1</b> | <b>INTRODUCTION</b>                                                                        | pag.61 |
|            | <i>CoA carrier</i> and associated diseases                                                 |        |
| <b>4.2</b> | <b>RESULTS</b>                                                                             | pag.65 |
|            | <b>4.2.1 Evolutionary analysis of human SLC25A42 homologs in eukaryotes</b>                | pag.65 |
|            | <b>4.2.2 Bacterial expression and functional characterization of dPCoAC-A and dPCoAC-B</b> | pag.67 |
|            | <b>4.2.3. Kinetic characteristics of the recombinant dPCoAC-A</b>                          | pag.71 |
|            | <b>4.2.4. Phenotype complementation of yeast LEU5 null strain by dPCoACs</b>               | pag.74 |
|            | <b>4.2.5. Dissection of the transport features of dPCoAC through structural analysis</b>   | pag.75 |
| <b>4.3</b> | <b>DISCUSSION</b>                                                                          | pag.79 |

|            |                                                                                                                                                                |         |
|------------|----------------------------------------------------------------------------------------------------------------------------------------------------------------|---------|
| <b>5</b>   | <b>STRUCTURAL REARRANGEMENTS FOR SUBSTRATE TRANSLOCATION IN THE MITOCHONDRIAL OXOGLUTARATE CARRIER</b>                                                         | pag.83  |
| <b>5.1</b> | <b>INTRODUCTION</b><br><i>Oxoglutarate carrier</i>                                                                                                             | pag.83  |
| <b>5.2</b> | <b>RESULTS</b>                                                                                                                                                 | pag.87  |
|            | 5.2.1 Expression, transport activity and kinetic analysis of the reconstituted K122R mutant.                                                                   | pag.87  |
|            | 5.2.2 Influence of sulfhydryl reagents on the WT OGC and K122R transport activities                                                                            | pag.89  |
|            | 5.2.3 Expression, transport activity and influence of sulfhydryl reagents on reconstituted C184, C221, C224, K122R/C184, K122R/C221 and K122R/C224 OGC mutants | pag.91  |
|            | 5.2.4 Influence of substrate on the inhibition of C224, K122R/C224, C221 and K122R/C221 mutants by MTSEA                                                       | pag.92  |
|            | 5.2.5 Molecular modeling studies of SLC25A11_OGC                                                                                                               | pag.94  |
| <b>5.3</b> | <b>DISCUSSION</b>                                                                                                                                              | pag.96  |
|            | <b>ABBREVIATIONS</b>                                                                                                                                           | pag.100 |
|            | <b>REFERENCES</b>                                                                                                                                              | pag.103 |



---

# ABSTRACT

---

The mitochondrial carriers (MCs) are transmembrane proteins found in the mitochondrial inner membrane, which catalyze the translocation of solutes through the membrane. These belong to a family of carrier proteins, the SLC25 or Mitochondrial Carrier Family (MCF). Their function is to create a connection between mitochondria and cytosol, facilitating the flow of a large variety of solutes across the permeability barrier of the inner mitochondrial membrane, which is necessary for many physiological processes.

The functional information obtained from the study of mitochondrial carrier was fundamental in correlating MCs physiological and pathological roles in cellular metabolism. It was possible to identify genes, and their possible defects, responsible for the onset of certain diseases such as the Stanley syndrome, Amish microcephaly, HHH syndrome (hyperornithinemia, hyperammonemia and homocitrullinuria) and type II citrullinemia, their molecular basis and their symptoms. Further studies on the functional characterization of the gene family SLC25 will clarify other diseases caused by a mitochondrial carrier deficiency.

This work was focused in particular on the study of some carriers belonging to the MCF:

- the mitochondrial glycine *carrier*, important in heme synthesis and congenital sideroblastic anemia;
- the mitochondrial dephosphocoenzyme A *carrier*, important in regulating the compartmentalization of the CoA, the study of which is crucial for a better understanding of some neurodegenerative diseases that depend on the biosynthesis of CoA;
- the mitochondrial oxoglutarate *carrier*, of which the functional and structural rearrangements required for substrate transport were analyzed.



**Mitochondrial glycine carrier**

The studies were focused on the biochemical and molecular characterization of human glycine carrier protein (GlyC) and its yeast homolog (Hem25p) providing evidence that they are mitochondrial carriers for glycine. Glycine carrier is required for the uptake of glycine in the mitochondrial matrix, where this amino acid is condensed with succinyl coenzyme A to yield  $\delta$ -aminolevulinic acid, necessary for heme biosynthesis. A detailed knowledge of this transporter could be helpful to clearly understand congenital sideroblastic anemia (CSA), caused by defects of heme biosynthesis in developing erythroblasts.

In particular, Hem25p was cloned into a bacterial expression system (*Escherichia coli* BL21), overexpressed at high levels as inclusion bodies, and purified by Ni<sup>2+</sup>-NTA-agarose affinity chromatography. The protein was then reconstituted in liposomes and its transport activity of glycine was observed. The kinetic constants, Km and Vmax, were calculated. Subsequently, other evidences of glycine uptake were obtained carrying out experiments on mitochondrial proteins from the yeast *wild-type* strain, the *hem25Δ* strain and the *hem25Δ* HEM25-pYES2. The protein subcellular localization was found to be mitochondrial. Furthermore, the *hem25Δ* mutant manifested a defect in the biosynthesis of  $\delta$ -aminolevulinic acid and displayed reduced levels of downstream heme and mitochondrial cytochromes. The observed defects were rescued by complementation with yeast *HEM25* or human *SLC25A38* genes.

This work may suggest new therapeutic approaches for the treatment of congenital sideroblastic anemia.

**Mitochondrial diphosphocoenzyme A carrier**

In human, the transport of CoA across the inner mitochondrial membrane has been attributed to two different genes, SLC25A16 and SLC25A42. Presumed orthologs of both genes are present in many eukaryotic genomes, but not in that of *D. melanogaster*, which contains only one gene, CG4241, phylogenetically close to SLC25A42. CG4241 encodes a long and a short isoform of the dPCoA carrier, respectively dPCoAC1 and dPCoAC2, which arise from an alternative translational start site. dPCoAC1 and dPCoAC2 were expressed as inclusion bodies in *E. coli* C0214, and reconstituted in proteoliposomes to observe the transport activity in order to characterize them functionally.



The functional characterization of the *D. melanogaster* dPCoA carrier is of particular interest as it is the first mitochondrial carrier showing a particular substrate specificity for dPCoA and ADP.

The expression of both isoforms in a *S. cerevisiae* strain lacking the endogenous putative mitochondrial CoA carrier restored the growth on respiratory carbon sources and the mitochondrial levels of CoA. The results reported here and the proposed subcellular localization of some of the enzymes of the fruit fly CoA biosynthetic pathway, suggest that dPCoA may be synthesized and phosphorylated to CoA in the matrix, but it can also be transported by dPCoAC to the cytosol, where it may be phosphorylated to CoA by the monofunctional dPCoA kinase. Thus, dPCoAC may connect the cytosolic and mitochondrial reactions of the CoA biosynthetic pathway without allowing the two CoA pools to get in contact.

This work will be useful in the near future to better understand the deficiency of enzymes involved in the CoA biosynthesis associated with a neurodegenerative disorder known as neurodegeneration with brain iron accumulation (NBIA).

### **Mitochondrial oxoglutarate carrier**

The oxoglutarate carrier (OGC) plays a key role in important metabolic pathways. Its transport activity has been extensively studied, and, to investigate new structural rearrangements required for substrate translocation, site-directed mutagenesis was used to conservatively replace lysine 122 by arginine. K122R mutant was kinetically characterized, exhibiting a significant  $V_{max}$  reduction with respect to the wild-type (WT) OGC, whereas  $K_m$  value was unaffected, implying that this substitution does not interfere with 2-oxoglutarate binding site.

Moreover, K122R mutant was more inhibited by several sulfhydryl reagents with respect to the WT OGC, suggesting that the reactivity of some cysteine residues towards these Cys-specific reagents is increased in this mutant. Different sulfhydryl reagents were employed in transport assays to test the effect of the cysteine modifications on single-cysteine OGC mutants named C184, C221, C224 (constructed in the WT background) and K122R/C184, K122R/C221, K122R/C224 (constructed in the K122R background). Cysteines 221 and 224 were more deeply influenced by some sulfhydryl reagents in the K122R background. Furthermore, the presence of 2-oxoglutarate significantly enhanced the degree of inhibition of K122R/C221,



K122R/C224 and C224 activity by the sulfhydryl reagent 2-Aminoethyl methanethiosulfonate hydrobromide (MTSEA), suggesting that cysteines 221 and 224, together with K122, take part to structural rearrangements required for the transition from the c- to the m-state during substrate translocation.



---

# 1. INTRODUCTION

---

## 1.1 Mitochondria – structure and function

Mitochondria (Fig. 1.1), frequently referred as the “powerhouses of the cell”, are essential mammalian organelles typical of animal, plant, algae and protozoa, with aerobic metabolism, surrounded by two lipid bilayers. These cytoplasmic organelles are responsible for many fundamental processes, including the production of ATP (adenosine-5'-triphosphate) that can be used in energy requiring reactions. This is possible due to different mitochondrial metabolic reactions, such as the fatty acid oxidation (FAO), the citric acid cycle and the oxidative phosphorylation (OXPHOS). Shape, size, number and distribution of mitochondria are closely associated with the cell type and function. Based on the energy demands, in the cell there can be a different amount of mitochondria, from a few to some hundreds. These organelles can also be distributed evenly or be grouped in the region with the most intense metabolic activity [1].

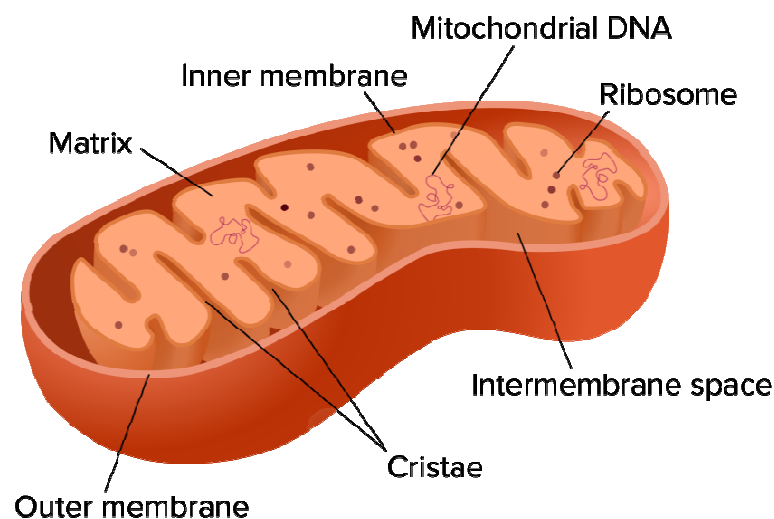


**Fig. 1.1** Schematic representation of a mitochondrion

Generally rod shaped, if observed under an optical phase contrast microscope, mitochondria may appear granular or filamentary. The dimensions may vary from  $1\mu\text{m}$  to  $10\mu\text{m}$  in length and from  $0.2\mu\text{m}$  to  $1\mu\text{m}$  of diameter [2].



The electron microscopy allows to ultrastructural analysis of these organelles, highlighting two membranes of about 6 nm of thicknesses. The outer mitochondrial membrane (OMM) is separated from the inner mitochondrial membrane (IMM) by a space of 6-8 nm, called intermembrane space (Fig. 1.2).

The IMM forms ridges within an aqueous solution, rich in protein and various metabolic intermediate molecules, called mitochondrial matrix. The number of mitochondrial ridges reflects the cellular metabolic activities: it is higher in kidney cells, striatum muscle and cardiac muscle, and is low in plant cells, depending on their different respiratory activity.

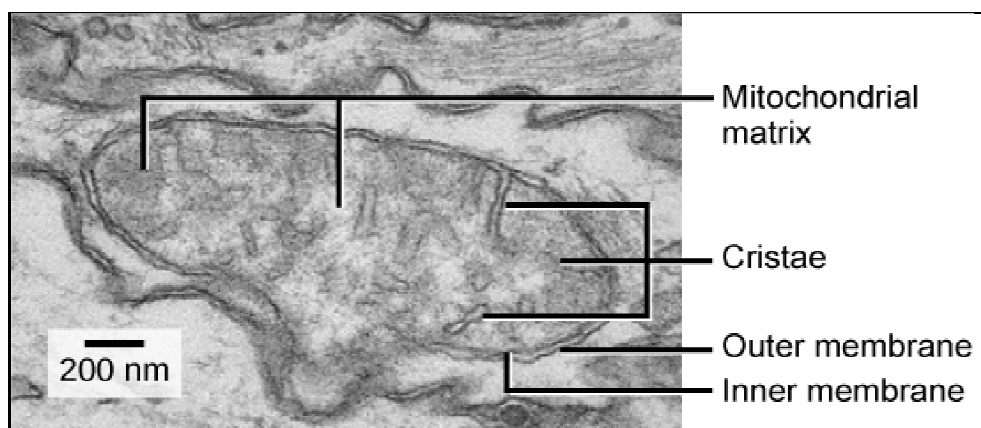


**Fig. 1.2** Electron microscope view of a mitochondrion

While the OMM is completely permeable to different substances and represents a barrier with low or no effectiveness for the regulation of the access of different substrates, the permeability of the IMM is rather limited. The "porins", channel proteins of the OMM, make it easily penetrable by ions and small molecules (with molecular weight of up to 10,000 Dalton), so that the composition of ions and substrates of the intermembrane space appears to be similar to the one of the cytosol.

The actual selection filter, between the cytosol and mitochondrial matrix, is represented, therefore, by the IMM. It is highly impermeable to ions and molecules with molecular weight greater than 100-150 Daltons. Such selectivity is mainly due to the presence of a high concentration of cardiolipin or diphosphatidylglycerol. Because of the different permeability of the two mitochondrial membranes, the matrix and the cytosol assume and maintain very different metabolic capacity and have different tasks.



Mitochondria are the only structure of of eucariotic non-plant cells, in addition to the nucleus, which contains genetic material. The mitochondrion has its own replication system; it contains the enzyme  $\gamma$ -DNA polymerase, which ensures a semiconservative replication.

The mitochondrial DNA (mtDNA) is relatively low, representing 1.5% of the cell total DNA, it is extremely small, contains, in fact, only 37 genes, in humans. Of these genes, 13 encode for some of the protein subunits of the respiratory chain complexes and 24 encode for molecules essential to the synthesis of these subunits (2 ribosomal RNAs, or rRNAs, and 22 transfer RNAs, or tRNAs). These proteins represent a small part of the proteins present in the mitochondria; in fact, in these organelles there are soluble proteins of the mitochondrial matrix, proteins of the outer membrane, and protein of the inner membrane, including mitochondrial transporters or *carriers*. All these proteins are encoded by nuclear genes, synthesized by cytoplasmic ribosomes and, subsequently, transferred into the mitochondria <sup>[3]</sup>.

Unlike other cellular organelles that are produced *ex-novo* during cell duplication, mitochondria are duplicated by binary fission, following their DNA duplication. The complete organelles are then inherited by daughter cells, according to what is called non-mendelian or cytoplasmic inheritance.

Another important characteristic of animal mitochondria is that, at the time of sexual reproduction, they are transmitted to the children only from the mother. During fertilization, the mitochondria present in the new individual (zygote) come only from the egg cell (oocyte). Therefore a mother carrying a mutation of the mtDNA transmit this mutation to all of her children, but only daughters transmit, in turn, to their progeny (matrilineal inheritance). Differently from nuclear genes, that are present in humans only in two copies (the maternal and paternal allele), there are hundreds of mtDNA molecules within each cell.

Mitochondria are also the center where cell life and death is regulated. They are the main target of aging processes; they tend to accumulate deletions and point mutations, which lead to a change in mitochondrial morphology and functionality. Aging, together



with loss of efficiency of mitochondria, compromise energy production and, often, lead to tissue death.

During aging processes or as a result of specific physiological signals, a series of processes, which involve structural modifications of mitochondrial membranes, are activated.

The apoptotic signals determine transition of mitochondrial permeability; the formation of pores in the IMM causes a reduction of the membrane potential and mitochondrial swelling. The signals can also cause increased permeability of the OMM, releasing an apoptosis trigger factor, the Cytochrome C, which passes from the mitochondria to the cytosol, and sets in motion proteolytic events of cell death <sup>[2]</sup>.

Since the mitochondria are present in all tissues, mitochondrial diseases can affect any organ of the body, but they mainly affect muscle and brain, because a bigger number of mitochondria are usually found in those tissues, due to their increased demand of energy.

### **1.2 Mitochondrial transport systems**

The high degree of impermeability, that characterizes the inner mitochondrial membrane, only allows some uncharged molecules, such as O<sub>2</sub> and CO<sub>2</sub>, to diffuse passively through it. However, numerous metabolic processes take place in the mitochondria and in the cytosol, because of the different enzyme compartmentalization. Thus, the internalization of metabolites produced outside of the mitochondria and the export in the cytosol of other metabolic intermediates that are formed in the mitochondrial matrix is necessary. Among the metabolites that migrate from the cytosol to the mitochondrial matrix we find: ADP and phosphate, involved in oxidative phosphorylation; substrates involved in the citric acid cycle, in the  $\beta$ -oxidation, in the biosynthesis of RNA and mitochondrial protein; coproporphyrinogen and iron, essential for the synthesis of heme, donors of functional groups (S-adenosylmethionine and folate) and co-enzymes (NAD<sup>+</sup>, FAD, TPP and CoA-SH). On the other hand, ATP, citrate, malate, PLP,  $\delta$ -aminolevulinate and citrulline need to be exported out of the mitochondria.

Since all these metabolites need to migrate across the inner mitochondrial membrane, the presence of a variety of transmembrane proteins, called transporters or *carriers*, is



required, and those proteins constitute a superfamily known as *Mitochondrial Carrier Family* (MCF) or *SLC25* (Solute Carrier 25) *family* <sup>[4-6]</sup>.

Numerous studies have been conducted on intact mitochondria, which allowed proving the existence of these carrier proteins. The importance of these proteins was clearly evident from the observation that the IMM possesses a protein fraction of about 76%, by far higher than the protein fraction of other biological membranes <sup>[7]</sup>. The majority of these proteins are mitochondrial *carriers*.

In humans, the 53 members of the MCF, known as mitochondrial carriers (MCs), are encoded by nuclear genes equally distributed in most chromosomes <sup>[5]</sup>. Different isoforms of many mitochondrial carriers exist, some of which are encoded by separate genes, while others are variants derived by alternative splicing the same gene; one example is the Phosphate carrier (PiC), responsible for the transport of phosphate, which is present in 2 isoforms derived by the SLC25A3 gene <sup>[8]</sup>.

The MCs are found in all eukaryotic organisms, both unicellular and multicellular. Their expression levels vary significantly; some are synthesized in virtually all tissues, while others are tissue-specific. The limited distribution of the latter reflects the implication in particular functions <sup>[9, 10]</sup>. Often, different isoforms of the same carrier have specific tissue distribution. Since all MCs are nucleus-encoded proteins, their cytosolic biosynthesis is followed by their transport to the inner mitochondrial membrane.

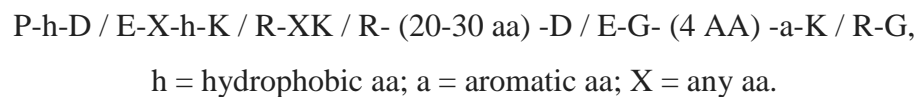
The common function of *carriers* is to provide a link between mitochondria and cytosol, to respond to the need of cellular metabolism. This link is essential, as some physiological processes require simultaneous participation of intra- and extra-mitochondrial enzymatic reactions.

In addition to this basic function, some mitochondrial carriers play an important role in regulating and maintaining a proper balance between phosphorylation and redox potentials in cytosol and mitochondrial matrix. Moreover, some flows control numerous metabolic pathways.



The transported substrates vary significantly in structure and size, from smaller H<sup>+</sup> ion [11, 12], to larger charged ones, such as the ATP<sup>4-</sup> [13, 14]. The majority of the transported substrates are anions; some are cations, other zwitterion.

All mitochondrial carriers with known functions have a primary structure with a tripartite sequence, which contains three homologous domains, repeated in tandem, of about 100 amino acids and a similar molecular mass of about 30-35 kDa [15-17]. Each domain, consisting of two hydrophobic regions, which cross the membrane with an  $\alpha$ -helix structure and that are connected to each other by long loops, shows a characteristic amino acid sequence, highly conserved [6]:



In the various mitochondrial *carriers* this sequence is partially modified, in one, two, or even in all three domains.

The typical tripartite structure, the presence of the two hydrophobic regions to  $\alpha$ -helix in each domain and of the conserved sequence, emphasizes the membership of those proteins to the same family.

Most mitochondrial *carriers* catalyze a reaction of a specific solutes exchange. Kinetic studies, obtained by varying the concentrations of both internal and external substrates, showed, with the exception of the carnitine *carrier*, that all mitochondrial *carriers* analyzed so far agree in the function of a sequential mechanism, which implies that the substrates, one internal and one external, form a ternary complex with the carrier, so that the translocation occurs. The carnitine *carrier*, on the other hand, follows a ping-pong mechanism which supposes the formation of a binary complex carrier substrate: the binding site of the carrier is alternately exposed to the sides of the membrane.

On the basis of the hydropathic profile and immunochemical and enzymatic data, it has been proposed a secondary structure model according to which this *carrier* should be organized in six hydrophobic transmembrane segments, probably with an  $\alpha$ -helix structure (Fig. 1.3).



Studies carried out using specific proteases and immunological studies showed that both the N-terminal and C-terminal end protrude in the cytoplasmic side of the membrane. The three hydrophilic segments, which connect the transmembrane domains in the side of the matrix, are called "loops" A, B, C. The two hydrophilic, shorter segments, that combine the three repeated elements, called a 'and b' protrude toward the cytoplasmic side of the mitochondrial membrane. It is possible that during the conformational change that occurs with the transport, one or more loops (A, B, C) can be inserted in the double layer lipid with a hairpin structure <sup>[6]</sup>.

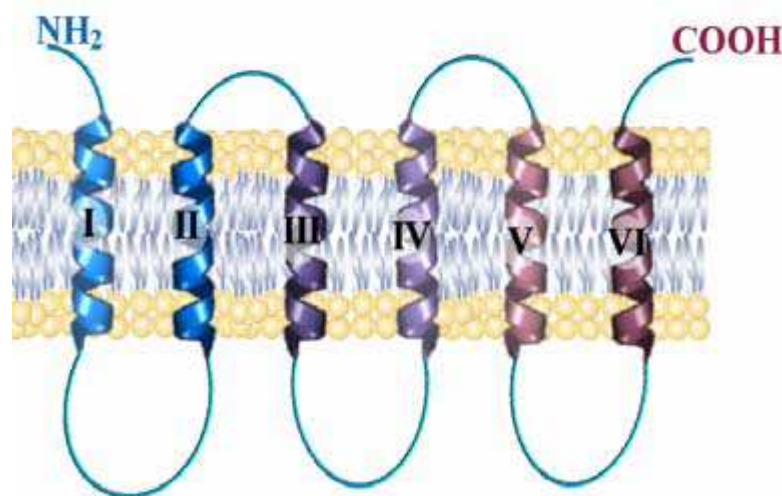


**Fig 1.3** Schematic representation of a *carrier* protein, with its typical tripartite structure

The tertiary structure of these proteins is not well known. This depends on the fact that these are membrane proteins, consequently hardly crystallizable due to their high hydrophobicity, their tendency to aggregate and their metastable nature.

All this does not allow a structural analysis. In fact, until now, the only crystallographic structure obtained with X-ray diffraction is the one of the *carrier* that catalyzes the transport of ADP/ATP (AAC1) in complex with the carboxyatractyloside <sup>[18]</sup>.

Most of the isolated mitochondrial *carriers* and probably all the members of the MCF form homodimers, even though this issue is controversial.

The role of homodimers in the transport mechanism has not been clarified yet; there could be a formation of a channel between the two protomers or the presence of two



identical channels, one for each protomer. If the mitochondrial carriers worked as dimers, these structures consist of twelve transmembrane segments, such as most of the carrier proteins <sup>[19]</sup>.

As said before, 53 members of mitochondrial *carriers* in human have been identified and their primary structures have been studied and connected to a specific transport, by functional reconstitution of proteins in artificial membrane systems (liposomes). Such *carriers* and their related isoforms are shown in Table 1 <sup>[5]</sup>. For many of them, the kinetical properties and the variation of their activities according to pH, membrane potential, phospholipids and other parameters, were clarified in detail.

| Human gene name | Protein name                            | Predominant substrates                             | Tissue distribution                                                                                                               | Link to disease                                                                  | Human gene locus |
|-----------------|-----------------------------------------|----------------------------------------------------|-----------------------------------------------------------------------------------------------------------------------------------|----------------------------------------------------------------------------------|------------------|
| SLC25A1         | CIC (citrate carrier)                   | Citrate, isocitrate, malate, PEP                   | Liver, kidney, pancreas (also in brain, lung, heart)                                                                              |                                                                                  | 22q11.21         |
| SLC25A2         | ORC2 (ornithine carrier 2)              | Ornithine, citrulline, lysine, arginine, histidine | Liver, testis, spleen, lung, pancreas, small intestine, brain, kidney                                                             |                                                                                  | 5q31             |
| SLC25A3         | PHC (phosphate carrier)                 | Phosphate                                          | Isoform A: heart, skeletal muscle and diaphragm; isoform B: liver, kidney, brain, thymus, lung, heart, skeletal muscle, diaphragm | Mitochondrial phosphate carrier deficiency                                       | 12q23            |
| SLC25A4         | ANT1 (adenine nucleotide translocase-1) | ADP, ATP                                           | Heart, skeletal muscle, much less in brain, pancreas, prostate, kidney, lung, thymus                                              | AAC1 deficiency, autosomal dominant progressive external ophthalmoplegia (adPEO) | 4q35             |



## 1. INTRODUCTION

|          |                                         |                                                      |                                                                              |                                                      |                 |
|----------|-----------------------------------------|------------------------------------------------------|------------------------------------------------------------------------------|------------------------------------------------------|-----------------|
| SLC25A5  | ANT2 (adenine nucleotide translocase-2) | ADP, ATP                                             | Brain, lung, kidney, pancreas, heart, skeletal muscle, spleen                |                                                      | Xq24-           |
| SLC25A6  | ANT3 (adenine nucleotide translocase-3) | ADP, ATP                                             | Brain, lung, kidney, liver, pancreas, heart, skeletal muscle, spleen, thymus |                                                      | Xp22.32, Yp11.3 |
| SLC25A7  | UCP1 (uncoupling protein 1)             | H <sup>+</sup>                                       | Brown adipose tissue                                                         | (obesity)                                            | 4q28-           |
| SLC25A8  | UCP2 (uncoupling protein 2)             | H <sup>+</sup>                                       | Lung, kidney, spleen, heart                                                  | obesity, type 2 diabetes, congenital hyperinsulinism | 11q13           |
| SLC25A9  | UCP3 (uncoupling protein 3)             | H <sup>+</sup>                                       | Skeletal muscle, lung                                                        | (obesity, type II diabetes)                          | 11q13           |
| SLC25A10 | DIC (dicarboxylate carrier)             | Malate, phosphate, succinate, sulphate, thiosulphate | Liver, kidney, heart, brain, lung, pancreas                                  |                                                      | 17q25.3         |
| SLC25A11 | OGC (oxoglutarate carrier)              | 2-oxoglutarate, malate                               | Heart, skeletal muscle, liver, kidney, brain, pancreas                       |                                                      | 17p13.3         |
| SLC25A12 | AGC1 (aspartate/glutamate carrier 1)    | Aspartate, glutamate                                 | Brain, heart, skeletal muscle, lung pancreas, kidney, but not in liver       | AGC1 deficiency, (autism)                            | 2q24            |



## 1. INTRODUCTION

|          |                                              |                                                                                    |                                                                                                  |                                                                                                   |          |
|----------|----------------------------------------------|------------------------------------------------------------------------------------|--------------------------------------------------------------------------------------------------|---------------------------------------------------------------------------------------------------|----------|
| SLC25A13 | AGC2<br>(aspartate/glutamate carrier 2)      | Aspartate,<br>glutamate                                                            | Liver, kidney,<br>pancreas, heart,<br>skeletal muscle,<br>brain                                  | Citrullinemia type<br>II (CTLN2),<br>neonatal<br>intrahepatic<br>cholestasis<br>(NICCD)           | 7q21.3   |
| SLC25A14 | UCP5 (uncoupling<br>protein 5)               | ?                                                                                  | Widely expressed,<br>with highest levels<br>in brain and testis                                  |                                                                                                   | Xq24     |
| SLC25A15 | ORC1 (ornithine<br>carrier 1)                | Ornithine,<br>citrulline, lysine,<br>arginine                                      | Liver, pancreas,<br>lung, testis, small<br>intestine, spleen,<br>kidney, brain, heart            | Hyperornithinemi<br>a-<br>hyperammonemi<br>a-<br>homocitrullinuria<br>(HHH) syndrome              | 13q14.11 |
| SLC25A16 | GDC (Graves' disease<br>carrier)             | ?                                                                                  | Liver, kidney,<br>thyroid, lung, heart,<br>skeletal muscle,<br>brain                             |                                                                                                   | 10q21.3  |
| SLC25A18 | GC2 (glutamate<br>carrier 2)                 | Glutamate                                                                          | Brain, testis, heart,<br>pancreas, kidney,<br>lung                                               |                                                                                                   | 22q11.2  |
| SLC25A19 | DNC<br>(deoxynucleotide<br>carrier)          | Thiamine<br>pyrophosphate,<br>thiamine<br>monophosphate,<br>(deoxy)nucleotid<br>es | Brain, testis, lung,<br>kidney, liver,<br>spleen, skeletal<br>muscle, heart                      | Congenital Amish<br>microcephaly<br>(MCPHA),<br>neuropathy with<br>bilateral striatal<br>necrosis | 17q25.3  |
| SLC25A20 | CAC<br>(carnitine/acylcarnit<br>ine carrier) | Carnitine,<br>acylcarnitine                                                        | Heart, skeletal<br>muscle, liver (also<br>in lung, kidney,<br>brain, pancreas,<br>lung,placenta) | Carnitine<br>acylcarnitine<br>carrier deficiency                                                  | 3p21.31  |



## 1. INTRODUCTION

|          |                             |                                                |                                                                                                   |                                |            |
|----------|-----------------------------|------------------------------------------------|---------------------------------------------------------------------------------------------------|--------------------------------|------------|
| SLC25A21 | ODC (oxoadipate carrier)    | Oxoadipate, oxoglutarate                       | Kidney, gall bladder, colon, liver, placenta, testis, lung, spleen, skeletal muscle, brain, heart |                                | 14q11.2    |
| SLC25A22 | GC1 (glutamate carrier 1)   | Glutamate                                      | Pancreas, brain, liver, testis, spleen, kidney, heart, lung, small intestine, pancreatic b cells  | Early epileptic encephalopathy | 11p15.5    |
| SLC25A23 | APC2                        | ATP-Mg <sup>2+</sup> , ATP, ADP, AMP and Pi    | Kidney, lung, small intestine, pancreas, brain, liver, skeletal muscle, heart                     |                                | 19p13.3    |
| SLC25A24 | APC1                        | ATP-Mg <sup>2+</sup> , ATP, ADP, AMP and Pi    | Testis                                                                                            |                                | 1p13.3     |
| SLC25A25 | APC3                        | ?                                              | Brain, heart, skeletal muscle, liver, small intestine, lung, pancreas, testis                     |                                | 9q34.11    |
| SLC25A26 | SAMC                        | S-adenosyl-methionine, S-adenosyl-homocysteine | Ubiquitous (testis)                                                                               |                                | 3p14.1     |
| SLC25A27 | UCP4 (uncoupling protein 4) | ?                                              | Brain                                                                                             |                                | 6p11.2-q12 |
| SLC25A28 | Mitoferrin 2 (Mfrn2)        | Fe <sup>2+</sup>                               | Ubiquitous (heart, liver, kidney)                                                                 |                                | 10q23-q24  |
| SLC25A29 | ORNT3                       | Ornithine, acylcarnitine                       | Heart, skeletal muscle, liver, brain                                                              |                                | 14q32.2    |
| SLC25A30 | UCP6 (KMCP1)                | ?                                              | Kidney                                                                                            |                                | 13q14.12   |



1. INTRODUCTION

|          |                                              |                        |                                                          |                        |          |
|----------|----------------------------------------------|------------------------|----------------------------------------------------------|------------------------|----------|
| SLC25A31 | AAC4, ANT4<br>(adenine nucleotide carrier 4) | ADP, ATP               | Testis                                                   | (spermatogenesis )     | 4q28.1   |
| SLC25A32 | MFT                                          | Folate                 |                                                          |                        | 8q22.3   |
| SLC25A33 | PNC1 (pyrimidine nucleotide carrier 1)       | UTP                    | Ubiquitous                                               |                        | 1p36.22  |
| SLC25A34 |                                              | ?                      |                                                          |                        | 1p36.21  |
| SLC25A35 |                                              | ?                      |                                                          |                        | 17p13.1  |
| SLC25A36 | PNC2 (pyrimidine nucleotide carrier 2)       | Pyrimidine nucleotides |                                                          |                        | 3q23     |
| SLC25A37 | Mitoferrin 1 (Mfrn1)                         | Fe <sup>2+</sup>       | Fetal liver, bone marrow, spleen, placenta, liver, brain |                        | 8p21.2   |
| SLC25A38 |                                              | Glycine                | Erythroid cells                                          | Sideroblastic anemia   | 3p22.1   |
| SLC25A39 |                                              | ?                      | Ubiquitous                                               |                        | 17q12    |
| SLC25A40 |                                              | ?                      | Ubiquitous at low levels                                 |                        | 7q21.12  |
| SLC25A41 | APC4                                         | ATP-Mg/Pi              | Brain, testis, liver                                     |                        | 19p13.3  |
| SLC25A42 |                                              | CoA, ADP, ATP, dPCoA   | Ubiquitous (adipose tissue)                              | Mitochondrial myopathy | 19p13.11 |
| SLC25A43 |                                              | ?                      | Brain, adrenal gland, skeletal muscle                    |                        | Xq24     |
| SLC25A44 |                                              | ?                      | Ubiquitous                                               |                        | 1q22     |
| SLC25A45 |                                              | ?                      | Skeletal muscle, intestine, brain, testis                |                        | 11q13.1  |
| SLC25A46 |                                              | ?                      | Ubiquitous                                               |                        | 5q22.1   |



|          |        |   |  |  |                 |
|----------|--------|---|--|--|-----------------|
| SLC25A47 |        | ? |  |  | 14q32.2         |
| SLC25A48 |        | ? |  |  | 5q31.1          |
| SLC25A49 | MTCH1  | ? |  |  | 6pter-<br>p24.1 |
| SLC25A50 | MTCH2  | ? |  |  | 11p11.2         |
| SLC25A51 | MCART1 | ? |  |  | 9p13.3-<br>p12  |
| SLC25A52 | MCART2 | ? |  |  | 18q12.1         |
| SLC25A53 | MCART6 | ? |  |  | Xq22.2          |

**Table 1.1** Schematic representation of the genes codifying for transport proteins, their substrates, tissue distribution, the human gene locus and the possible link to diseases <sup>[5]</sup>. The mitochondrial *carriers* analyzed in this work are marked with different color.

The mitochondrial *carriers* currently known can be divided into electrogenic and electroneutral transporters; in particular, the functional characterization of the known *carriers* allows us to further divide them into three categories, according to the type of substrate transported:

- *Carriers* that catalyze an electrogenic transport such as the  $\text{ADP}^{4-} / \text{ATP}^{3-}$  transporter;
- *Carriers* that catalyze an electroneutral transport, in which the charges transported inward are balanced by equal charges outward (symport: anion/ $\text{H}^+$ ) or opposite charges inward (antiporter: anion/ $\text{OH}^-$ ), as the phosphate *carrier*;
- *Carriers* that catalyze a neutral transport in which the transported molecule does not have an electric charge, as in the case of the carnitine *carrier*.

### 1.3 Disorders related to mitochondrial carrier deficiency

Since almost all of the known substrates of the MCF members are involved in reaction sequences that ultimately produce ATP for the cell, efficient transport is required for mitochondrial function and cellular survival. Furthermore, amino acid mutations caused



by single nucleotide polymorphisms in MCF proteins have been documented in humans and are linked to clinical diseases <sup>[5]</sup>.

The diseases caused by deficiencies of mitochondrial transport proteins are metabolic disorders caused by mutations in genes that encode for them, and they are transmitted as autosomal recessive, with the exception of Progressive External Ophthalmology (adPEO), inherited as autosomal dominant.

Diseases related to mitochondrial *carriers* can be divided into two groups <sup>[20]</sup>:

- Diseases with a genetic defect of mitochondrial *carriers*, whose function is linked to the oxidative phosphorylation;
- Diseases due to the alteration of mitochondrial function of those *carriers* that are not involved in oxidative phosphorylation but determine an alteration of physiological concentrations of important intermediates of some metabolic pathways. The symptoms in this case depend on the metabolic pathway and the type of affected tissue (tissue distribution of the *carrier*).

The dysfunction of oxidative phosphorylation is due to the ADP/ATP *carrier* and to the Pi *carrier*, which transport ADP and Pi, used by the complex ATP synthase for the production of ATP, in the mitochondrial matrix.

In the first group we find:

- Sengers' syndrome,
- AAC1 deficiency,
- PiC deficiency
- Progressive External Ophthalmology (adPEO).

The symptoms of the diseases related to these genes defects are caused by insufficient production of ATP, especially in those tissues where these carriers are strongly expressed and where is present a high activity of the oxidative phosphorylation.

In this group of diseases is also included PEO, even though the heterozygous mutation of isoform 1 of the carrier of ADP/ATP does not lead to a direct action on the energy dysfunction, but it contributes to the mitochondrial DNA instability <sup>[20]</sup>.



The known diseases of the second group are:

- CAC deficiency,
- HHH syndrome,
- ACG2 deficiency,
- Microcephaly of the Amish population
- Neonatal myoclonic epilepsy <sup>[20]</sup>.

Other carriers may be jointly responsible for diseases, but the mechanisms have not been clarified yet. For example, the carrier of citrate (CIC), encoded by the SLC25A1 gene seems to be involved in DiGeorge Syndrome (DGS) and the veil-craniofacial syndrome (VCFS) <sup>[20]</sup>.

| Disorder                        | Gene     | Carrier | Substrates               |
|---------------------------------|----------|---------|--------------------------|
| AAC1 deficiency                 | SLC25A4  | AAC1    | ADP/ATP                  |
| Sengers' syndrome               | ?        | AAC1    | ADP/ATP                  |
| PiC deficiency                  | SLC25A3  | PiC     | Phosphate                |
| adPEO                           | SLC25A4  | AAC1    | ADP/ATP                  |
| CAC deficiency                  | SLC25A20 | CAC     | Carnitine/acylcarnitines |
| HHH syndrome                    | SLC25A15 | ORC1    | Ornithine/citrulline     |
| NICCD/CTLN2                     | SLC25A13 | AGC2    | Aspartate/glutamate      |
| Amish microcephaly              | SLC25A19 | TPC     | Thiamine pyrophosphate   |
| Neonatal myoclonic epilepsy     | SLC25A22 | GC1     | Glutamate                |
| Congenital sideroblastic anemia | SLC25A38 |         | Glycine                  |

**Table 1.2** Diseases associated with mitochondrial carriers



---

## 2. MATERIALS AND METHODS

---

### 2.1 Construction of Expression Plasmids

The coding sequence of the selected proteins (yeast *HEM25* and human *SLC25A38* for the glycine carrier; *dPCoAC-A* and *dPCoAC-B*, the two isoforms of the *D. melanogaster* gene GC4241; the *B. taurus OGC*) were cloned into expression vectors, respectively into pET21b, pRUN and pMW7 vectors for expression in *E. coli*, and into the yeast pYES2 expression vector (*HEM25* and *SLC25A38* - *dPCoAC-A* and *dPCoAC-B*).

Transformants selected on LB plates containing ampicillin (100 µg/ml) were screened by direct colony PCR and by restriction digestion of the purified plasmid DNA <sup>[21]</sup> and verified by DNA sequencing.

#### 2.1.1 Expression Plasmids for Glycine Carrier

The *HEM25* open reading frame was amplified from *S. cerevisiae* genomic DNA by PCR, using primers corresponding to the extremities of the coding sequences with additional *NdeI* and *HindIII* sites.

The coding sequence of the human *SLC25A38* gene was obtained by RT-PCR reaction, using total RNA extracted from HepG2 cells as template <sup>[22, 23]</sup>, and the primers with additional *NdeI* and *HindIII* sites. The amplified products were cloned into the *NdeI-HindIII* sites of the expression vector pET21b that had been previously modified by cloning into *HindIII-XhoI* sites a cDNA sequence coding for a V5 epitope followed by six histidines <sup>[24]</sup>.

The *HEM25*-pYES2 and *SLC25A38*-pYES2 plasmids were constructed by cloning the coding sequences of *HEM25* and *SLC25A38*, respectively, into the yeast pYES2 expression vector. In order to create the *HEM25*-pYES2, the *HEM25* cDNA was amplified by PCR using the *HEM25*-pET21b construct as template. The forward and reverse primers carried *BamHI* and *XhoI* restriction sites, respectively, as linkers. The reverse primer also carried a cDNA sequence coding for a V5 epitope. Similarly, to generate the *SLC25A38*-pYES2 construct,



the coding sequence of *SLC25A38* was obtained by PCR using *SLC25A38*-pET21b as template and the primers with additional *Bam*HI and *Xho*I sites. The pET21b and pYES2 vectors, prepared as above, were transformed into *E. coli* DH5 $\alpha$  cells.

### 2.1.2 Expression Plasmids for dPCoA Carriers

The first isoform, dPCoAC-A, corresponded to a 1098 bp open reading frame (RefSeq accession no. NM\_206522) and encoded a protein of 365 residues (RefSeq accession no. NP\_650891). The second one, dPCoAC-B, corresponded to an 873 bp open reading frame (RefSeq accession no. NM\_169901) and encoded a protein of 290 residues (RefSeq accession no. NP\_732519). Both splicing isoforms were amplified by PCR, using an Oregon-R adult flies cDNA as template and two primers (sense and antisense) carrying suitable restriction sites at their 5' ends for the further cloning of the amplified inserts in the *E. coli* and *S. cerevisiae* expression vectors, pRUN<sup>[25]</sup> and pYES2 (Invitrogen<sup>TM</sup>), respectively. We introduced the R103S mutation into the wild-type dPCoAC-A cDNA by overlap-extension PCR<sup>[26]</sup>.

### 2.1.3 Expression Plasmids for OGC Carrier and site direct mutagenesis

The coding region for BtOGC was amplified by polymerase chain reaction (PCR) method from bovine heart cDNA<sup>[27]</sup>. The forward and reverse oligonucleotide primers corresponded to the extremities of the coding sequence for OGC with *Nde*I and *Hind*III sites. The WT OGC cDNA was employed as a template to replace lysine 122 by arginine. K122R cDNA was employed as a template to construct triple mutants having a single cysteine residue: K122R/C184, K122R/C221 and K122R/C224. As the WT OGC contains three native cysteines (in position 184, 221 and 224), in K122R/C184 cDNA cysteines located in position 221 and 224, in K122R/C221 cDNA cysteines 184 and 224 and in K122R/C224 cDNA cysteines 184 and 221 were replaced by serines, respectively. Further mutants, named C184, C221 and C224, each containing a single cysteine residue (184, 221 and 224, respectively), were constructed in the



WT OGC background, as previously described [28, 29]. All of the mutations were introduced in the WT or in the K122R OGC cDNA by the overlap extension PCR method [26], using oligonucleotides with appropriate mutations in their sequences. The PCR products were cloned into the expression vector pMW7 and transformed into *E. coli* TG1 cells.

### 2.2 Bacterial expression and purification of recombinant proteins

All the cloned expression vectors were overexpressed as inclusion bodies in the cytosol of *E. coli* cells, BL21(DE3) for Hem25p and GlyC, C0214(DE3) for dPCoAC-A, R103S dPCoAC-A mutant, dPCoAC-B and the OGC mutants.

A colony was inoculated into growth medium containing ampicillin (100 µg/ml) and the culture was grown at 37 °C for 4-5 h, or until the optical density of the culture at 600 nm was 0.7-1.0. Then isopropyl-β-D-thiogalactopyranoside was added to a final concentration of 0.4 mM to induce the expression of the carrier proteins, and incubation was continued for a further 4 to 5 hours [30]. Control cultures with the empty vector were processed in parallel. The cells were harvested by centrifugation, and used for the preparation of inclusion bodies. Cells were resuspended in TE buffer disrupted using either a French Press or a Sonicator, and then centrifuged at 4°C at 27000 g for 15 min. The pellet was resuspended in a smaller volume of the same buffer and fractionated by centrifugation at 131000 g for 4.5 h at 4°C, through a step gradient made of 40 %, 53 % and 70 % (w/v) solutions of sucrose (sucrose density gradient) [31]. Inclusion bodies were collected, washed at 4°C with TE buffer (10 mM Tris/HCl, 1 mM EDTA, at the appropriate pH), and finally resuspended in the same buffer [32].

Hem25p and GlyC proteins were solubilized in 2% (w/v) sarkosyl and purified by centrifugation and Ni<sup>2+</sup>-NTAagarose affinity chromatography, as described previously [33].

### 2.3 Reconstitution of recombinant proteins into liposomes and transport measurements

The recombinant proteins were solubilized in Sarkosyl® (N-dodecanoyl-N-methylglycine sodium salt) and then reconstituted into liposomes by cyclic removal of



the detergent with a hydrophobic column of Amberlite beads (Bio-Rad) <sup>[34]</sup> in the presence or absence of substrates <sup>[35]</sup>.

After vortexing, this mixture was recycled 13 times through the Amberlite column (4.0 × 0.5 cm). All operations were performed at 4 °C, except the passages through Amberlite, which were carried out at room temperature.

External substrate was removed from proteoliposomes on Sephadex G-75 columns, pre-equilibrated with 50 mM NaCl/10 mM HEPES at pH 7.5 (for Hem25p and GlyC) or PIPES at pH 7 (for dPCoACs and OGC) <sup>[36]</sup>.

The first 600 µl of turbid eluate from the Sephadex G- 75 column were collected, and 100 µl were transferred to reaction vessels and used for transport measurements by the “inhibitor stop method” <sup>[24, 34, 36]</sup>.

Transport at 25°C was started by adding, at the indicated concentrations, respectively, L- [<sup>14</sup>C] glycine, [<sup>14</sup>C] ADP, 2-oxo [1-<sup>14</sup>C] glutarate or other indicated labeled compounds, to substrate-loaded proteoliposomes (exchange) or to empty proteoliposomes (uniport).

Transport was terminated by adding PLP (pyridoxal-5'-phosphate) and BAT (bathophenanthroline), which, in combination and at high concentrations, completely inhibit the activity of several mitochondrial carriers <sup>[35]</sup>. Each sample was run in duplicate. Finally, the external substrate was removed by a Sephadex G-75 column, the proteoliposomes were eluted with 50 mM NaCl, collected in a scintillation mixture and the accumulation of radioactive substrate in the liposomes was measured by liquid scintillation (Fig. 2.1) <sup>[24, 36]</sup>. The experimental values were corrected by subtracting control values.



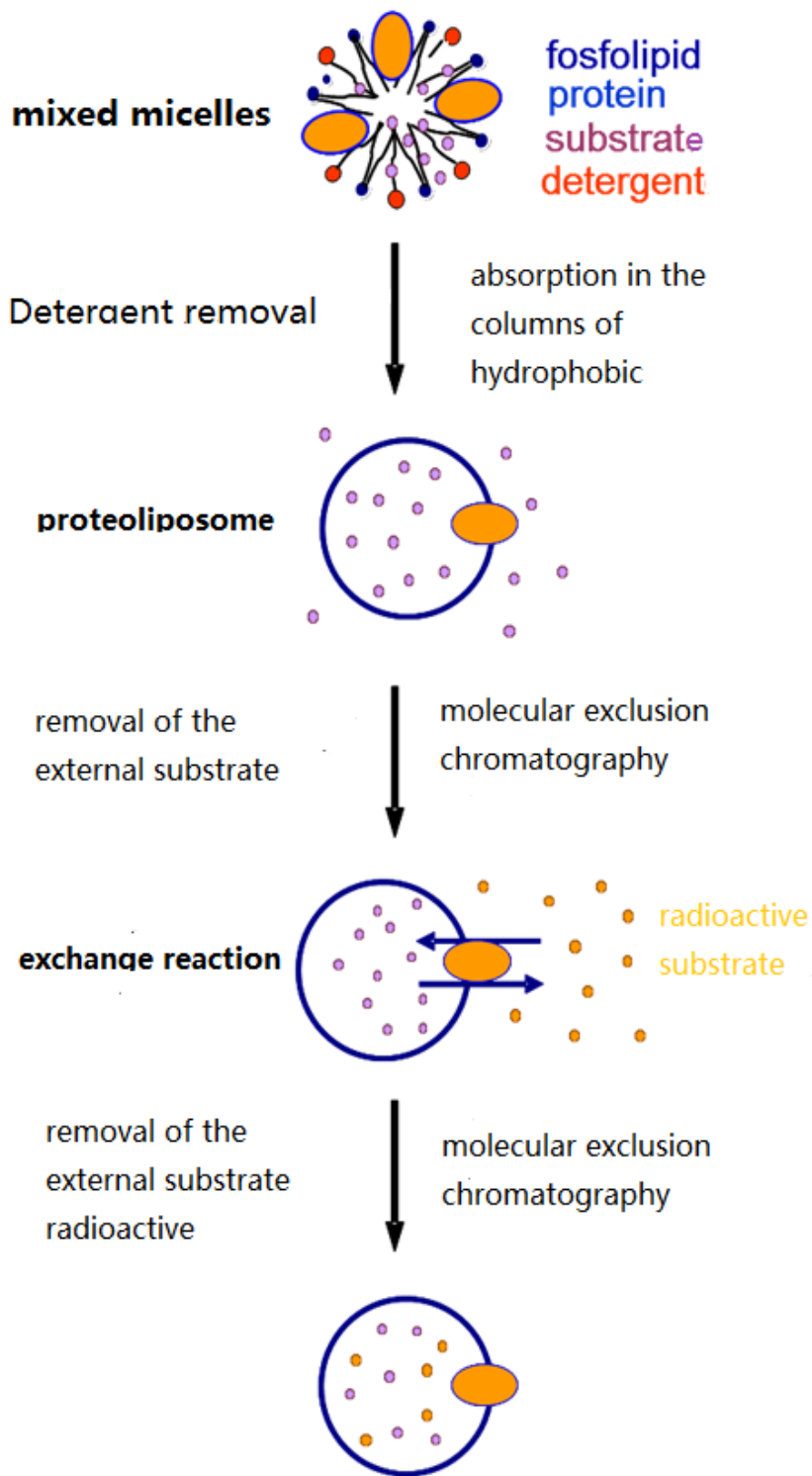


**Fig. 2.1** Formation of proteoliposomes and determination of transport.



The reconstitution mixture for each group of proteins contained:

- **Hem25p and GlyC**

100  $\mu$ l of purified proteins (0.5-1  $\mu$ g of protein)

90  $\mu$ l of 10% (w/v) Triton X-114

90  $\mu$ l of 10% (w/v) L- $\alpha$ -phosphatidylcholine from egg yolk (Sigma-Aldrich), as sonicated liposomes

10 mM glycine (except where otherwise indicated)

20 mM HEPES at pH 7.5 (except where otherwise indicated)

water to a final volume of 700  $\mu$ l.

- **dPCoAC-A, R103S dPCoAC-A mutant, dPCoAC-B**

55  $\mu$ l of purified proteins (10  $\mu$ g of protein)

70  $\mu$ l of 10% (w/v) Triton X-114

90  $\mu$ l of 10% (w/v) L- $\alpha$ -phosphatidylcholine from egg yolk (Sigma-Aldrich), as sonicated liposomes

10 mM ADP (except where otherwise indicated)

20 mM PIPES at pH 7 (except where otherwise indicated)

0.4 mg of cardiolipin (Sigma-Aldrich)

water to a final volume of 700  $\mu$ l.

- **OGC and mutants**

100  $\mu$ l of purified proteins

98  $\mu$ l of 10% (w/v) Triton X-114

90  $\mu$ l of 10% (w/v) L- $\alpha$ -phosphatidylcholine from egg yolk (Sigma-Aldrich), as sonicated liposomes

20 mM oxoglutarate (except where otherwise indicated)

20 mM PIPES at pH 7.0 (except where otherwise indicated)

2.3 mg/ml asolectin from soybean

water to a final volume of 700  $\mu$ l.

The initial transport rate was calculated from the radioactivity taken up by proteoliposomes after 1 or 2 min (in the initial linear range of substrate uptake).

For efflux measurements, proteoliposomes containing 2 mM substrate were loaded with 5  $\mu$ M of labeled substrate, by carrier-mediated exchange equilibration<sup>[34]</sup>. After 30 min, the external radioactivity was removed by passing the proteoliposomes through



Sephadex G-75. Efflux was started by adding unlabeled external substrate or NaCl to aliquots of proteoliposomes and terminated by adding the inhibitors indicated above.

In the OGC experiments, the influence of several sulfhydryl reagents such as mersalyl, pCMBS, MTSEA, MTSES and MTSET, was investigated on single-cysteine replacement mutants through transport assays. Proteoliposomes were pre-incubated at 25 °C in the presence or absence of each sulfhydryl reagent at the desired concentration for 2 min (mersalyl or pCMBS) <sup>[31]</sup> or for 10min (MTSEA, MTSES or MTSET) <sup>[29, 37, 38]</sup>. After removal of unbound reagent by Sephadex G-75 chromatography, transport was started by adding 0.3 mM 2-oxo[1-<sup>14</sup>C]glutarate and stopped after 30 s <sup>[39]</sup>. The influence of substrate on the inhibition of some OGC mutants by MTSEA was tested by pre-incubating proteoliposomes, preloaded with 20 mM 2-oxoglutarate, with this sulfhydryl reagent and its concentration was chosen in order to obtain only partial (approximately 50%) transport inhibition. After removal of unbound reagent and external substrate by Sephadex G-75 chromatography, transport was initiated by the addition of 1 mM 2-oxo[1-<sup>14</sup>C]glutarate and terminated after 30 s.

#### **2.4 Overexpression in *Saccharomyces cerevisiae* of recombinant proteins and mitochondrial isolation**

The resulting yeast expression plasmids were introduced in the deleted strain, and transformants were selected on SC agar plates without uracil, supplemented with 2% (w/v) glucose. A colony was precultured on SC medium without uracil supplemented with 2% (w/v) glucose for 14-16 h, diluted to a final OD<sub>600</sub> = 0.05 in YP supplemented with 3% (w/v) glycerol and 0.1% (w/v) glucose and grown to early-exponential phase. Galactose (0.4% w/v) was added 4 h before harvesting to induce recombinant protein overexpression.

Cells were pelleted by centrifugation at 3000g for 5 min at room temperature and washed with distilled water. Subsequently, they were resuspended in 2 ml/g of cells (v/w) DTE buffer (100 mM Tris-H<sub>2</sub>SO<sub>4</sub>, pH 9.4, 10 mM 1,4-Dithioerythritol) and shaken slowly for 10 min at 30°C. After incubation with DTE buffer, the cells were centrifuged again at 3000g for 5 min and then washed with sorbitol 1.2M.

The pellet was suspended with zymolyase buffer (1.2 M sorbitol, 20 mM potassium



phosphate, pH 7.4) and then incubated with the addition of 4 mg/g (w/w) Zymolyase-20T (Seikagaku Kogyo Co.) for 30-60 min at 30°C to obtain spheroplasts. Cells were then washed again with sorbitol 1.2M.

Cells were homogenized by 50 strokes in a glass-teflon potter in 14 ml/g (v/w) ice-cold homogenization buffer (0.6 M sorbitol, 10 mM Tris-HCl, pH 7.4, 1 mM PMSF, 0.2% BSA).

Cell debris and nuclei in the homogenate were removed by centrifugation at 3000g for 5 min at 4°C. The supernatant was collected and centrifuged twice at 12,000g for 15 min at 4°C in order to recover the mitochondrial fraction which was resuspended in ST buffer (0.25 M Sucrose, 10 mM Tris-HCl, pH 7) <sup>[40, 41]</sup>.

After protein quantification, mitochondria were stored at -80 °C until use.

Mitochondria were solubilized in a buffer containing 3% (w/v) Triton X-100, 20 mM NaCl, 10 mM HEPES pH 7.5 or PIPES p7 and supplemented with cardiolipin. After incubation for 20 min at 4°C, the mixture was centrifuged at 8000 x g for 20 min thereby obtaining a supernatant, referred to as mitochondrial extract. The mitochondrial extract was reconstituted by cyclic removal of detergent <sup>[33]</sup>.

### 2.5 Subcellular localization of recombinant proteins

Indirect immunofluorescence experiments were carried out according to Pringle's procedure with some modifications <sup>[42, 43]</sup>. Cells were grown in glycerol supplemented YP medium until early logarithmic phase, and the expression of recombinant proteins was induced adding 0.4% (w/v) galactose for 4 h at 30°C. Then, formaldehyde solution was added directly to the cells in growth medium to a final concentration of 3.7% (w/v). After 1 h at 30°C, the cells were pelleted by centrifugation at 1301 x g for 5 min at room temperature and resuspended in phosphate-buffered paraformaldehyde containing 100 mM potassium phosphate, pH 6.5, 1 mM MgCl<sub>2</sub> and 3.7% (w/v) paraformaldehyde. After 16 h at 30°C, the cells were washed with distilled water and then incubated for 10 min at 30°C in 1 ml solution containing 200 mM Tris/HCl, pH 8.0, 1 mM EDTA and 1% (v/v) β-mercaptoethanol. The pellet was resuspended in 1 ml zymolyase buffer (1.2 M sorbitol, 20 mM potassium phosphate, 1 mM MgCl<sub>2</sub>, pH 7.4). Zymolyase-20T (Seikagaku Kogyo Co., Japan) (5 mg/g of cell, wet weight) was added and the suspension was incubated for 30-60 min at 30°C with gentle shaking for conversion into



spheroplasts. After digestion, cells were spun down at 1301 x *g* and washed once with 1.2 M sorbitol, then resuspended gently and incubated for 2 min in 1.2 M sorbitol and 2% (w/v) SDS. Cells were washed twice with 1.2 M sorbitol.

Spheroplasts (20  $\mu$ l) were incubated for 1 h at 30°C in the presence of 100 nM MitoTracker Red, 32 nM FM 4-64 Dye (*N*-(3-Triethylammoniumpropyl)-4-(6-(4-(Diethylamino) Phenyl) Hexatrienyl) Pyridinium Dibromide) or 1  $\mu$ g/ml DAPI (4',6-Diamidino-2 -Phenylindole, Dihydrochloride) (Molecular Probes, The Netherlands), washed twice with PBS containing 5 mg/ml BSA (PBS-BSA) before adding a primary antibody against V5 (1  $\mu$ g/ml in PBS-BSA) and incubated for 1 h at 30°C. After washing twice for 5 min with PBS-BSA, the secondary antibody anti-mouse FITC conjugate (Santa Cruz Biotechnology, Inc., CA, USA) was added at 1:100 dilution in PBS-BSA for 1 h at 30°C. In the final step, the coverslips were washed three times in PBS-BSA and the cells were observed by a confocal laser scanning microscope (LSM 700, Zeiss, <http://www.zeiss.com/>). Observations were performed as described in <sup>[44]</sup>.

### 2.6 Sample preparation for yeast metabolite analysis

A previous procedure for preparation of yeast cell lysates described by Villas-Bôas was used <sup>[45]</sup>. Yeast cultures were grown overnight shaking in YP media supplemented with 2% (w/v) glucose at 30°C to OD<sub>600</sub> = 3.5 and then were quenched by quickly adding 10 ml of overnight cultures to 40 ml of chilled methanol-water solution (60% v/v). Cells were harvested for 5 min at 1540 x *g* (0°C) and the pellets were resuspended in 3 ml chilled 100% (v/v) methanol. A 1ml aliquot of this suspension was snap frozen in liquid nitrogen, thawed in an ice-bath and centrifuged at 770 x *g* for 20 min (0°C). The supernatant was collected and an additional 0.5 ml of chilled 100% (v/v) methanol was added to the pellet and vortexed for 30 seconds. Suspensions were centrifuged at 770 x *g* for 20 min (0°C) and both supernatants were pooled. Metabolite extractions were carried out on yeast mitochondria isolated from wild-type, *hem25* $\Delta$  and *HEM25*-pYES2 cells. Yeast mitochondria were obtained as described above.



### 2.7 Glycine and ALA analysis by gas chromatography coupled to tandem mass spectrometry (GC-MS/MS)

Yeast lysates and mitochondria obtained from wild-type, *hem25Δ* and *HEM25-pYES2* cells were centrifuged, and the supernatant was transferred into a glass vial; norleucine (Sigma-Aldrich, Italy) was added as internal standard (10  $\mu$ l of an 80 ng/ $\mu$ l norleucine solution) and freeze dried [46, 47]. The residue was reconstituted with 200  $\mu$ l of DMF (N,N-dimethylformamide) (VWR International PBI S.r.l., Italy) and 50  $\mu$ l of MTBSTFA (N-tertbutyldimethylsilyl- N-methyltrifluoroacetamide) (Sigma-Aldrich, Italy) [48]. Derivatization with MTBSTFA was performed at 60°C for 30 min. If not otherwise indicated, samples were placed on the GC-MS/MS autosampler tray immediately after preparation. After cooling the solution at room temperature for 5 min, 1  $\mu$ l of the solution was injected into the GC-MS/MS. Samples were run on a GC-QqQ-MS (Bruker 456 gas chromatograph coupled to a triple quadrupole mass spectrometer Bruker Scion TQ) equipped with an autosampler (GC PAL, CTC Analytics AG). 1  $\mu$ l of the sample was injected in split mode (split ratio 5:1). The GC was operated at a constant flow of 1.2 mL/min and analytes were separated on a Restek Rxi 5Sil MS capillary column (30 m with a 10 m “built-in” guard column, inner diameter 250  $\mu$ m and film thickness 0.25  $\mu$ m). The oven was kept at 130°C for 2 min after injection, then a temperature gradient of 5°C/min was employed until 220°C was reached and of 10°C/min up to 300°C. The oven was then held at 300°C for 10 min. The total run time was 38 min. The mass detector was operated at 70 eV in the electron impact (EI) ionization mode. The ion source and transfer line temperature were 200°C and 280°C, respectively. The collision gas was argon. For both ALA and Gly quantification, an MS/MS procedure was employed in Multiple Reaction Monitoring (MRM) mode using argon 99.999% (w/v) (Sapio BIC) as collision gas at a pressure of 1.5147 mbar in the collision cell. To ensure a reliable identification of analytes, two MS/MS transitions were selected within  $\pm$  0.2 min of the compounds’ retention time. Product ion abundance was maximized by optimal collision energy voltage. The dwell time per transition was 0.1 s. For identity confirmation both the match in retention time and the confirmation ratio (Q/qi), i.e. the ratio between the intensity of the quantification (Q) and confirmation (qi) transitions recorded for each compound, were required to confirm positive identification in a sample. Bruker MS Workstation 8 application manager was used to process the data. Method validation included determination of linear range, limit



of detection (LOD), limit of quantification (LOQ), recovery, and repeatability (Table 1 gives an overview of the relevant data). Linearity was evaluated by least-squares regression and expressed as  $r^2$ . The calibration curve was linear in the investigated range of six concentration levels (0.04, 0.1, 0.2, 0.4, 0.7, and 1.0 ng/ $\mu$ l). LOQ and LOD were estimated, respectively, from the calibration curve as the concentration for which there is a 5% chance of having a false-positive and the concentration for which there is a coefficient of variation on the expected value less than 10%. Experiments to evaluate surrogate or marginal recovery were performed with samples spiked with 100 ng Gly and ALA: the average recoveries were calculated on five different experiments. The repeatability of the present method was estimated during the entire analytical procedure (sample pretreatment, derivatization, and GC/MSMS separation) using standard solutions (0.4 ng/ $\mu$ l ALA; 0.1 ng/ $\mu$ l Gly). The intraday and interday precision values, expressed in terms of relative standard deviation (RSD), were assessed by performing an analysis three times on the same day and by conducting the analysis on five different days in one month, respectively.

### 2.8 Determination of mitochondrial heme and cytochrome content

Mitochondria were isolated from wild-type, *hem25* $\Delta$ , *HEM25*-pYES2 and *SLC25A38*-pYES2 cells and solubilized in 1% (w/v) Triton-X100. Heme was quantified by spectrophotometry according to the method of Drabkin with some modifications<sup>[49]</sup>. To determine fluorescence spectra of heme, equal amounts of mitochondrial protein were mixed with 2 mol/L oxalic acid, heated to 95°C for 30 minutes to release iron from heme and generate protoporphyrin IX. Samples were then centrifuged for 10 minutes at 1000 g at 4°C to remove debris. The fluorescence intensity of the supernatant was measured with a JASCO FP 750 fluorimeter (Jasco Corporation, Japan). The excitation wavelength was 405 nm and emission was measured at 600 nm. The 662 nm emission peak has lower fluorescence than the peak at 600 nm, but also has other interference<sup>[50]</sup>. Determination of the contents of cytochromes *aa3*, *b*-type (*bII* + *bH* + *bL*) and *c* type (*c* + *c1*) in isolated mitochondria was carried out in 1 ml of respiratory buffer (300 mM sucrose, 1 mM EDTA, 5 mM Mops, 10 mM KH<sub>2</sub>PO<sub>4</sub>, 2 mM MgCl<sub>2</sub>, 0.1% (w/v) BSA and 5 mM succinate, pH 7.4)<sup>[50]</sup>. Individual fully reduced (with excess sodium



dithionite) or fully oxidized (with excess ferricyanide) absorbance spectra were recorded between 500 and 650 nm, and the concentration of each type of cytochrome was determined from the difference (reduced/oxidized) spectrum at the maximum absorption value for each one, normalized by the absorbance of the respective isosbestic point. Values were calculated by the Beer-Lambert law, as described previously<sup>[51]</sup>, and expressed relative to protein concentration.

### 2.9 Mitochondrial respiration efficiency

Mitochondrial respiration (0.2 mg of mitochondrial protein/ml) was measured in a medium consisting of 300 mM sucrose, 1 mM EDTA, 5 mM Mops, 10 mM KH<sub>2</sub>PO<sub>4</sub>, 2 mM MgCl<sub>2</sub>, 0.1% (w/v) BSA and 5 mM succinate, pH 7.4, by means of a Clark oxygen electrode at 30°C. After 2 min, *state 3* respiration was induced by the addition of 0.2 mM ADP. The rate of oxygen uptake by yeast mitochondria (V) was expressed as nmol O<sub>2</sub> x ml<sup>-1</sup> x min<sup>-1</sup>/mg protein. The RCR was calculated by dividing V3 (rate of oxygen uptake measured in the presence of respiratory substrates + ADP, i.e., *state 3* of respiration or active state of respiration) by V4 (rate of oxygen uptake measured with respiratory substrates alone, i.e., *state 4* of respiration or resting state of respiration)<sup>[52]</sup>. The enzymatic bc1 complex activity was determined by measuring the reduction of oxidized cytochrome *c* at 550 nm as described previously<sup>[53]</sup>.

### 2.10 Comparative modelling and docking investigations

Computational approaches for protein function investigations<sup>[54]</sup> have been employed to investigate the function of the analyzed proteins.

Modeller<sup>[55]</sup> was used to calculate a 3D comparative model of dPCoAC-A and BtOGC by using as template the structure of the bovine AAC1 (protein data bank accession code: 1okc), crystallized in complex with its powerful inhibitor carboxyatractyloside (CATR)<sup>[18]</sup>. The structural properties of the dPCoAC-A and SLC25A11\_OGC comparative models with the best energy function were evaluated using the biochemical/computational tools of the WHAT IF Web server<sup>[56]</sup>. Q-site Finder<sup>[57]</sup> was used to predict the potential binding sites of dPCoAC-A best model. For docking



analysis, CoA and dPCoA ligands were docked into the proposed binding sites of dPCoAC-A by using Autodock 1.5.2. [58].

### **2.10.1 Comparative modelling and docking investigations of dPCoAC**

A multiple sequence alignment (MSA) between dPCoAC-A and dPCoAC-B proteins and their putative orthologs from *H. sapiens* and *S. cerevisiae* was obtained by using ClustalW [59]. The sequence of crystallized bovine ADP/ATP carrier (AAC1) [18] was introduced in the alignment in order to use the secondary structure of the bovine AAC1 to weigh gap insertions [55]. The characterizing triplet set of dPCoACs was obtained by aligning the three repeats of the analyzed mitochondrial carriers, building an inter-repeat multiple sequence alignment (MSA) [60].

### **2.10.2 Comparative modelling and docking investigations of BtOGC mutants**

By using the obtained 3D model of BtOGC as a protein template, mutagenesis in silico analysis was also performed to build the single OGC mutant K122R, and the triple mutants (K122R/C184, K122R/C221 and K122R/C224), in order to investigate the role played by K122R in 2-oxoglutarate translocation and, more in general, the influence of cysteine residues in 2-oxoglutarate uptake. Due to the availability of in vitro transport assays in the presence or absence of cysteine specific reagents MTSEA was added to cysteine residues of 3D models (WT OGC and triple mutants) in order to explain results from transport assays in the context of a 3D protein model. More in detail, MTSEA was alternatively added to the cysteine residues within the triple mutants K122R/ C184, K122R/C221 and K122R/C224. For docking analysis the 2-oxoglutarate ligand was docked into the proposed binding site of our 3D models using Autodock 1.5.2. [58]. A gridbox involving the residues protruding towards the WT OGC and the triple mutants carrier cavity from the c-gate to the m-gate, surrounding residues that form the MCs common substrate binding site [61, 62], and overlapping with the carboxyatractyloside binding region described in the crystallized AAC1 [18], was built to investigate the binding of 2-oxoglutarate substrate to OGC. Docking



simulations were performed according to validated protocols <sup>[54]</sup>, in order to screen the putative binding modes of 2 oxoglutarate at this region in the WT OGC 3D model and in the analysed triple mutants in the presence or absence of MTSEA.

### 2.11 Molecular evolution analysis

14 eukaryotic model organisms for which whole genome sequences were available were selected, i.e. two yeast species (*Saccharomyces cerevisiae* and *Schizosaccharomyces pombe*), two plant species (*Arabidopsis thaliana* and *Zea mays*), two nematode species (*Caenorhabditis elegans* and *Caenorhabditis briggsae*), two insect species (*Drosophila melanogaster* and *Anopheles gambiae*), two fish species (*Danio rerio* and *Tetraodon nigroviridis*), two amphibian species (*Xenopus laevis* and *Xenopus tropicalis*), and two mammalian species (*Mus musculus* and *Homo sapiens*). The human protein sequence encoded by the SLC25A42 gene was queried against the non-redundant reference RNA sequence database using the tblastn version implemented in the NCBI website (<https://blast.ncbi.nlm.nih.gov/>). The obtained transcripts were filtered for e-value  $\leq 10^{-40}$  and coverage  $\geq 80\%$ , and only one protein isoform per gene, i.e. the longest one, was retained for subsequent analyses. The 65 homologous proteins collected were multi-aligned with ClustalW <sup>[59]</sup>. N- and C-termini sequences were removed from multiple sequence alignment (MSA) and 6 MSA blocks (255 alignment columns) were retained for the following evolutionary analyses, since they correspond to the most informative mitochondrial carrier amino acids <sup>[5, 61]</sup>. After having used MEGA6 <sup>[63]</sup> to find the best amino acid substitution model for the maximum likelihood (ML) analysis, a phylogenetic tree was built in PhyML <sup>[64]</sup>, using the LG substitution model with four substitution rate categories. The tree branch support was tested in PhyML using two methods, i.e. aBayes <sup>[65]</sup> and 100 bootstrap samplings.



---

## 3. CHARACTERIZATION OF THE MITOCHONDRIAL GLYCINE CARRIER

---

### 3.1 INTRODUCTION

#### **Glycine carrier and associated diseases**

The human glycine *carrier* (human SLC25A38) is a nuclear encoded protein, localized in the inner mitochondrial membrane. This *carrier* belongs to the mitochondrial carrier family, and, similarly to all SLC25A family members, mediates the exchange of metabolites across the inner mitochondrial membrane and possesses a tripartite structure, typical of the mitochondrial inner membrane transporter family, consisting of three tandemly repeated sequences of approximately 100 amino acids length <sup>[5]</sup>. The gene, mapped on chromosome 3.p22.1, has a length of 14kb, presents 7 exons coding for a protein of 303 amino acids and about 33kDa <sup>[66]</sup>.

SLC25A38 is highly and preferentially expressed in transferrin receptor (CD71) positive erythroid cells. Mutations in SLC25A38 cause congenital sideroblastic anemia <sup>[67]</sup>. As its name indicates, this disease is characterized by severe anemia with hypochromia, microcytosis and ringed sideroblasts in the bone marrow, formed by iron-loaded mitochondria clustered around the erythroblast nucleus <sup>[68]</sup>. Patients are nonsyndromic and present no developmental anomalies.

Unlike the acquired sideroblastic anemia, which occurs after exposure to certain drugs or alcohol and with copper deficiency <sup>[69]</sup>, congenital sideroblastic anemia (CSA) is a rare and heterogeneous disease caused by mutations of genes involved in heme biosynthesis, iron-sulfur (Fe-S) cluster biogenesis or Fe-S cluster transport and mitochondrial metabolism. The definition of this disease at molecular level has provided insight into cellular pathways associated with dysfunctional mitochondrial iron metabolism <sup>[68]</sup>.

X-linked sideroblastic anemia (XLSA) is a form of non-syndromic CSA caused by a defect of the  $\delta$ -aminolevulinate synthase 2 (*ALAS2*) gene, which encodes the first



mitochondrial enzyme of heme biosynthesis in erythroid cells<sup>[70]</sup>. The ALAS2 catalyzes the condensation into mitochondria of glycine with succinyl-coenzyme A to yield  $\delta$ -aminolevulinic acid (ALA), and requires pyridoxal 5'-phosphate (PLP; vitamin B6) as cofactor<sup>[71]</sup>. Following its synthesis, ALA is exported to the cytosol where it is converted to coproporphyrinogen III (CPgenIII). All the remaining steps of heme biosynthesis take place inside mitochondria. CPgenIII is imported into the mitochondrial intermembrane space where it is converted to protoporphyrinogen IX by coproporphyrinogen oxidase. Then, protoporphyrinogen IX is oxidized to protoporphyrin IX (PPIX) by protoporphyrinogen oxidase. Lastly, ferrous iron is incorporated into PPIX to form heme in the mitochondrial matrix, a reaction catalyzed by ferrochelatase (Fig 3.1)<sup>[72]</sup>. While all the enzymatic steps leading to the production of heme are well characterized, it is still not completely understood how ALA, CPgenIII and heme and glycine are transported across the two mitochondrial membranes.

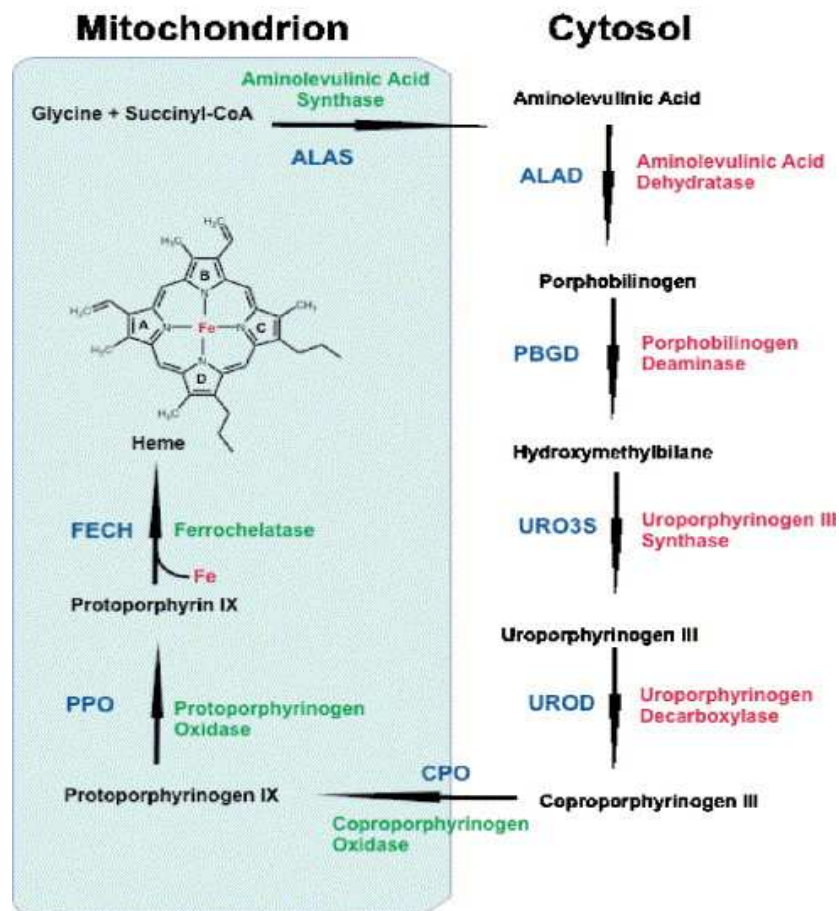


**Fig. 3.1** The heme biosynthetic pathway. Mitochondrial enzymes are depicted in green and cytosolic enzymes in red<sup>[72]</sup>.



Missense mutations in SLC25A38 gene have been found recently, by Guernsey et al, in patients with severe non-syndromic CSA resembling XLSA but lacking ALAS2 mutations. Knocked down zebrafish orthologues of SCL25A38 (*slc25a38a* and *slc25a38b*) caused an anemic phenotype, showing the importance of this gene for red blood cells production and function<sup>[67]</sup>.

Furthermore, the genetic deletion of the *Saccharomyces cerevisiae* SLC25A38 orthologue *YDL119c* (also named *HEM25*) produces a respiratory phenotype (unable to grow on glycerol), indicative of mitochondrial involvement, and shows a significant reduction of ALA levels, the first product in the heme biosynthetic pathway<sup>[67]</sup>.

Based on these findings and on their structure (particularly because of a conserved arginine-aspartate (RD) dipeptide sequence present in transmembrane helix 4, typical of amino acid *carriers*), SLC25A38 and its yeast orthologue Hem25p were hypothesized to facilitate ALA production by importing glycine into mitochondria or by exchanging glycine for ALA across the inner mitochondrial membrane. Thus, it would transport one or two substrates required in the first steps of heme biosynthesis.



## 3.2 RESULTS

### 3.2.1 Bacterial expression of Hem25p

Hem25p was overexpressed at high levels in *Escherichia coli* BL21 (DE3) as inclusion bodies and purified by Ni<sup>2+</sup>-NTA-agarose affinity chromatography (Fig. 3.2A, lanes 4 and 5). The apparent molecular mass of the purified protein was about 36 kDa. The protein was not detected in bacteria harvested immediately before the induction of expression (Fig. 3.2A, lane 2) or in cells harvested after induction but lacking the coding sequence in the expression vector (Fig. 3.2A, lane 3). Approximately 90 mg of purified protein was obtained per liter of culture. The identity of the purified protein was confirmed by Western blot analysis (Fig. 3.2B, lanes 4 and 5).

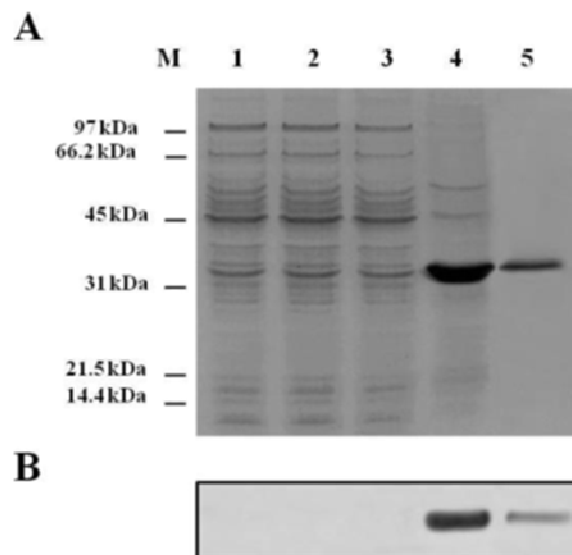


**Fig 3.2 Expression in *Escherichia coli* and purification of Hem25p**  
 Proteins were separated by SDS-PAGE and stained with Coomassie blue dye (A) or transferred to nitrocellulose and immunodetected with an anti-V5 monoclonal antiserum (B). Lane M, markers (phosphorylase b, serum albumin, ovalbumin, carbonic anhydrase, trypsin inhibitor and lysozyme); lanes 1-4, *E. coli* BL21 (DE3) containing the expression vector, without (lanes 1 and 3) and with (lanes 2 and 4) the coding sequence for Hem25p. Samples were taken at the time of induction (lanes 1 and 2) and 1 h later (lanes 3 and 4). The same number of bacteria was analyzed in each sample. Lane 5, purified Hem25p (5  $\mu$ g) originating from bacteria shown in lane 4.

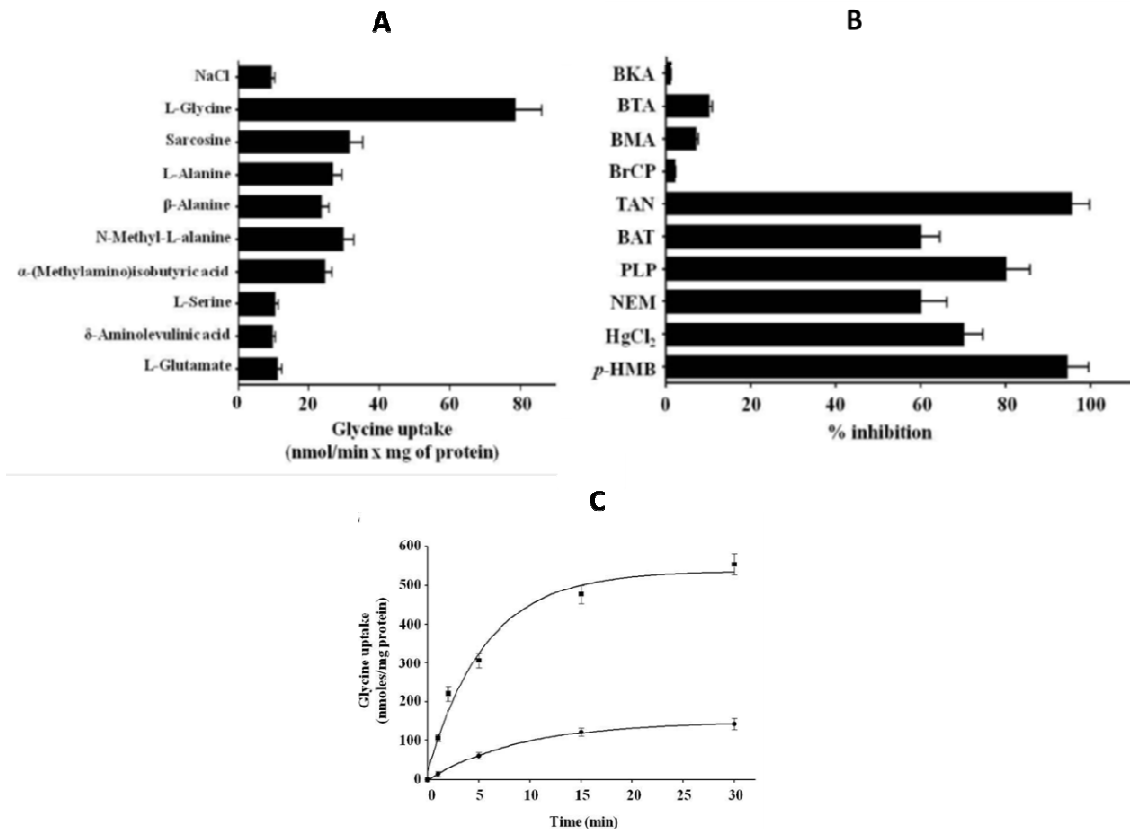


### 3.2.2 Functional characterization of recombinant Hem25p

Since it has been hypothesized that Hem25p facilitates ALA production by importing glycine into mitochondria [67, 73], the recombinant and purified Hem25p was reconstituted into liposomes and its ability to transport glycine was tested. Proteoliposomes reconstituted with Hem25p catalyzed active [<sup>14</sup>C]glycine/glycine exchange, which was abolished by a mixture of the inhibitors pyridoxal 5'-phosphate (PLP) and bathophenanthroline (BAT). Reconstituted Hem25p did not catalyze significant homoexchanges for aspartate, glutamate, glutamine, asparagine, ornithine, lysine, arginine, proline, and threonine (internal concentration, 10 mM; external concentration, 1 mM). No [<sup>14</sup>C]glycine/glycine exchange was observed with Hem25p that had been boiled before incorporation into liposomes or after reconstitution of sarcosyl-solubilized material from bacterial cells either lacking the expression vector for Hem25p or harvested immediately before the induction of expression. The substrate specificity of purified and reconstituted Hem25p was investigated in detail by measuring the uptake of [<sup>14</sup>C]glycine into proteoliposomes which had been preloaded with various potential substrates (Fig. 3.3A). External glycine was significantly exchanged only in the presence of internal glycine. Furthermore, transport activities were also observed with internal sarcosine, L-alanine and N-methyl-L-alanine. A low exchange was found with  $\beta$ -alanine and  $\alpha$ -(methylamino)isobutyric acid while the activity observed with L-serine, ALA and L-glutamate was approximately the same as that observed in the absence of internal substrate (Fig. 3.3A). Reconstituted Hem25p, therefore, exhibits a very narrow substrate specificity, which is virtually confined to glycine. The effects of known mitochondrial inhibitors on the [<sup>14</sup>C]glycine/glycine reaction catalyzed by reconstituted Hem25p were also examined (Fig. 3.3B). The activity of the recombinant protein was markedly inhibited by tannic acid [74], PLP and BAT [34] (known inhibitors of several mitochondrial carriers) as well as by thiol reagents (*p*-hydroxymercuribenzoate, mercuric chloride and N-ethylmaleimide) [34, 39]. In addition, no significant inhibition was observed with butylmalonate [21], 1,2,3-benzenetricarboxylate [75] and bongkreic acid [14], specific inhibitors of the dicarboxylate carrier, citrate carrier and ADP/ATP carrier, respectively. Also bromocresol purple [74] had no effect on the activity of the yeast reconstituted protein (Fig. 3.3B). The time-course of uptake by proteoliposomes of 1 mM [<sup>14</sup>C]glycine measured either as exchange (with 10 mM glycine inside the proteoliposomes) or as



uniport (without internal substrate) is shown in figure 2C. All curves fitted a first-order rate equation with rate constants ( $k$ ) for the exchange and uniport reactions of approximately  $0.18 \text{ min}^{-1}$  and  $0.11 \text{ min}^{-1}$ , respectively. The initial rates of glycine uptake (the product of  $k$  and intraliposomal quantity of glycine taken up at equilibrium) were about  $95.96 \pm 4.55$  and  $16.36 \pm 0.72 \text{ nmol/min} \times \text{mg protein}$  for the exchange and uniport reactions, respectively. The addition of 10 mM unlabeled glycine to proteoliposomes after incubation with 1 mM [ $^{14}\text{C}$ ]glycine for 30 min, when radioactive uptake had almost reached equilibrium, caused an extensive efflux of radiolabeled glycine from both glycine-loaded and unloaded proteoliposomes. This efflux shows that [ $^{14}\text{C}$ ]glycine taken up by exchange or unidirectional transport is released in exchange with externally added substrate (results not shown). The kinetic constants of recombinant purified Hem25p were determined by measuring the initial transport rate at various external [ $^{14}\text{C}$ ]glycine concentrations in the presence of a constant saturating internal concentration (10 mM) of glycine. The  $K_m$  and  $V_{max}$  values (measured at  $25^\circ\text{C}$ ) were  $0.75 \pm 0.084 \text{ mM}$  and  $169.8 \pm 13.7 \text{ nmol/min} \times \text{mg protein}$ , respectively (means of 5 experiments). The activity was calculated by taking into account the amount of Hem25p recovered in the proteoliposomes after reconstitution.

**Fig 3.3****(A) Dependence of Hem25p transport activity on internal substrate.**

Proteoliposomes were preloaded internally with various substrates (concentration 10 mM). Transport was started by adding 0.75 mM [<sup>14</sup>C]glycine to proteoliposomes reconstituted with Hem25p and terminated after 1 min.

**(B) Effect of inhibitors on the [<sup>14</sup>C]glycine/glycine exchange mediated by Hem25p.**

Proteoliposomes were preloaded internally with 10 mM glycine. Transport was initiated by adding 0.75 mM [<sup>14</sup>C]glycine to proteoliposomes reconstituted with Hem25p and was stopped after 1 min. The inhibitors were added 3 min before the labeled substrate. The final concentrations of the inhibitors were 10 mM (pyridoxal 5'-phosphate, PLP; bathophenanthroline, BAT), 2 mM (1,2,3- benzenetricarboxylate, BTA; butylmalonate, BMA), 1 mM (N-ethylmaleimide, NEM), 100  $\mu$ M (phydroxymercuribenzoate, *p*-HMB; mercuric chloride, HgCl<sub>2</sub>; bromocresol purple, BrCP), 10  $\mu$ M (bongkreic acid, BKA), and 0.1% (w/v) (tannic acid, TAN). The extent of inhibition (%) from a representative experiment is reported.

**(C) Kinetics of [<sup>14</sup>C]glycine transport in proteoliposomes reconstituted with Hem25p.**

1 mM [<sup>14</sup>C]glycine was added to proteoliposomes containing 10 mM glycine (exchange, solid squares) or 10 mM NaCl and no substrate (uniport, solid circles).



### 3.2.3 Impaired glycine uptake in mitochondria lacking Hem25p

In other experiments, the uptake of [ $^{14}$ C]glycine was measured in proteoliposomes that had been reconstituted with Triton X-100 extracts of mitochondria isolated from wild-type, *hem25* $\Delta$  and *hem25* $\Delta$  transformed with *HEM25*-pYES2 plasmid (Fig. 3A). A very low glycine/glycine exchange activity was observed upon reconstitution of mitochondrial extract from the knockout strain. This activity was more than double in mitochondria extracts from wild-type and was considerable even in mitochondrial extracts from *HEM25*-pYES2 (Fig. 3.4A). As a control, the [ $^{14}$ C]malate/phosphate exchange (the defining reaction of the dicarboxylate carrier, known as Dic1) <sup>[76]</sup> was virtually the same for all types of reconstituted mitochondrial extracts (Fig. 3.4B). Therefore, the absence of *HEM25* does not affect the expression or the activity of other mitochondrial carriers.

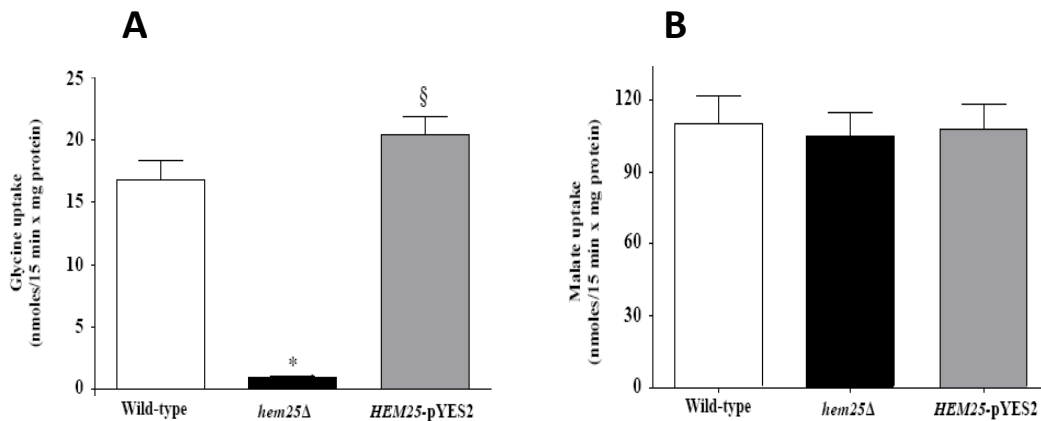


**Fig 3.4**

**(A)(B) Glycine exchange activities in proteoliposomes reconstituted with mitochondrial extracts.**

The mitochondrial extract (30  $\mu$ g protein) from the wild-type (open bars), *hem25* $\Delta$  (solid bars) and *hem25* $\Delta$  strains transformed with *HEM25*-pYES2 plasmid (gray bars) were reconstituted into liposomes preloaded with 10 mM glycine or 20 mM phosphate. Transport was started by adding 0.75 mM [ $^{14}$ C]glycine or 0.1 mM [ $^{14}$ C]malate, respectively, and terminated after 15 min. The [ $^{14}$ C]malate/phosphate exchange, the defining reaction of the dicarboxylate carrier, was used as control. \* $P < 0.001$  vs wild-type cells; § $P < 0.001$  vs *hem25* $\Delta$  cells.

### 3.2.4 Subcellular localization of Hem25p

Given that some mitochondrial carrier members are localized in non-mitochondrial membrane <sup>[77]</sup>, the intracellular localization of the recombinant Hem25p was

investigated (Fig. 3.5). Hem25p-expressing cells exhibited green fluorescence (Fig. 3.5A, E and I). Upon staining with MitoTracker Red (mitochondrial specific dye) (Fig. 3.5B), FM4-64 (vacuolar specific dye) (Fig. 3.5F) and DAPI (nucleic acid dye) (Fig. 3.5L), the same cells showed a pattern of fluorescence that merged only with the mitochondrial network (Fig. 3.5C). From the overlapping images it is clear that recombinant Hem25p was localized to mitochondria (Fig. 3.5C). Structural integrity of the cells was documented by phase contrast microscopy (Fig. 3.5D, H and N).

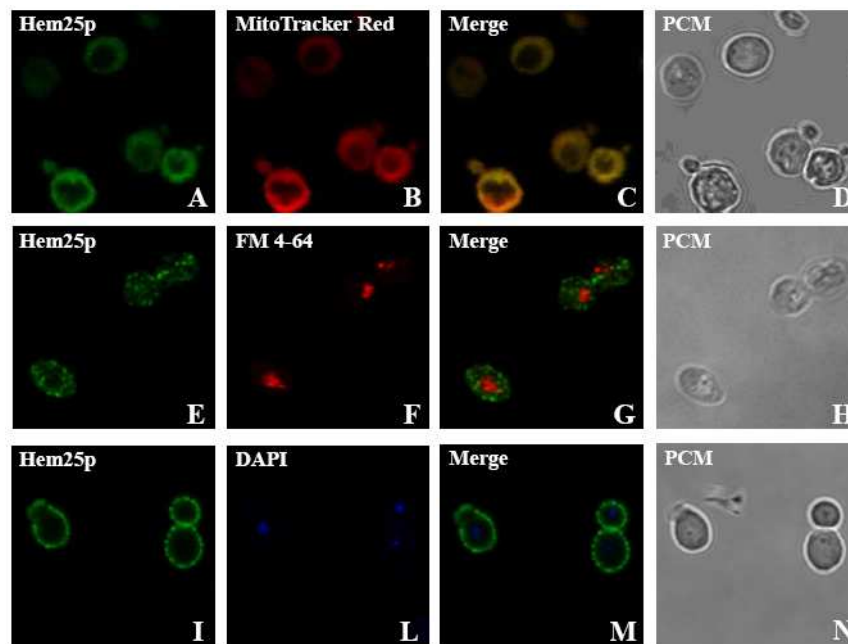


**Fig. 3.5**

***Subcellular localization of recombinant Hem25p after expression in Saccharomyces cerevisiae cells.***

Staining of the Hem25p/V5 protein was performed with mouse anti-V5 monoclonal antibody and anti-mouse antibody with conjugated FITC (A, E and I). MitoTracker Red (B), FM 4-64 (F) and DAPI (L) were used to locate mitochondria, vacuoles and nucleic acid in the cells, respectively. Co-localization of the Hem25p/V5 protein and mitochondria are seen as yellow fluorescence in the red and green merged image (C). Phase contrast microscopy (PCM) was used to monitor the integrity of the cells (D, H and N). The same cells were photographed first with a FITC-green filter set and then with the MitoTracker or FM 4-64 red filter set or with the DAPI blue filter set.

Identical fields are presented in panels A-D, E-H or I-N.

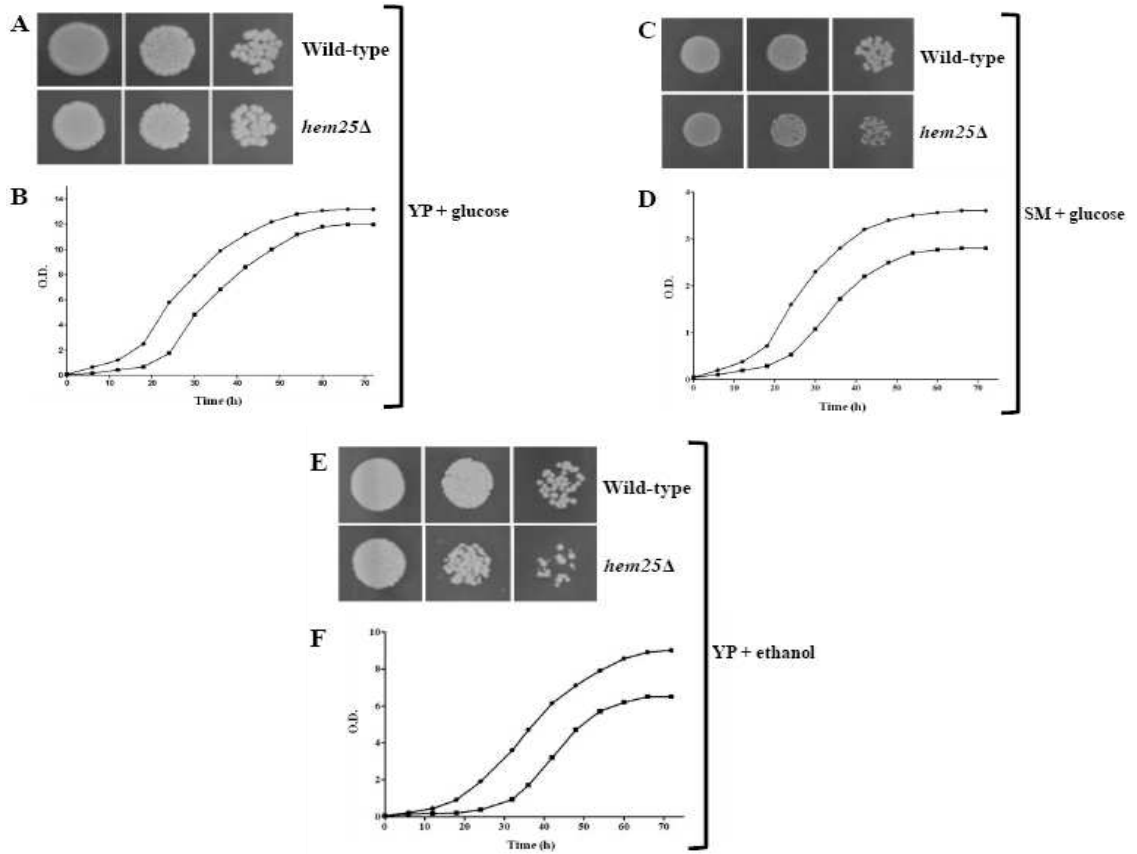


### 3.2.5 Growth characteristics of wild-type and *hem25Δ*

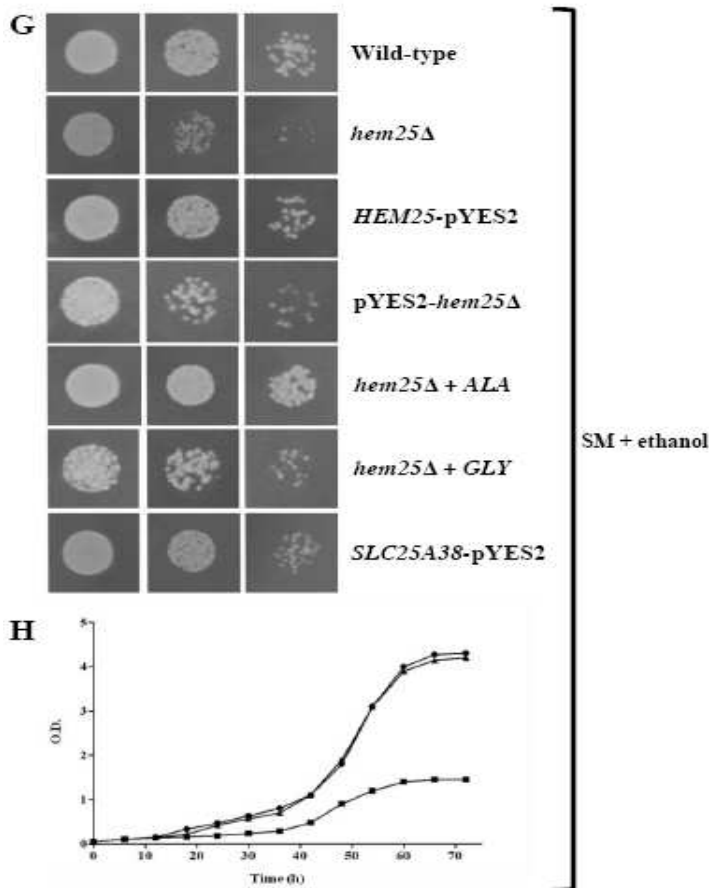
The effect of deletion of the *HEM25* gene on yeast cells was investigated. On YP and SM media supplemented with glucose, *hem25Δ* exhibited a slight but definite growth defect as compared to wild-type cells (Fig. 3.6A-D). However, *hem25Δ* displayed a growth delay in the YP medium supplemented with ethanol (Fig. 3.6E-F).

In the SM medium, growth of *hem25Δ* cells on ethanol was very poor after 70 h (Fig. 3.6G-H); in addition, a slower lag-phase of growth was observed more in the SM medium than in the YP medium (Fig. 3.6H). The growth phenotype of *hem25Δ* cells was restored when these cells were transformed with *HEM25*- pYES2, demonstrating that the impaired phenotype is the result of the absence of *HEM25* and not of a secondary effect. The observed defect can also be rescued by supplementation of the SM medium with 10 mM ALA (Fig. 3.6G), whereas the addition of glycine at a high concentration (10 mM) did not restore their lack of growth (Fig. 3.6G). All together, these results indicate that the defect of *hem25Δ* cells to grow on non-fermentable carbon source is overcome by expression of Hem25p in mitochondria or by supplementation of ALA, indicating that the defect is related to glycine transport.

Importantly, figure 3.6G shows that the *hem25Δ* cell transformed with plasmid carrying the human *SLC25A38* gene restored growth of the *hem25Δ* strain on ethanol.





**Fig. 3.6****Growth behavior of wild-type and mutant strains under various conditions.**

Three-fold serial dilutions of wild-type and *hem25Δ* cells were plated on solid YP medium supplemented with glucose (A) or ethanol (E) and solid SM medium supplemented with glucose (C) or ethanol (G). *hem25Δ* cells were also spotted on solid ethanol-supplemented SM medium in the presence of 10 mM  $\delta$ -aminolevulinic acid (ALA) or 10 mM glycine (GLY) (G). Wild-type and *hem25Δ* cells were inoculated in liquid glucose-supplemented YP (B), glucose-supplemented SM (D), ethanol-supplemented YP (F) or ethanol-supplemented SM medium (H). *hem25Δ* cells transformed with the *HEM25-pYES2* plasmid were spotted (G) or inoculated (H) on ethanol-supplemented SM medium. *hem25Δ* cells transformed with the *SLC25A38-pYES2* plasmid were also plated on ethanol-supplemented SM medium (G). The optical density (O.D.) values at 600 nm given in (B), (D), (F) and (H) refer to cell cultures after the indicated growth times. Wild type, solid circle; *hem25Δ*, solid square; *hem25Δ + HEM25-pYES2*, solid triangle.

Furthermore, SLC25A38, expressed in *E. coli* and reconstituted in liposomes, shows a significant transport of glycine demonstrating without a doubt that it is the human ortholog of Hem25p and then, the human mitochondrial glycine carrier (GlyC) (Fig. 3.7).

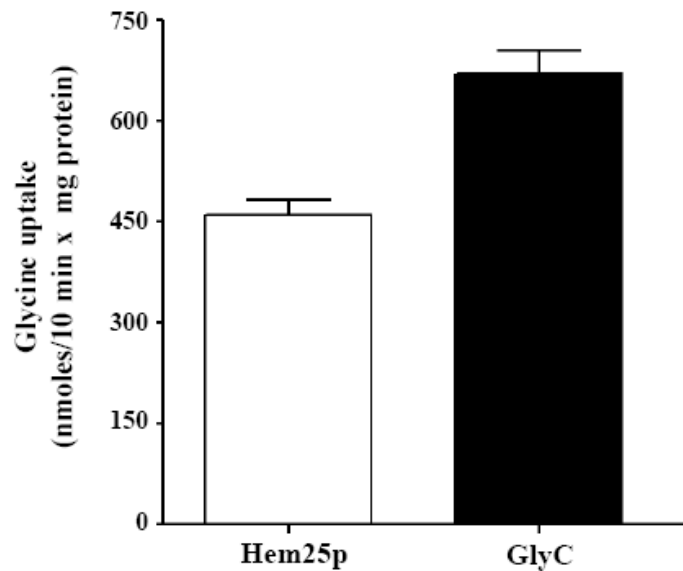


**Fig. 3.7**  
***Glycine uptake in proteoliposomes reconstituted with recombinant Hem25p or GlyC.*** [<sup>14</sup>C]glycine (0.75 mM) was added to proteoliposomes reconstituted with Hem25p (open bar) or GlyC (solid bar) containing 10 mM glycine. The exchange rate was measured after 10 min. Data are means  $\pm$  S.D. of at least five independent experiments.

### 3.2.6 Hem25p is required for the entry of glycine into mitochondria

To confirm the transport function of Hem25p *in vivo*, we investigated the effect of *HEM25* deletion on glycine content in the cellular lysates and mitochondrial extracts from wild-type cells, *hem25* $\Delta$  cells, and *hem25* $\Delta$  cells transformed with the *HEM25*-pYES2 plasmid grown on ethanol-supplemented medium. GC-MS/MS analysis revealed that in mitochondria isolated from *HEM25*-pYES2 cells the amount of glycine is comparable to that determined in wild-type cells ( $3.21 \pm 0.24$  nmol/mg protein and  $2.17 \pm 0.15$  nmol/mg protein, respectively) (Fig. 3.8). On the other hand, *hem25* $\Delta$  cells



revealed a ~70% decrease of intramitochondrial glycine ( $0.64 \pm 0.034$  nmol/mg protein). In agreement with Guernsey<sup>[67]</sup>, no reduction was documented in the amount of total cellular glycine between wild-type (220 ng/107 cells) and *hem25Δ* (251 ng/107 cells) strains. Furthermore, the level of mitochondrial ALA was also measured and, again, in agreement with Guernsey<sup>[67]</sup>, the amount of mitochondrial ALA in the *hem25Δ* strain was reduced compared with control (0.04 nmol/mg protein vs 0.4 nmol/mg protein), highlighting that loss of Hem25p impairs ALA biosynthesis *in vivo*. ALA was reinstated in the wild-type levels when the mutant was complemented with the missing gene (0.5 nmol/mg protein) (Fig. 3.8).

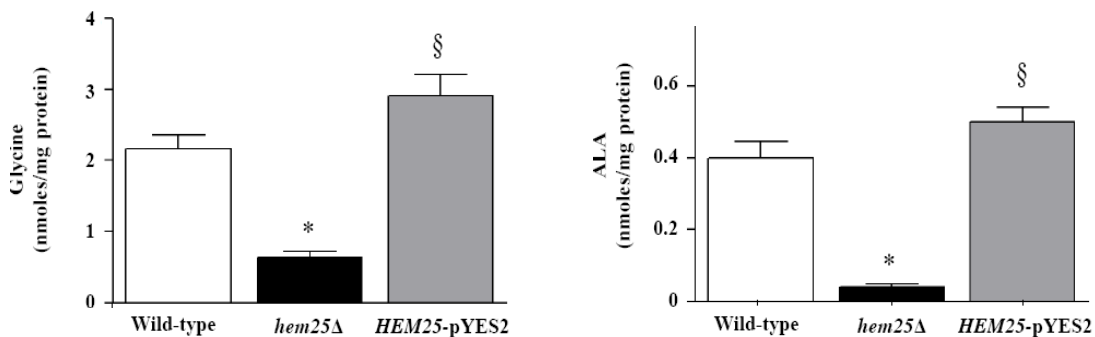


**Fig.3.8**  
**Quantification of glycine and ALA levels in mitochondria extracts by GC-MS/MS analysis.** Mitochondria were extracted from wild-type (open bars), *hem25Δ* (solid bars) and *hem25Δ* strains transformed with the *HEM25-pYES2* plasmid (gray bars). Data represent means  $\pm$  S.D. of at least five independent experiments. \* $P < 0.001$  vs wild-type cells; § $P < 0.001$  vs *hem25Δ* cells.

### 3.2.7 Hem25p and GlyC deficiency cause defects in respiratory chain components

The involvement of Hem25p in heme synthesis implies that the products of the heme pathway could be altered. One of these is heme b, which is incorporated into complexes II and III of the respiratory chain and is present in cytochrome *c*<sup>[78]</sup>. Figure 3.9 shows immunoblotting of mitochondrial extracts from wild-type, *hem25Δ*, *HEM25-pYES2* and *SLC25A38-pYES2* cells. In the *hem25Δ* lysates we observed a reduction of approximately 80% of cytochrome *b* protein (Cyt *b*) (Fig. 3.9A, lane 2) compared to the wild-type, *HEM25-pYES2* and *SLC25A38 pYES2* strains (Fig. 3.9A, lanes 1, 3 and 4).

Cyt *b* is part of the catalytic core of cytochrome *bc1* complex together with cytochrome *c1* (Cyt *c1*) and Rieske iron-sulfur protein (Rip 1) [53]. Furthermore, Cyt *c1* forms a subcomplex with the two core proteins Cor1 and Cor2 [79]. A Western blot analysis using specific antibodies against Cyt *c1* (Fig. 3.9B) and the Cor1 and Cor2 proteins (Fig. 3.9C) shows that the expression of Cyt *c1* and Cor1 and Cor2 proteins were also markedly decreased only in the *hem25Δ* cells (Fig. 3.9B and C, lane 2). To exclude the possibility of a disturbance of the overall protein content by Hem25p, we immunodetected wild-type, *hem25Δ*, *HEM25*-pYES2 and *SLC25A38*-pYES2 mitochondrial lysates with polyclonal antisera directed against yeast Dic1 [76]. In all samples, Dic1 was present in equal amounts (Fig. 3.9D, lanes 1-4).

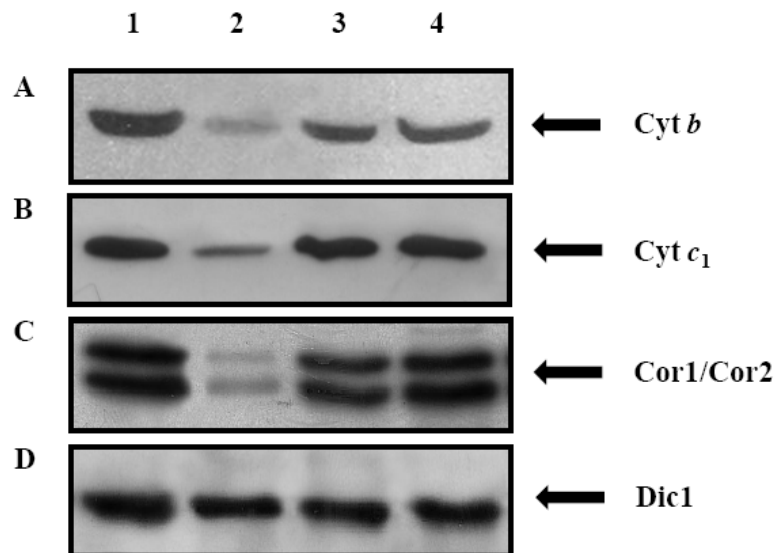


**Fig. 3.9**

***Hem25p deficiency impairs the expression of cytochrome *bc1* complex as evaluated by specific antibodies for cytochrome *b*, cytochrome *c1*, Cor1 and Cor2.***

Mitochondria (30 μg of protein) were extracted from wild-type (lane 1), *hem25Δ* (lane 2), *HEM25*-pYES2 (lane 3) and *SLC25A38*-pYES2 (lane 4) and separated by

SDS-PAGE, transferred to nitrocellulose and immunodetected with antibodies directed against the Cyt *b* (A), Cyt *c1* (B), Cor1 and Cor2 (C) and Dic1 (D) proteins.

Anti-Dic1 was used as control.

We also measured the heme content in mitochondria isolated from wild-type, *hem25Δ*, *HEM25*-pYES2 and *SLC25A38*-pYES2 cells; the corresponding results of the spectrophotometric analysis are shown in figure 3.10A. Taken together, these results indicate that the activity of the Hem25p and GlyC carriers is correlated to the



mitochondrial heme concentration and the expression of some protein components of yeast cytochrome *bc1* complex. To further confirm these results, we assayed cytochrome *aa3*, *b*-type (*bII* + *bH* + *bL*), and *c*-type (*c* + *c1*) content in mitochondria isolated from the wild type, *hem25Δ*, *HEM25*- pYES2 and *SLC25A38*-pYES2 cells. To perform an absolute determination of the respiratory cytochromes we calculated nmoles of each cytochrome type per milligram of mitochondrial protein from different absorbance spectra (experimental data are reported in figure 3.10B). The *hem25Δ* strain displayed a marked decrease in mitochondrial cytochromes compared with control, proving once again that the Hem25p and GlyC carriers are relevant for glycine transport into mitochondria, for subsequent mitochondrial synthesis of the heme group and therefore for respiratory cytochromes. Furthermore, cytochromes were reinstated to the wild-type levels when the mutant was complemented with the *HEM25* or *SLC25A38* genes (Fig. 3.10B).

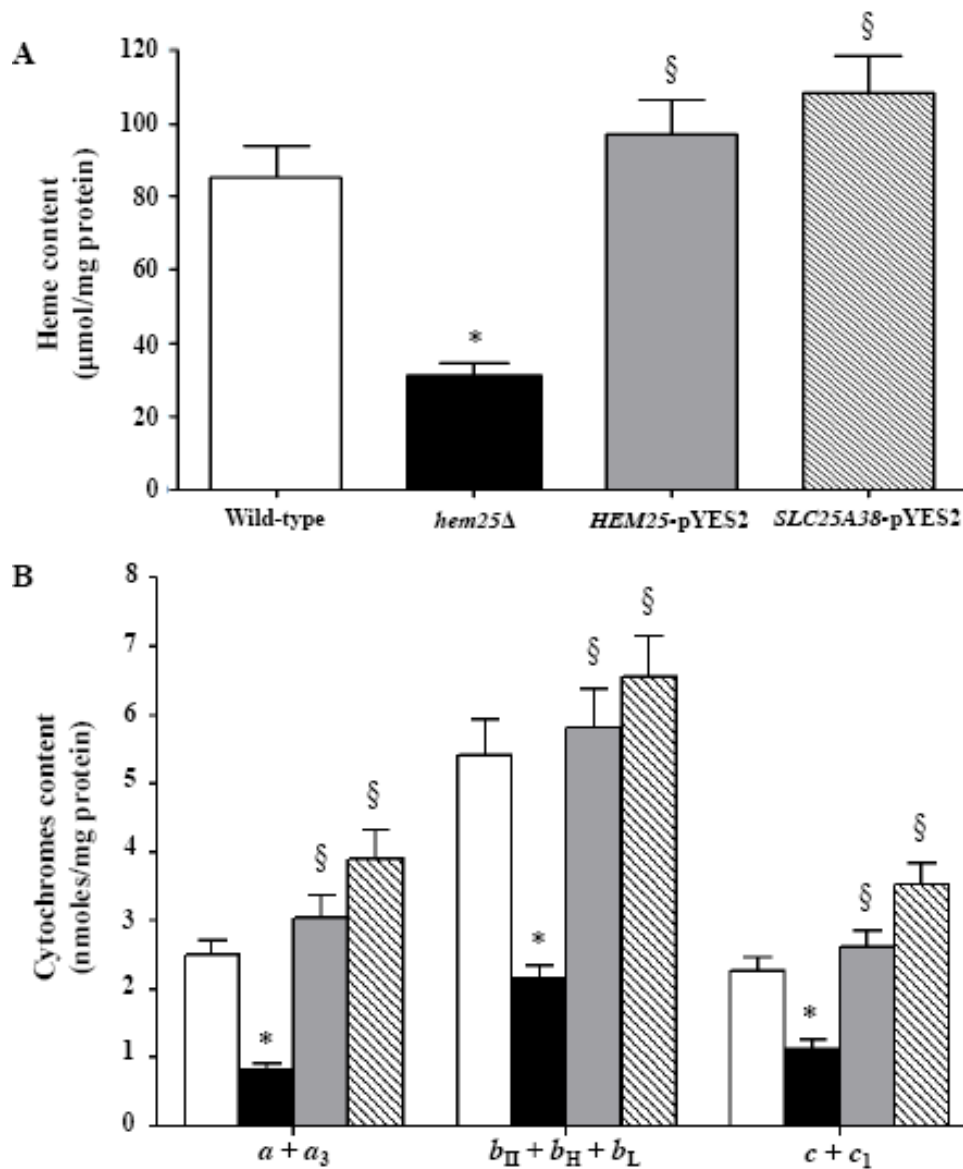


**Fig. 3.10**

***Hem25p* deficiency influences mitochondrial content of heme and cytochromes.**

Mitochondrial heme level (A) and cytochrome *aa<sub>3</sub>*, *b*-type and *c*-type content (B) were measured by spectrophotometry in mitochondria extracted from the wild-type (open bars), *hem25Δ* (solid bars) and *hem25Δ* strain transformed with the *HEM25-pYES2* plasmid (gray bars) or with *SLC25A38-pYES2* plasmid (hatched bars). Data represent means ± S.D. of at least five independent experiments. \**P* < 0.005 vs wild-type cells; §*P* < 0.005 vs *hem25Δ* cells.



### 3.2.8 Respiratory analysis of isolated mitochondria

To better characterize the effects of altered mitochondrial heme content on the oxidative properties of yeast cells, we analyzed the respiratory efficiency of mitochondria freshly isolated from wild-type, *hem25Δ*, *HEM25*- pYES2 and SLC25A38-pYES2 cells grown on SM medium supplemented with ethanol. As shown in figure 3.11, the addition of 5 mM succinate to mitochondria isolated from wildtype cells promoted significant oxygen consumption corresponding to 36 nmol x ml<sup>-1</sup> x min<sup>-1</sup>/mg protein. This rate, indicated as V<sub>4</sub>, corresponds to the so-called resting state of mitochondrial respiration (respiration state 4). The subsequent addition of 0.2 mM ADP doubled the oxygen consumption rate in wildtype mitochondria (77 nmol O<sub>2</sub> x ml<sup>-1</sup> x min<sup>-1</sup>/mg protein). This rate, indicated as V<sub>3</sub>, corresponds to the active state of mitochondrial respiration (respiration state 3). In mitochondria isolated from *hem25Δ* cells, a significant reduction in state 4 and state 3 oxygen consumption (V<sub>4</sub> = 11 nmol O<sub>2</sub> x ml<sup>-1</sup> x min<sup>-1</sup>/mg protein and V<sub>3</sub> = 21.5 nmol O<sub>2</sub> x ml<sup>-1</sup> x min<sup>-1</sup>/mg protein, respectively) was found when compared with wild-type. When this respiratory defect was rescued in *hem25Δ* transformed with *HEM25*-pYES2 or SLC25A38- pYES2, the V<sub>3</sub> values were 70 or 81 nmol O<sub>2</sub> x ml<sup>-1</sup> x min<sup>-1</sup>/mg protein, respectively, while V<sub>4</sub> values were 34 or 43 nmol O<sub>2</sub> x ml<sup>-1</sup> x min<sup>-1</sup>/mg protein, respectively (Fig. 3.11). However, no significant variation was observed in respiratory control ratio (RCR) values (calculated ratio between V<sub>3</sub> and V<sub>4</sub>) among the different samples of mitochondria suggesting, on the one hand, a good coupling between respiration and phosphorylation and, on the other hand, well preserved integrity of the organelles<sup>[80]</sup>. In a more selective approach we assayed the activity of cytochrome *bc1* complex<sup>[81]</sup>. A significant decrease of activity was only found in mitochondria isolated from *hem25Δ* cells (2.78 ± 0.19 μmol/min x mg protein) with respect to wild-type (12.03 ± 1.05 μmol/min x mg protein).

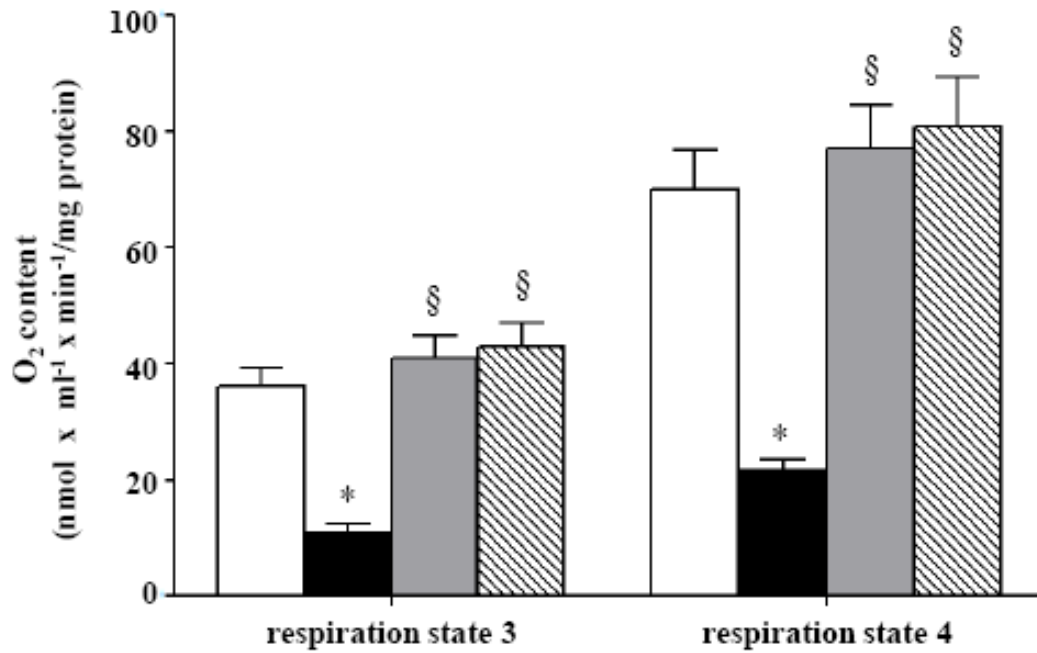


**Fig.3.11**

***Respiratory efficiency of freshly isolated mitochondria by oxygraphic methods.***

Mitochondria isolated from wild-type (open bars), *hem25*Δ (solid bars) and *hem25*Δ cells transformed with the *HEM25*- pYES2 plasmid (gray bars) or with *SLC25A38*-pYES2 plasmid (hatched bars) were grown on SM medium supplemented with ethanol. The rate of oxygen uptake in the presence of added ADP (respiration states 3) and the rate observed when added ADP had been completely phosphorylated to ATP (respiration state 4) were measured by means of a Clark oxygen electrode at 30°C. The rate of oxygen uptake by yeast mitochondria was expressed as nmol O<sub>2</sub> x ml<sup>-1</sup> x min<sup>-1</sup>/mg protein. Data represent means ± S.D. of at least five independent experiments. \**P* < 0.001 vs wild-type cells; §*P* < 0.001 vs *hem*Δ cells.



### 3.3 DISCUSSION

Together with its importance in protein biosynthesis, glycine appears to be a major source of one carbon units in mitochondria. In yeast glycine biosynthesis depends on two different pathways: a 'glycolytic' pathway, during growth on glucose, and a 'gluconeogenic' pathway, during growth on non-fermentable carbon sources such as ethanol and acetate <sup>[82]</sup>.

During the 'glycolytic' pathway, glycine can be synthesized starting from the glycolytic intermediate 3-phosphoglycerate, and also in the reaction catalyzed by the cytosolic L-threonine aldolase, as a product of the catabolism of threonine (L-threonine  $\leftrightarrow$  glycine + acetaldehyde). During the 'gluconeogenic' pathway, glycine can be produced starting from glyoxylate, a product of the anaplerotic glyoxylate cycle, by the alanine-glyoxylate aminotransferase 1 <sup>[83]</sup>.

Other enzymes, important in the synthesis and catabolism of glycine in yeast, are the serine hydroxymethyltransferase (Shm1p and Shm2p) isoenzymes <sup>[84]</sup>. Shm2p is localized in the cytoplasm and it is mainly involved in the breakdown of serine, producing one-carbon units and glycine, while Shm1p is mitochondrial and catalyzes principally the synthesis of serine, consuming glycine and one-carbon units <sup>[85]</sup>.

Since the synthesis of glycine occurs mainly in the cytosol, through the enzyme threonine aldolase, it is necessary the presence of a transporter that will facilitate glycine uptake into mitochondria, where glycine is required for protein synthesis, heme synthesis and for the activity of some enzymes such as glycine cleavage T-protein, a folate-dependent enzyme that is part of the complex responsible for the incorporation of one-carbon units from glycine into folate-dependent pathways <sup>[86]</sup>.

The study here presented, through the results about transport and kinetic characteristics of the recombinant Hem25p (encoded by the yeast *YDL119c* gene, also known as *HEM25*) and its localization to mitochondria, demonstrated that the main function of Hem25p is to catalyze the uptake of glycine into mitochondria. This transporter, moreover, showed a very narrow substrate specificity confined to glycine.

Hem25p was found to be the first mitochondrial protein shown to be capable to transport glycine, and it has been the first *carrier* with this characteristics identified in any organism. Previously, only one study showed evidences for the existence of a

glycine-transport system: exogenous glycine was found to be taken up by isolated mitochondria of rat brain and liver <sup>[87]</sup>.

The only protein sequences that showed a significant homology (~30% amino acid identity) with Hem25p, resulted to be all orthologs of this *carrier* in other organisms: SLC25A38 (*Homo sapiens*); slc25a38a and slc25a38b (*Danio rerio*). On the other hand, Hem25p did not show any significant sequence homology with other mitochondrial *carriers* functionally identified until now in yeast, mammals and plants <sup>[5, 88]</sup>, and SLC25A38 is not particularly related with other members of the SLC family <sup>[5, 67]</sup>.

The data showed in this in this work demonstrate that both Hem25p and the human GlyC (encoded by SLC25A38) control the uptake of glycine into mitochondria. Three relevant suppositions support this affirmation:

1. The levels of glycine and ALA, a precursor of heme, were found to be lower in mitochondria of *hem25Δ* cells, and the normal intramitochondrial levels were restored after complementation with the missing gene. ALAS2 activity assay showed no significant difference between the wild type and the *hem25Δ* strains, which means that the reduced amount of ALA in the mitochondria were due exclusively to the impaired transport of glycine. In addition, glycine uptake was strongly reduced in the reconstituted *hem25Δ* mitochondrial extract compared to wild type.

Recently, Ymc1p has been proposed as a secondary glycine transporter, due to the fact that the double mutant (*hem25Δymc1Δ*) presented a lower level of heme compared to the single mutants (*hem25Δ* and *ymc1Δ*) <sup>[73]</sup>. However, YMC1 and its paralog YMC2 resulted to be related with the mitochondrial 2-oxodicarboxylate transporters, Odc1p and Odc2p, and to be involved in oleic acid and glycerol utilization <sup>[89]</sup>; moreover, they were found to have an anaplerotic role in the TCA cycle, by transferring intermediates to mitochondria and contributing to the utilization of energy substrates (e.g., long chain fatty acids) <sup>[90]</sup>.

2. The growth delay of the *hem25Δ* strain was seen only on non-fermentable carbon sources, and the regular growth was restored after complementation with Hem25p or the human GlyC, and by the addition of ALA to the media, while the addition of glycine alone was insufficient to restore the growth defect. Thus,



since glycine transport into mitochondria is required for the synthesis of ALA, the growth phenotype of *hem25Δ* is probably due to an insufficient synthesis of ALA.

3. The reduced amount of mitochondrial ALA is the main cause of an impaired synthesis of heme, resulting in a reduced level of it. Since heme is contained into cytochromes and oxidative phosphorylation complexes <sup>[78, 91]</sup>, low level of it will be causing defects in state 3 and state 4 respiration. *hem25Δ* mutant had an impaired expression and activity of the yeast cytochrome *bc<sub>1</sub>* complex, and the *hem25Δ* isolated mitochondria had a significant reduction of state 3 and state 4 oxygen consumption, compared with wild-type. However, the defects were rescued when the mutant was complemented with the yeast or human missing gene.

Taken together, these results highlight that Hem25p is the main mitochondrial *carrier* involved in heme synthesis and suggest that Hem25p plays an important role in cell life and respiratory growth. Human GlyC is able to transport glycine and complement defects caused by the absence of Hem25p, and this demonstrates that human SLC25A38 has the same function of HEM25 in yeast. These conclusions provide novel insights into the biochemical characterization and molecular mechanisms involved in mitochondrial glycine transport and may offer new avenues to develop innovative therapies for SLC25A38-related disorders. A schematic view of the supposed mechanism for GlyC involvement into heme biosynthesis is shown in Fig. 3.12.

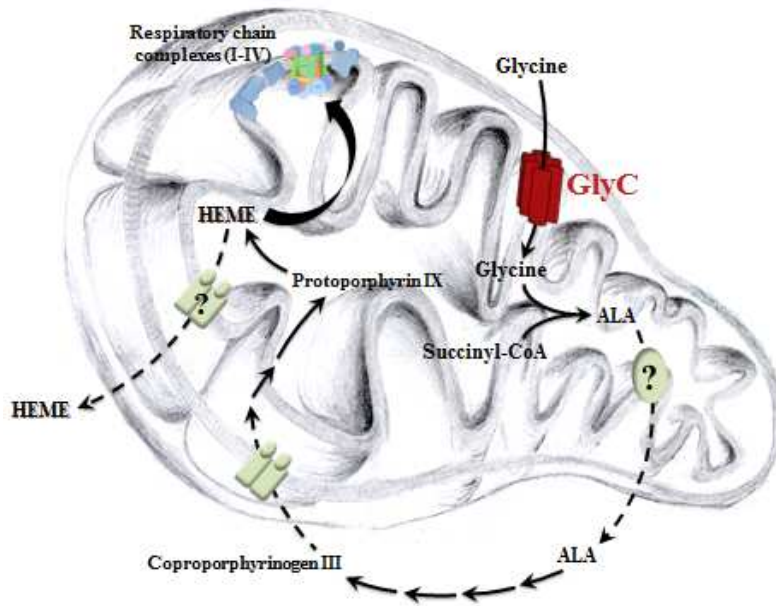


**Fig. 3.12** GlyC transport activity and heme biosynthesis in mitochondria



---

## 4. CHARACTERIZATION OF THE MITOCHONDRIAL DEPHOSPHOCOENZYME-A CARRIER

---

### 4.1 INTRODUCTION

#### **CoA carrier and associated diseases**

Coenzyme A is an essential cofactor for all organisms and holds a central position in a multitude of biochemical reactions. Therefore synthesis of CoA from pantothenic acid is present in both prokaryotes and eukaryotes. The synthesis CoA from pantothenic acid is a five steps pathway (Fig. 4.1) <sup>[92]</sup>.

In the first step, PanK catalyzes the phosphorylation of pantothenic acid to form phosphopantothenate. In the second step, the product from the first step binds to cysteine and the reaction is catalyzed by CoaB, 4'-phosphopantothenoylcysteine synthase. In the third step, the product undergoes decarboxylation reaction to form 4'-phosphopantetheine. This step is catalyzed by CoaC, 4'-phosphopantothenoylcysteine decarboxylase. During the step four, 4'-Phosphopantetheine was catalyzed by CoaD (Phosphopantetheine adenylyltransferase) to form dephospho-CoA. In the fifth and final step, dephospho-CoA is phosphorylated by CoaE (dephospho-CoA kinase) at the 3'-OH of the ribose to form CoA <sup>[93]</sup>.

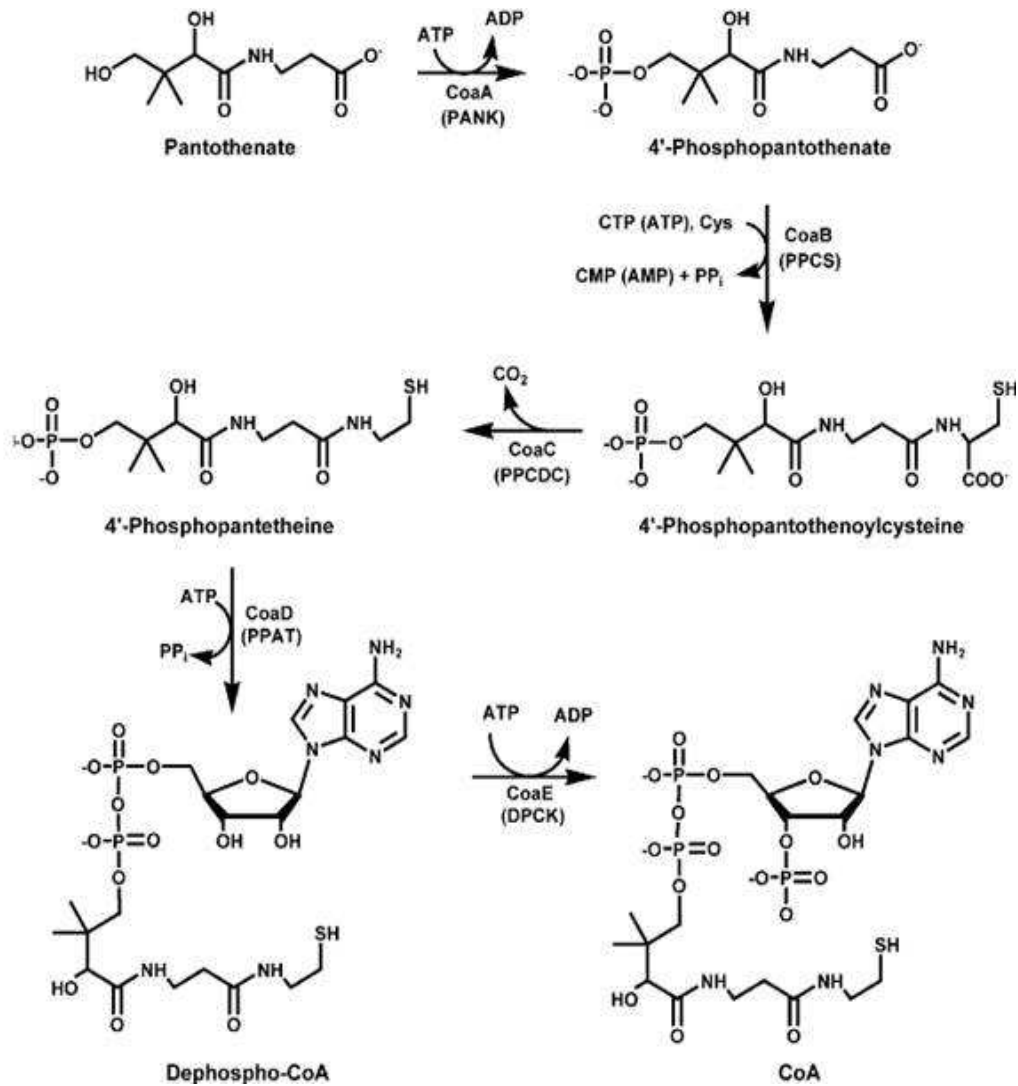


**Fig. 4.1** Biosynthetic pathway of Co-A <sup>[92]</sup>

Even though its biosynthetic pathway is well known, the subcellular localization of the eukaryotic biosynthetic enzymes is still under debate; furthermore, eukaryotic cells have a scarce cytosolic availability of CoA since most of it is sequestered in the mitochondrial and peroxisomal matrices <sup>[92]</sup>. The mechanism behind the cytosolic and mitochondrial CoA pools compartmentalization appear to be tightly regulated since it can modulate metabolic fluxes through CoA-dependent reactions <sup>[92]</sup>. This information led to the proposal of the existence of a CoA transport system.

In human, the transport of Coenzyme A (CoA) across the inner mitochondrial membrane has been attributed to two different genes, *SLC25A16* <sup>[94]</sup> and *SLC25A42* <sup>[95]</sup>.



The SLC25A42 gene, mapped on chromosome 19, codifies for a 418 amino acids long protein with two splicing variants, highly expressed in virtually all tissues, in most at higher levels than many other SLC25 family members. The protein resulted particularly highly expressed in adipose tissue. The next highest levels were detected in brain section VII, hypothalamus, and section IV <sup>[66]</sup>. The presence of mRNA for *Slc25a42* in all brain regions, including high levels in the hypothalamus and brainstem, possibly suggests an important basal physiological function <sup>[66]</sup>. SLC25A42 was proved to be a mitochondrial transporter for CoA and PAP (adenosine 3',5'-diphosphate). The evidences were provided directly overexpressing SLC25A42 in *Escherichia coli*, and reconstituting it in phospholipid vesicles, and the results showed a transport of CoA, dephospho-CoA, PAP, and (deoxy) adenine nucleotides <sup>[95]</sup>. The main function of SLC25A42 is been speculated to be the catalysis of the entry of CoA into the mitochondria in exchange for adenine nucleotides and PAP, since CoA synthesis was thought to take place outside the inner mitochondrial membrane <sup>[96]</sup>.

The SLC25A16, also called GDC (Graves' Disease *Carrier*), was isolated for the first time by screening a human thyroid expression library with antibody-rich sera from patients with Graves' disease, an autoimmune disease <sup>[97]</sup>. The gene was localized to chromosome 10, and subsequently mapped to 10q21.3-q21.1 <sup>[98]</sup>. Unfortunately, it was not possible to reconstitute this protein in a functional way, so there is lack of information on its actual transport activity. However, the SLC25A16, consisting of 348 amino acids, showed 35% identity with the yeast mitochondrial *carrier* protein Leu5, identified as a CoA transporter into the mitochondrial matrix <sup>[94]</sup>, a protein of *Saccharomyces cerevisiae* encoded by the gene *YHR002w* <sup>[99]</sup>. Subcellular localization and function of Leu5p were studied, and this protein was the first mitochondrial carrier suggested to be involved in the transport of CoA or one of its precursors across the inner mitochondrial membrane. Study on a yeast strain lacking of the *leu5* gene showed a defect in CoA transport or biosynthesis, since very low levels of CoA were found in the mitochondrial matrix. This caused also a severe growth defect on non-fermentative carbon sources <sup>[94]</sup>, which was rescued by the expression of the human genes SLC25A16 <sup>[94]</sup> and SLC25A42 <sup>[95]</sup>.

Presumed orthologues of both genes are present in many eukaryotic genomes, but not in that of *D. melanogaster*, which contains only one gene, CG4241, phylogenetically close to SLC25A42. CG4241 encodes a long isoform (dPCoAC1) and a short (dPCoAC2) of the dPCoA carrier, which arise from an alternative translational start site. The presence of only one mitochondrial transporter involved in the CoA transport in fruit fly, could help to better understand the CoA trafficking across the inner mitochondrial membrane. Recent published results on the mitochondrial matrix localization of the Coenzyme A Synthase (COASY) <sup>[100]</sup>.

In fact, studies revealed that a missense variant in the SLC25A42 gene cause a mitochondrial myopathy in humans <sup>[101]</sup>. Myopathies are heterogeneous disorders characterized clinically by weakness and hypotonia, and mitochondrial dysfunction is a frequent cause of myopathy. The impaired transport of CoA and its metabolites (the proposed substrates for this *carrier*) across the inner mitochondrial membrane is supposed to be the cause of those pathologies. Furthermore, the deficiency of enzymes involved in the CoA biosynthesis is associated with a neurodegenerative disease known as neurodegeneration with brain iron accumulation (NBIA) <sup>[100]</sup>. This because CoA is a necessary cofactor used by about 4% of all known enzymes and is involved in more than a hundred of biosynthetic and catabolic reactions <sup>[102]</sup>.

Shedding light on the molecular mechanism maintaining the CoA pools separated is crucial for a better understanding of CoA metabolism and its connection with numerous pathology.



## 4.2 RESULTS

### 4.2.1 Evolutionary analysis of human SLC25A42 homologs in eukaryotes

While analyzing different *carrier* proteins sequences, 65 homologous proteins of SLC25A42 were found in 14 model organisms of metazoans, yeasts and plants. The most similar sequences to SLC25A42 in human were SLC25A16 and three ATP-Mg/Pi carrier proteins, i.e. SLC25A23, SLC25A24 and SLC25A25<sup>[103]</sup>, whereas in yeast the most similar sequences were Leu5p<sup>[94]</sup> and Ypr011cp<sup>[104]</sup>. To clarify the evolutionary relationships among these human paralogs and all the other homologs in the analyzed species, we built a phylogenetic tree including all the collected protein sequences. A unique sequence cluster identifies a single SLC25A42 ortholog in all the metazoan species, including the *D. melanogaster* protein, here called dPCoAC-A, which was encoded by the gene CG4241 (arrow in Fig. 4.2). No lineage-specific gene duplication event was observed in the SLC25A42 cluster. The next closest group to SLC25A42 orthologs hosts SLC25A16 together with its orthologous proteins in some vertebrates and in the two yeast species, including the *S. cerevisiae* protein Leu5p. No SLC25A16 orthologs were present in insects and nematodes, according to the present analysis. The known CoA carriers in the two plants<sup>[105]</sup> were in the outer branch of both the SLC25A42 and SLC25A16 groups, and they further underwent a plant-specific duplication event. Regarding the ATP-Mg/Pi transporters (green branches in Fig. 4.2), we observed several duplication events independently in the plant, nematode and vertebrate lineages. The latter gave rise to the human paralogs SLC25A23, SLC25A24 and SLC25A25, while both yeasts and insects kept a single orthologous protein. According to the tree, other three independent clusters of plant and/or yeast sequences were detectable without a clear evolutionary relationship to CoA transporters and to ATP-Mg/Pi transporters (black branches in 4.2). One of those clusters hosted the *S. cerevisiae* Ypr011cp protein, i.e. the yeast mitochondrial transporter of APS and PAPS<sup>[104]</sup> together with a putative ortholog in plants, although this cluster is supported by only one of the two branch supporting methods.

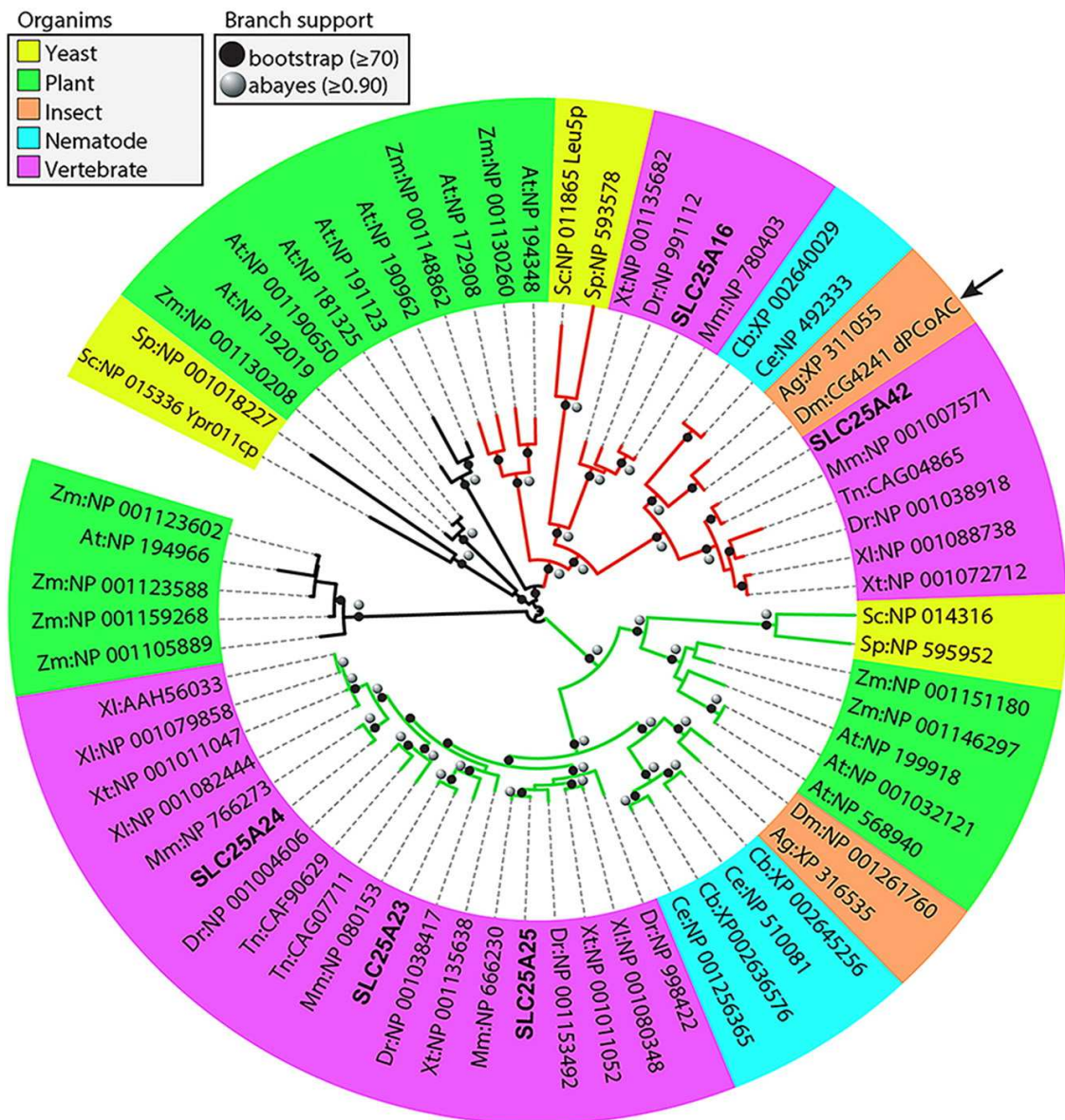


**Fig. 4.2 Evolutionary relationships among SLC25A42 homologs.**

Reported is a maximum likelihood tree obtained from 65 protein sequences collected by sequence similarity from the genome of 14 model species of eukaryotes. The tree leaf indicates the protein identifier following the species names, i.e. Sc: *S. cerevisiae*; Sp: *S. pombe*, At: *A. thaliana*, Zm: *Z. mais*, Ce: *C. elegans*, Cb: *C. briggsae*, Dm: *D. melanogaster*, Ag: *A. gambiae*, Dr.: *D. rerio*, Tn: *T. nigroviridis*, Xi: *X. laevis*, Xt: *X. tropicalis*, Mm: *M. musculus* and Hs: *H. sapiens*. Organisms from different lineages are also color-coded. The branch color indicates proteins clustering with SLC25A16 and SLC25A42 (red), with SLC25A23, SLC25A24, and SLC25A25 (green) and other clusters (black). Branch support symbols are indicated when support is greater than the cut-off value, i.e. aBayes likelihood  $\geq 0.90$  and/or bootstrap samplings  $\geq 70$ .



#### 4.2.2 Bacterial expression and functional characterization of dPCoAC-A and dPCoAC-B

CG4241 gene, also called “att” (alternative testis transcripts), was an alternatively spliced gene <sup>[106]</sup>, which gave rise to three tissue-specific transcripts, one somatic- and two testis-specific. The somatic form encoded for a 365 amino acids long protein, here called dPCoAC-A and one of the testis-specific forms encoded for a 290 amino acids long protein, here called dPCoAC-B which has never been confirmed in vivo, but only in reticulocyte lysates <sup>[106]</sup>. dPCoAC-A and dPCoAC-B protein sequences are identical, but the latter lacked the N-terminal portion till to the sixth amino acid of the first transmembrane helix according to the crystal structure of the bovine mitochondrial adenine nucleotide carrier <sup>[18]</sup>. The amino acid identity between dPCoAC-A (dPCoAC-B) and the human SLC25A42, SLC25A16 and the yeast LEU5 gene products were 47% (50%), 28% (28%) and 31% (30%), respectively. The dPCoAC-A and dPCoAC-B recombinant proteins were overexpressed in *E. coli* C0214 (DE3) strain. The proteins were accumulated as inclusion bodies and purified by centrifugation on a sucrose gradient and washed. The isolated proteins gave an almost pure single band by SDS-PAGE with apparent molecular masses of 40 and 32 kDa (Fig. 4.3A, lanes 7 and 9, respectively).

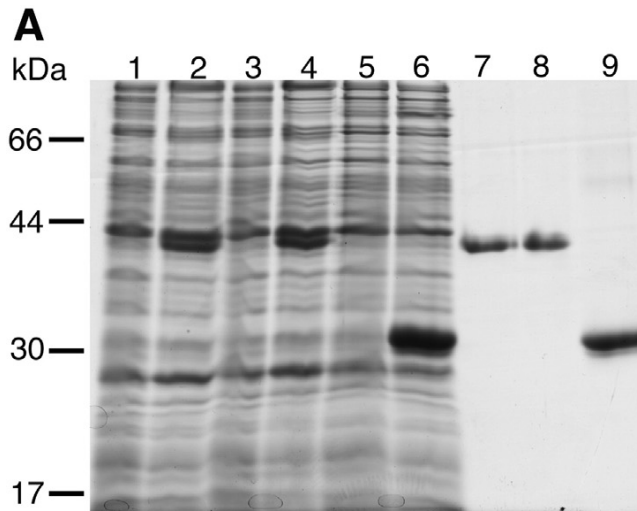


**Fig. 4.3A Overexpression in *E. coli* of recombinant dPCoACs and transport assays into proteoliposomes with dPCoAC-A**

Proteins were separated by SDS-PAGE and stained with Coomassie Blue dye. Markers in the left-hand column (bovine serum albumin, ovoalbumin, carbonic anhydrase and myoglobin); lanes 1–6, *E. coli* C0214(DE3) containing the expression vector with the coding sequence of dPCoAC-A (lanes 1 and 2), R103S dPCoAC-A mutant (lanes 3 and 4) and dPCoAC-B (lanes 5 and 6). Samples were taken at the time of induction (lanes 1, 3 and 5) and 5 h later (lanes 2, 4 and 6). The same number of bacteria was analyzed in each sample. Lanes 7–9, dPCoAC-A, R103S dPCoAC-A mutant, and dPCoAC-B purified from bacteria in lanes 2, 4 and 6, respectively.

Both recombinant proteins were reconstituted into liposomes and their substrate specificity for a variety of nucleotides was assayed in homo-exchange experiments (i.e. with the same substrate inside and outside the proteoliposomes). Using external and internal substrate concentrations of 1 and 10mM, respectively, dPCoAC-A catalyzed active [ $^{14}$ C] ADP/ADP, [ $^{14}$ C] AMP/AMP, and [ $^{14}$ C]ATP/ATP exchange reactions (Fig. 4.3B) that were inhibited completely by pyridoxal-5'-phosphate and bathophenanthroline. By contrast, despite the long incubation period (i.e. 30 min), virtually no homo-exchange activity was observed using GTP, CTP, TTP and UTP and NAD $^{+}$  (Fig. 4.3B). No [ $^{14}$ C]ADP/ADP and [ $^{14}$ C]AMP/AMP exchange activities were detected with boiled, unfolded reconstituted dPCoAC-A or with proteoliposomes reconstituted with sarkosyl-solubilized material from bacterial cells either lacking the expression vector for dPCoAC A or harvested immediately before the induction of



expression (data not shown). It should be noted that differently from dPCoAC-A, the recombinant and reconstituted dPCoAC-B showed no transport activity under any of the experimental conditions tested, by varying many parameters that could influence the solubilization of the inclusion bodies and the reconstitution of the protein into liposomes. The lack of any transport activity with dPCoAC-B, was most probably due to the reconstitution of a misfolded recombinant protein, a situation similar to that encountered with the human recombinant SLC25A16 gene product (Vozza, Paradies and Fiermonte, unpublished data) and many other recombinant carriers <sup>[21, 103]</sup>. For this reason, all further experiments into liposomes were carried out only on the recombinant dPCoAC-A. The substrate specificity of dPCoAC-A was determined by measuring the uptake of [<sup>14</sup>C] ADP into proteoliposomes preloaded with a variety of potential substrates (Fig. 4.3C). The highest [<sup>14</sup>C] ADP uptake into proteoliposomes was found with internal dPCoA, ADP, dADP, AMP and dAMP (Fig. 4.3C). To a lesser extent [<sup>14</sup>C] ADP was also exchanged with internal ATP, dATP, PAP, PAPS, AP4 and pyrophosphate. In contrast, the uptake of [<sup>14</sup>C]ADP was negligible in absence of internal substrate (NaCl present) or in the presence of internal CoA, acetyl-CoA, malonyl-CoA and pantothenate (Fig. 4.3C) and not shown APS, sulfate, NAD<sup>+</sup>, NADP<sup>+</sup>, FAD, ThMP, ThPP, cAMP, 3'-AMP, adenosine, adenine, phosphate, CDP, TDP, UDP and GDP. This sharp peculiarity of effective dPCoA transport but not CoA, that characterized dPCoAC-A with respect to the human SLC25A42 <sup>[95]</sup>, was further investigated by competitive inhibition experiments.

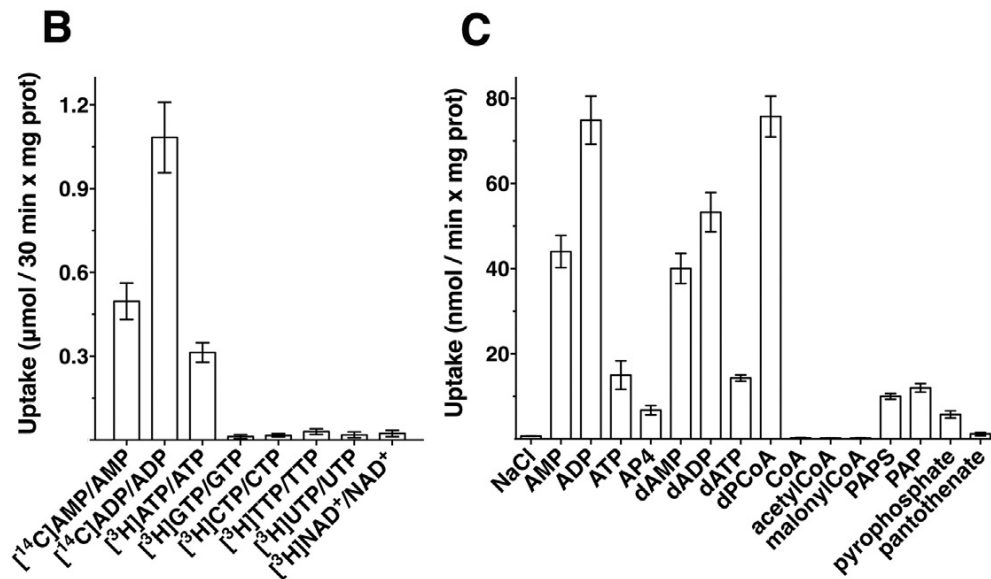


**Fig. 4.3B Nucleotide homo-exchanges.**

Transport was initiated by adding 1 mM of radioactive substrate to dPCoAC-A-reconstituted proteoliposomes preloaded internally with 10 mM of the same substrate. The reaction was terminated after 30 min.

**Fig. 4.3C Substrate specificity of dPCoA-A.**

Proteoliposomes were preloaded internally with various substrates (concentration, 10 mM).

Transport was started by the addition of 140  $\mu\text{M}$  [ $^{14}\text{C}$ ] ADP and terminated after 2 min.

Values are means  $\pm$  S.D. from at least four independent experiments.

The effects of inhibitors of other mitochondrial carriers on the [ $^{14}\text{C}$ ] ADP/ADP exchange reaction catalyzed by the reconstituted dPCoAC-A were also examined (Fig. 4.4A). The reaction catalyzed by the reconstituted dPCoAC-A was completely inhibited by pyridoxal-5'-phosphate, bathophenanthroline, tannic acid, and bromocresol purple (effective inhibitors of several mitochondrial carriers) and only partially by  $\alpha$ -cyano-4-hydroxycinnamate, butylmalonate, phenylsuccinate and 1,2,3-benzenetricarboxylate (Fig. 4.4A). In contrast, little effect was observed with thiol-blocking reagents as N-ethylmaleimide, mersalyl and p-hydroxymercuribenzoate in agreement with the absence of cysteine residues in the amino acid sequence of dPCoAC-A. Interestingly, dPCoAC-A showed a different sensitivity towards bongkrekic acid and carboxyatractyloside, two very powerful inhibitors of the mitochondrial ADP/ATP carrier<sup>[18, 107]</sup>, being inhibited significantly (61%) by the former and weakly (3%) by the latter. In addition, the [ $^{14}\text{C}$ ] ADP/ADP exchange reaction was strongly inhibited by



externally-added substrates such as dPCoA, CoA, AMP and dADP, to a lesser extent by ATP, dAMP, dATP, PAP, APS and PAPS, and only slightly by AP4, and PPi (Fig. 4.4B).

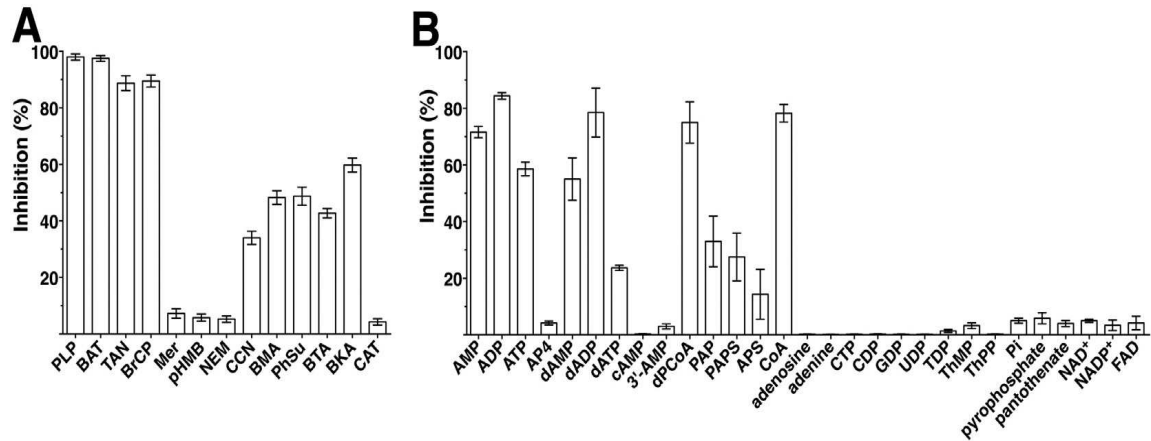


**Fig. 4.4 Inhibition of [<sup>14</sup>C]ADP uptake by inhibitors and substrates externally added to proteoliposomes reconstituted with dPCoAC-A.**

Inhibitors (A) and unlabeled substrates (B) were added to proteoliposomes preloaded internally with 10 mM ADP, transport was initiated by adding 140  $\mu$ M [<sup>14</sup>C]ADP and stopped after 2 min. Thiol reagents and CCN were added 2 min before the labeled substrate.

The final concentrations of the inhibitors were 10  $\mu$ M (CAT and BKA), 20 mM (PLP and BAT), 0.2 mM (pHMB and MER), 1 mM (NEM and CCN), 2 mM (BMA, PhSu and BTA), 0.1% (TAN), and 0.1 mM (BrCP). External substrates (1.4 mM) were added together with [<sup>14</sup>C]ADP. The values are expressed as a percentage of the [14C]ADP/ADP exchange activity, which was 86 (A) and 81.5 (B) nmol/min  $\times$  mg of protein. Values are means  $\pm$  S.D. from at least four independent experiments.

### 4.2.3. Kinetic characteristics of the recombinant dPCoAC-A

The uptake of 1 mM [<sup>14</sup>C] ADP into proteoliposomes was measured both as uniport (in the absence of internal substrate) or as exchange (in the presence of internal 10 mM ADP) (Fig. 4.5A). The uptake of [<sup>14</sup>C] ADP followed a first-order kinetics (rate constant 0.126 min<sup>-1</sup>; initial rate 0.136  $\mu$ mol/min  $\times$  mg protein) with isotopic equilibrium being approached exponentially (Fig. 4.5A). By contrast, no [<sup>14</sup>C] ADP uptake was observed without an internal substrate, indicating that dPCoAC-A does not catalyze the uniport of ADP, but only the exchange reaction. The uniport mode of transport was further investigated by measuring the efflux of [<sup>14</sup>C] ADP from prelabeled active proteoliposomes because it provides a more convenient assay for detecting an unidirectional transport<sup>[34]</sup>. In the absence of external substrate (10 mM of NaCl), no

efflux was observed after an incubation time of 30 min (Fig. 4.5B, ○), whereas extensive effluxes occurred upon the addition of external ADP or dPCoA (Fig. 4.5B, ▼ and ●, respectively); as expected no efflux of internal labeled substrate was observed upon the addition of external CoA (Fig. 4.5B, ▽), acetyl-CoA and malonyl-CoA (not shown). These results demonstrated that the reconstituted dPCoAC-A catalyzed an obligatory exchange reaction of substrates. The kinetic constants of the recombinant purified dPCoACA were determined by measuring the initial transport rate at various external [<sup>14</sup>C]ADP concentrations in the presence of a constant saturating internal concentration of ADP (10mM). The Km and Vmax values (measured at 25 °C) were  $140 \pm 11 \mu\text{M}$  and  $158 \pm 12 \text{ nmol/min} \times \text{mg protein}$ , respectively (means of 30 experiments). The transport activity was measured by taking into account the amount of dPCoAC-A recovered from proteoliposomes after reconstitution.



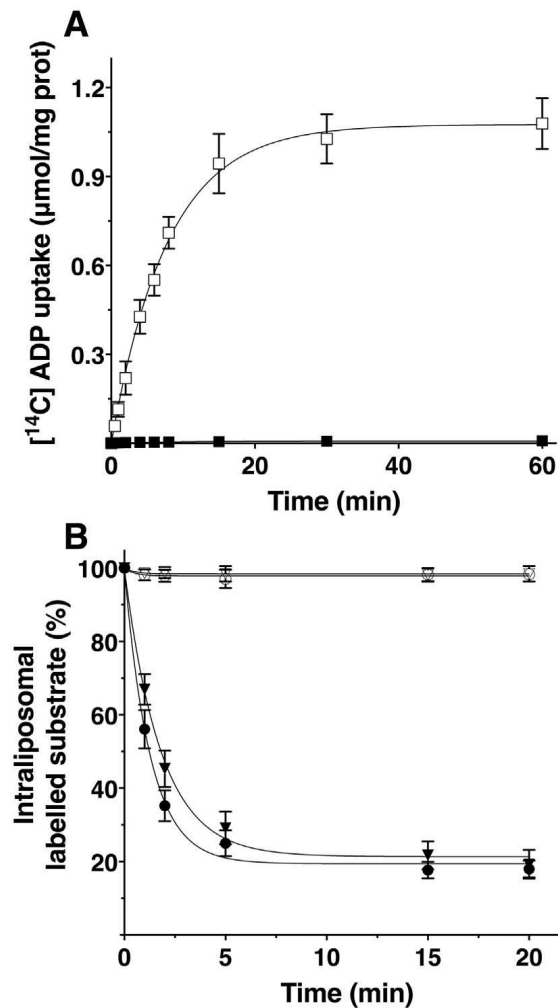


**Fig. 4.5 Kinetics of [14C]ADP transport.**

(A) Uptake of [ $^{14}\text{C}$ ]ADP in proteoliposomes reconstituted with dPCoAC-A. [ $^{14}\text{C}$ ]ADP (1 mM) was added to proteoliposomes containing ADP (10 mM) (exchange,  $\square$ ) or NaCl (10 mM) and no substrate (uniport,  $\blacksquare$ ). Similar results were obtained in three independent experiments. (B) Efflux of [ $^{14}\text{C}$ ]ADP (2 mM) from proteoliposomes reconstituted with dPCoAC-A. The internal substrate pool was labeled with 5  $\mu\text{M}$  [ $^{14}\text{C}$ ]ADP by carrier-mediated exchange equilibration. Then the proteoliposomes were passed through Sephadex G-75. [ $^{14}\text{C}$ ]ADP efflux was initiated by adding 10 mM of NaCl ( $\circ$ ), ADP ( $\blacktriangledown$ ), dPCoA ( $\bullet$ ), or CoA ( $\nabla$ ). Values are means  $\pm$  S.D. from at least three independent experiments.

Several external substrates acted as competitive inhibitors of [ $^{14}\text{C}$ ]ADP uptake (Table 4.1) since they increased the apparent  $K_m$  without changing the  $V_{max}$  (data not shown). These results showed that the dPCoAC-A affinity for dPCoA was higher than that for ADP, dADP, AMP, ATP, CoA, PAP and PAPS. Furthermore, the  $K_i$  value of dPCoA was N40-fold lower than that of CoA (Table 4.1).

| Competitive inhibition by various substrates of<br>[ <sup>14</sup> C]ADP uptake in proteoliposomes containing dPCoAC-A. |           |
|-------------------------------------------------------------------------------------------------------------------------|-----------|
| Substrate                                                                                                               | Ki (μM)   |
| dPCoA                                                                                                                   | 3.3 ± 0.2 |
| CoA                                                                                                                     | 137 ± 12  |
| dADP                                                                                                                    | 186 ± 15  |
| PAP                                                                                                                     | 820 ± 49  |
| PAPS                                                                                                                    | >1000     |
| AMP                                                                                                                     | >1000     |
| ATP                                                                                                                     | >3000     |

**Table 4.1** The values were calculated from Lineweaver–Burk plots of the rate of [<sup>14</sup>C] ADP uptake versus substrate concentrations. The competing substrates at appropriate constant concentrations were added together with 0.005–1.25 mM [<sup>14</sup>C]ADP to proteoliposomes containing 10mMADP. The data represent the mean ± S.D. of at least five independent experiments.

#### 4.2.4. Phenotype complementation of yeast LEU5 null strain by dPCoACs

The yeast LEU5 null mutant did not grow on respiratory carbon sources and showed a mitochondrial CoA deficiency <sup>[94]</sup>. This phenotype was explained by the ability of Leu5p to transport CoA or one of its precursors through the inner mitochondrial membrane. Thus, we checked if the expression of a mitochondrial carrier protein that recognized dPCoA as a substrate could mitigate or abolish the growth defect of the leu5Δ yeast strain. The dPCoAC-A and, to a lesser extent, dPCoAC-B expressed in leu5Δ cells via the yeast vector pYES2 restored the growth of the leu5Δ strain on glycerol, lactate and acetate (Fig. 4.6A), by contrast, when leu5Δ cells were transformed with the empty vector, no growth restoration was observed (Fig. 4.6A). The positive effect of dPCoAC on the mitochondrial CoA metabolism of the Leu5p deficient yeast strain was further confirmed by the meaningful levels of CoA found in the mitochondria (Fig. 4.6B). These results clearly indicated that the transport of dPCoA was sufficient to restore the mitochondrial CoA metabolism of the yeast leu5Δ strain.

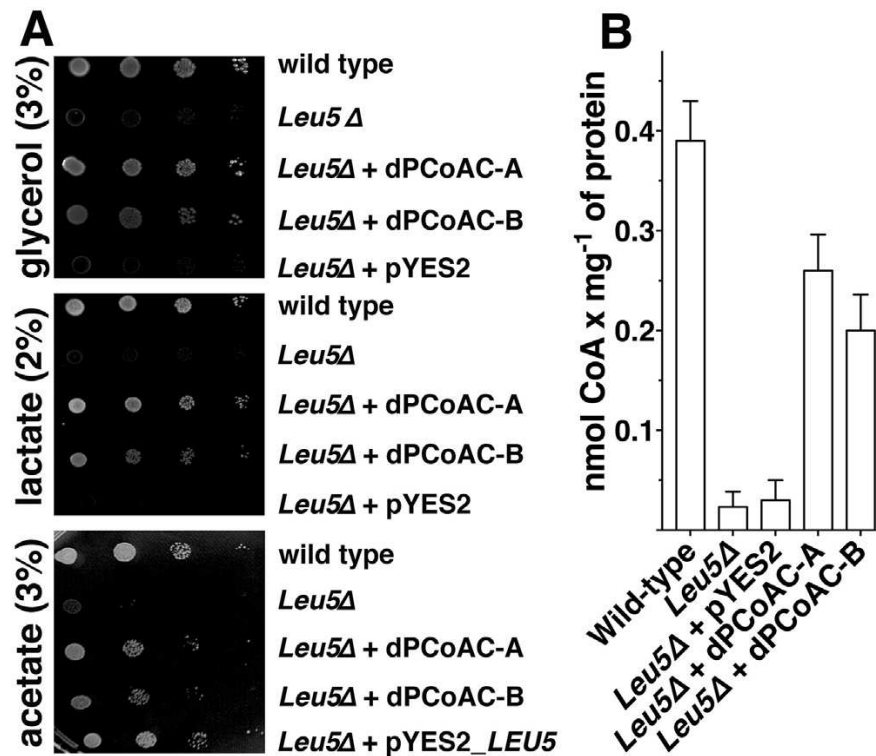


**Fig. 4.6 Effects of dPCoAC-A and dPCoAC-B expression in the *leu5Δ* yeast strain.**  
 (A) Complementation of the growth defect of *leu5Δ* cells by dPCoAC-A and dPCoAC-B. Fourfold serial dilutions of wild-type, *leu5Δ* and *leu5Δ* cells transformed with different pYES2 constructs were plated for 72 h at 30 °C on YP medium supplemented with 0.1% galactose and different non-fermentable carbon sources.  
 (B) Effects of dPCoAC-A and dPCoAC-B expression on the mitochondrial CoA contents of *leu5Δ* yeast cells. Mitochondria were isolated from the wild-type and transformed yeast strains shown in (A), grown in the presence of 3% glycerol. Mitochondrial CoA levels were determined by mass spectrometry. Values are means  $\pm$  S.D. from at least three independent experiments.

#### 4.2.5. Dissection of the transport features of dPCoAC through structural analysis

Comparative multiple sequence analysis and molecular modelling studies have been performed by comparing dPCoACs with the human SLC25A42, SLC25A16, Leu5p and bovine AAC1 proteins (Figs. 4.7 and 4.8A-D). It has been recently shown that mitochondrial carrier (MC) subfamilies can be defined by specific amino acid triplets resulting from MC inter-repeat MSAs<sup>[108]</sup>. The calculation of the inter-repeat MSA



makes sequence comparison faster and consequently allows to predict MC function more rapidly, provided that an homologous protein of the investigated carrier has been experimentally characterized. Therefore in order to determine the dPCoACs characterizing triplets, we calculated the inter-repeat sequence alignment of dPCoACs and BtAAC1 and compared the aligned triplet residues (Fig. 4.7) with those proposed for the human mitochondrial CoA/PAP carrier subfamily<sup>[108]</sup>. The set of characterizing triplets in this subfamily, i.e. “23 (K[A/V]Q), 34 (I[A/V]R), 88 ([K/Q]SS)”<sup>[108]</sup>, that arise from comparison of the functionally characterized human SLC25A42<sup>[95]</sup> and the yeast Leu5p<sup>[94]</sup>, is highly conserved<sup>[108]</sup> in the dPCoACs. The only exception is triplet 23 that is constituted of amino acids “KQQ” in dPCoACs instead of residues “KAQ” and “KVQ” detected in human SLC25A42 and yeast Leu5p, respectively. In order to highlight the role of the observed differences in amino acid sequence composition, 3D comparative models of dPCoAC-A and SLC25A42 (Fig. 4.8) were built by using Modeller. In the 3D comparative model of dPCoAC-A and SLC25A42 it was found that residues of the substrate binding area<sup>[61]</sup> overlapped with the carboxyatractyloside binding site detected in the crystallized BtAAC1<sup>[18]</sup>. This region extended between proline–glycine (PG) level 1 and PG level 2, a known MC region deeply involved in conformational changes occurring during substrate translocation<sup>[60]</sup>. It should be noticed that this region contained the characteristic dipeptide GV (G234-V235, second contact point at triplets 80–81<sup>[109]</sup>) shared by most of nucleotide and dinucleotide MCs<sup>[60, 109]</sup>. By comparing other residues of the substrate binding area and the matrix gate (m-gate) area, it was observed the presence of an arginine-rich region at the level of triplets 39–41 (R103, R201 and R296). Notably, among those arginine residues, R103 (triplet 39, also conserved in the other sampled drosophilidae, data not shown) was the only one that protruded towards the carrier cavity just below the m-gate (Fig. 4.8). Since R103 is not conserved in the human SLC25A42 (and other mammalian), SLC25A16 and Leu5p (Fig. 4.7), it could be involved in specific conformational changes that stabilize dPCoAC c-conformation in presence of CoA, preventing CoA translocation through dPCoAC. To verify this hypothesis, we replaced R103 within dPCoAC-A with a serine, since in the human SLC25A42 and the yeast Leu5p we observed a serine residue in correspondence of the arginine 103 of dPCoAC-A (Figs. 4.7, 4.8C and D). With this aim the R103S dPCoAC-A mutant was constructed, expressed in *E. coli* and reconstituted into liposomes. Interestingly, the R103S dPCoAC-A mutant catalyzed a

significant CoA/ADP transport exchange activity (Fig. 4.8E), which was absent in the wild-type protein.

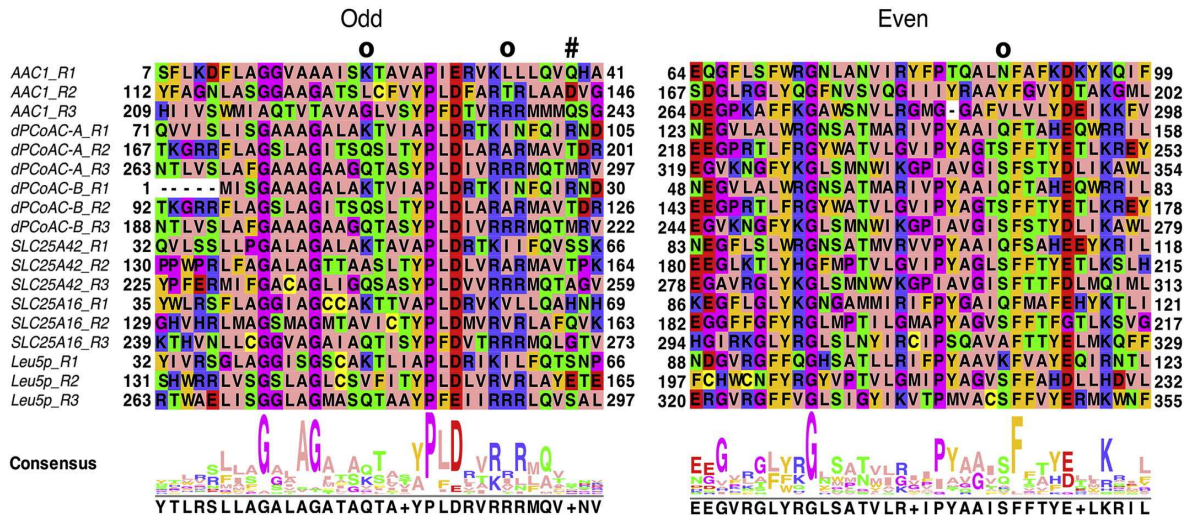


**Fig. 4.7 Inter-repeat sequence analysis of fruit fly dPCoAC.**

Multiple sequence alignment of the three repeats (R1–3) of *D. melanogaster* (dPCoAC-A and dPCoAC-B), human (SLC25A42 and SLC25A16) and yeast (Leu5p) carriers involved in the CoA metabolism and the bovine ADP/ATP carrier (BtAAC1). For each carrier and each repeat (R1, R2, R3) only the odd transmembrane helices (H1, H3, H5) and the even transmembrane helices (H2, H4, H6) preceded by 10 amino acids are shown. Amino acids are colored according to the default JalviewZappo style (<http://www.jalview.org/>). A consensus sequence is reported on the bottom of the figure where the sequence motif of the mitochondrial carrier family PX[D/E]XX[K/R], EGXXXXAr[R/K]G is recognizable. Circles “ ” indicate the positions of the characterizing amino acid triplets of the mitochondrial carrier CoA subfamily, e.g. the first “ ” indicates vertical triplet 23 (KLG in BtAAC1 and KQQ in dPCoAC-A and dPCoAC-B, respectively); hash “#” indicates the position of vertical triplet 39 (e.g., QDQ in BtAAC1, RTM in dPCoAC-A and dPCoAC-B, STA in SLC25A42; HQG in SLC25A16 and SES in ScLeu5p).

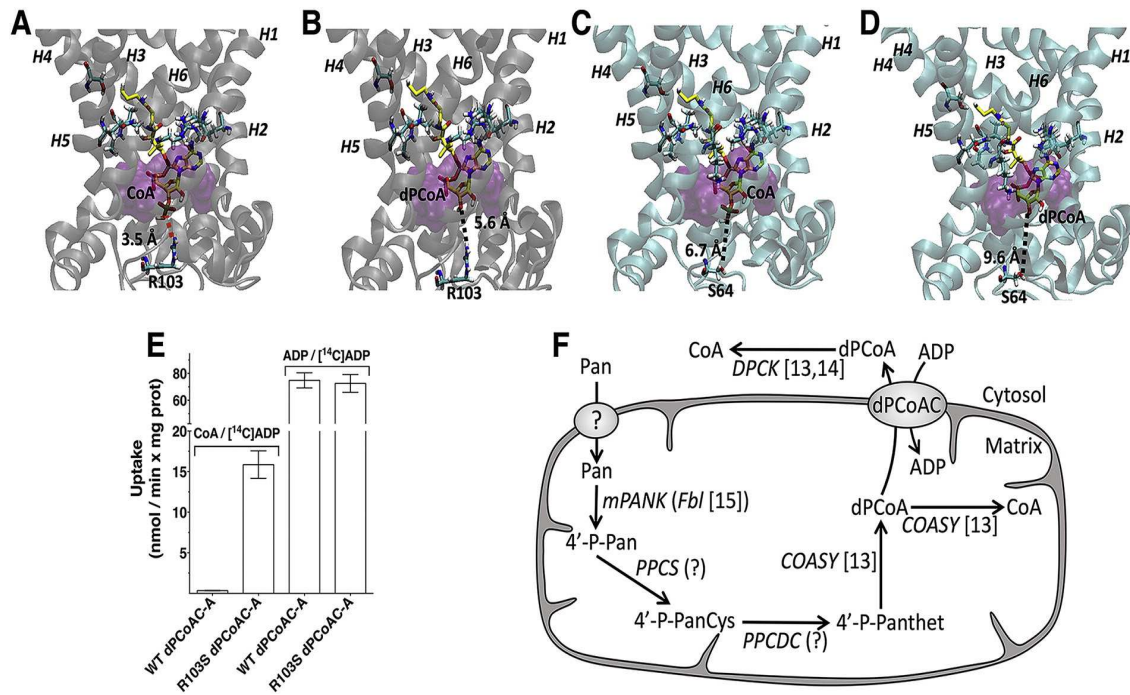


**Fig. 4.8 Structural analysis and suggested physiological role of dPCoAC.**

A–D, side view of the structural comparative models of dPCoAC (A and B) and human SLC25A42 (C and D) highlighting the substrate binding sites in presence of CoA (A and C) and dPCoA (B and D). The 3D models show the transmembrane H1–H6 six-helix bundle in grey cartoon (dPCoAC) or cyan cartoon (SLC25A42) representations. The bottom part of H1 (residues 90–120 in fruit fly and 50–80 in human) is transparent for allowing the carrier cavity inspection. Hydrophilic residues within 4 Å from CoA or dPCoA in SLC25A42 (K48, R99, S204, Q241, K294, R252) and in dPCoAC (K87, R139, Q183, S242, Q279, R290) are shown in cyan sticks. The distances between the R103 or S64 and dPCoA or CoA are shown for comparative purposes. The putative ionic interaction between the 3'-phosphate group of the CoA and the side chain of R103 is reported with a red dashed line. Residues of the matrix gate of the dPCoAC (D94 K97 D190 R193 D286 R289) and SLC25A42 (D55 K58 D153 R156 D248 R251) are reported in transparent pink representation. (E) ADP/[14C]ADP and CoA/[14C]ADP exchange reactions catalyzed by the recombinant wild-type and R103S mutant dPCoAC-A. Proteoliposomes were preloaded internally with 10 mM of unlabeled substrates. Transport was started by the addition of 140 μM [14C]ADP and terminated after 2 min. Values are means ± S.D. from at least four independent experiments. (F) Proposed physiological role of dPCoAC in *D. melanogaster*. (?) denote the enzymes of the CoA biosynthetic pathway with an unknown subcellular localization.



### 4.3 DISCUSSION

CoA is an essential cofactor used by about 4% of all known enzymes and is involved in more than a hundred of biosynthetic and catabolic reactions. The biosynthesis of CoA from pantothenate is conserved amongst species and occurs by the subsequent action of five enzymes.

The final two steps of the pathway are catalyzed by the COASY, a bifunctional enzyme which catalyzes the reversible adenylation of 4'-phosphopantetheine to dPCoA, by its phosphopantetheine adenylyltransferase activity (PPAT), and the final 3'-phosphorylation of dPCoA to CoA, by its kinase activity (DPCK). Although COASY has been recently localized into the matrix of mammalian mitochondria <sup>[100,110]</sup>, the existence of a cytosolic monofunctional DPCK activity has been also demonstrated <sup>[111, 112]</sup>. The proposed enzyme compartmentalization suggested that the dPCoA, at least in mammals, can be synthesized only in the matrix by the PPAT activity of COASY and then converted to CoA both in the matrix by the COASY itself, by its DPCK activity, and in the cytosol by the monofunctional DPCK.

In the latter case, a carrier would be required to transport dPCoA from the matrix to the cytosol.

The human SLC25A42 gene, the only functionally characterized mitochondrial transporter able to transport dPCoA and CoA in a reconstituted lipid system <sup>[95]</sup>, could be responsible of such a transport, but the different phenotype found in patients affected by SLC25A42 deficiency <sup>[101]</sup> compared to that found in the deficiency of other enzymes involved in the CoA metabolism (NBIA) <sup>[100, 113]</sup>, together with the fact that SLC25A42 showed a transport activity and a substrate affinity for dPCoA and CoA slightly lower than those for PAP and ADP <sup>[95]</sup>, suggested the possible presence of another mitochondrial dPCoA transporter.

A possible candidate could be SLC25A16, the second human gene able to complement the growth defect of the yeast *leu5Δ* strain <sup>[94]</sup>. Unfortunately, we failed to reconstitute this recombinant carrier in an active form into liposomes. Thus the organization and compartmentalization of mitochondrial and cytosolic CoA pools in human cells <sup>[92]</sup> remained an open question.

Phylogenetic analysis of all the complete eukaryotic genomes revealed that fruit fly, differently from many metazoan species, had the SLC25A42 ortholog, the gene CG4241, but lacked that of SLC25A16. The functions of SLC25A42 and CG4241 only partially overlapped, suggesting that the two human paralogs, SLC25A42 and SLC26A16, have undergone subfunctionalization or neofunctionalization following the duplication event. In fact, although both recombinant dPCoAC A and SLC25A42 efficiently transported mono- and di-phosphate adenine nucleotides, they showed important differences in their substrate specificity<sup>[95]</sup> (Fig. 4.3C), particularly in their ability to transport CoA and dPCoA: the human carrier transported both molecules at a rate lower than that of ADP, but still significant<sup>[95]</sup>, while the fruit fly ortholog efficiently transported dPCoA (Fig. 4.3C), showing for this metabolite the highest substrate affinity (Table 4.1) but did not transport at all CoA (Figs. 4.3C and 4.5B). Thereby the fruit fly carrier was here called dephosphocoenzyme A carrier (dPCoAC).

The human and fruit fly carriers also profoundly differed for their specificity towards PAP, which was well transported by SLC25A42<sup>[95]</sup>, but only poorly translocated by dPCoAC-A (Fig. 4.3C). The substrate specificity showed by dPCoAC-A suggested that the fruit fly carrier could be strictly involved in the CoA metabolism and not in that of PAP as previously suggested for the human carrier<sup>[95]</sup>. This last observation was also supported by the inhibitory effects produced by the externally added unlabeled substrates on the [<sup>14</sup>C]ADP/ADP exchange reaction catalyzed by the reconstituted dPCoAC-A (Fig. 4.4B). In fact, while PAP poorly affected the exchange reaction catalyzed by dPCoAC-A, CoA although not transported (Figs. 4.3C and 4.4B), powerfully and competitively inhibited the exchange reaction catalyzed by dPCoAC-A (Fig. 4.4B), which showed for this molecule the third highest affinity among all tested substrates (Table 4.1).

A structural modelling analysis revealed that, although in the substrate binding area, dPCoAC-A and SLC25A42 contained similar residues (Fig. 4.8A–D)<sup>[108]</sup>, important differences in amino acid composition were observed at residues of the m-gate area<sup>[61]</sup> deeply involved in interactions with the transported substrate and in conformational changes along substrate translocation<sup>[108]</sup>. It was previously observed that residues of the m-gate area may be able to bind the substrate during translocation just before reaching the transition state and the following opening of the carrier on the matrix side<sup>[61]</sup>.

The different substrate specificity shown by dPCoAC-A and SLC25A42<sup>[95]</sup>, and the putative role played by charged residues of the m-gate area, were investigated by in silico docking experiments using CoA and dPCoA as ligands. A gridbox involving residues of the substrate binding area and the m-gate area<sup>[61, 109]</sup> was built to investigate the binding of CoA or dPCoA at this region. Autodock showed that dPCoAC-A and SLC25A42 bound CoA and dPCoA in a very similar way (Fig. 4.8A–D). Beyond the residues of the proposed binding region, CoA and dPCoA formed with dPCoACA and SLC25A42 further ionic interactions with basic residues of triplets 33 (K97 and R289 in dPCoAC-A; K58 and R251 in SLC25A42) and 34 (R290 in dPCoAC-A and R252 in SLC25A42) that participated in the m-gate stabilization<sup>[61]</sup>. A further ionic interaction was observed between the phosphate group of the CoA (but not dPCoA) ribose ring and R103 (a residue of triplet 39) of dPCoAC-A. This ionic interaction is absent in SLC25A42 as the R103 in dPCoAC-A is replaced by a serine (S64). The ionic interactions established by this arginine residue (R103, triplet 39 “RTM”) and the 3'-phosphate group of CoA could stabilize the conformation closed towards the matrix, preventing CoA translocation.

This hypothesis was also supported by the finding that all ligands carrying a 3'-phosphate group on the ribose ring, structurally related to the CoA (in particular, PAP) and transported by the human SLC25A42, were poorly transported by dPCoAC-A and acted as competitive inhibitors of the [<sup>14</sup>C]ADP/ADP exchange reaction catalyzed by dPCoAC-A. Thus, the first residue of triplet 39 (R103 within dPCoAC-A and S64 within SLC25A42) could play a key role in closing the c-conformation on the matrix face in presence of ligands structurally related to CoA and carrying a 3' phosphate on the ribose ring. In order to verify this hypothesis, we mutated R103 into serine and we observed that the mutant R103S was able to translocate CoA, at variance with the dPCoAC-A wild type (Fig. 4.8E). Also other residues, beyond R103 may be responsible for CoA specificity and translocation. R103 may play a key role in the substrate uptake/release in the mitochondrial matrix, reflecting a species-specific physiological role played by dPCoAC in fruit fly.

The transport activity of dPCoAC found into proteoliposomes was further confirmed in a yeast cell model. dPCoAC-A and dPCoAC-B were both able to complement the growth defect on non-fermentable carbon sources, of the yeast *leu5Δ* strain (Fig. 4.7). These results demonstrated that the mitochondrial matrix CoA deficiency induced by



the deletion of the yeast LEU5 gene<sup>[94]</sup> could be rescued by a mitochondrial transporter (dPCoAC) able to transport only dPCoA and not CoA, suggesting that Leu5p could also be the yeast dPCoAC. In fact, Prohl et al. were unable to find a CoA transport activity using isolated yeast mitochondria<sup>[94]</sup>. They explained this result by the presence of a CoA hydrolase, outside the mitochondria, that could rapidly metabolize the radiolabeled CoA, but it may be speculated that Leu5p can translocate dPCoA instead of CoA.

In conclusion, it was here reported the functional characterization of the *D. melanogaster* mitochondrial dephosphocoenzyme A carrier. It is the first eukaryotic mitochondrial transporter which shows a very narrow substrate specificity essentially towards dPCoA and ADP. Although the localization of *D. melanogaster* enzymes involved in the CoA biosynthetic pathway is poorly known, in humans, an isoform of the pantothenate kinase (fbl) and the COASY have been localized to mitochondria, and the existence of a cytosolic mono-functional DPCK has been suggested<sup>[111, 112, 114]</sup>. The data showed in this study, together with the ones in literature, suggests a possible physiological role of dPCoAC in the fruit fly CoA metabolism and compartmentalization, which has been reported in Fig. 4.8F. The first and last two steps of CoA biosynthesis may take place in the mitochondrial matrix, dPCoA, produced by the phosphopantetheine adenylyltransferase activity of COASY, is transported to the cytosol by dPCoAC in exchange for ADP. Once in the cytosol, the monofunctional DPCK transforms dPCoA to CoA. It should be noted that CoA competitively inhibits the dPCoAC, with a  $K_i$  of 137  $\mu\text{M}$ , a concentration of CoA similar to that found in the cytosol 20–140  $\mu\text{M}$ <sup>[92]</sup>. Thus, CoA itself may control its cytosolic concentration by inhibiting the dPCoAC from the cytosolic side.

Thus, when the matrix concentration of CoA is more than two-fold of magnitude higher than that of the cytosol and the two CoA pools must be kept separate and adequately constant<sup>[92]</sup>, a mitochondrial transporter, like dPCoAC, fits perfectly to connect the cytosolic and mitochondrial parts of the CoA biosynthetic pathway, without getting the two CoA pools in touch.

The functional characterization of the CG4241 gene reported here could help to better use *D. melanogaster* as model organism for the study of a human disease associated to CoA deficiency, called pantothenate kinase-associated neurodegeneration<sup>[114, 115]</sup>.

---

## 5. STRUCTURAL REARRANGEMENTS FOR SUBSTRATE TRANSLOCATION IN THE MITOCHONDRIAL OXOGLUTARATE CARRIER

---

### 5.1 INTRODUCTION

#### ***Oxoglutarate carrier***

The oxoglutarate carrier (OGC) is a nuclear encoded protein located in the inner mitochondrial membrane, where it catalyzes the electroneutral exchange of cytosolic malate for 2-oxoglutarate from the mitochondrial matrix <sup>[116, 117]</sup>.

This system plays an important role in some metabolic processes such as the gluconeogenesis from lactate, the nitrogen metabolism, the malate/aspartate and the 2-oxoglutarate/isocitrate shuttles.

This carrier is transported and inserted into the inner mitochondrial membrane through a specific protein complex, TIM 22. This complex uses the membrane potential  $\Delta\Psi$  created by the transport of electrons through the respiratory chain. The signal that directs OGC insertion is located at the level of its primary structure, in the third and last segment of the protein.

The OGC was first purified from mitochondria of bovine heart, swine heart and rat liver <sup>[117, 118]</sup> by chromatography on hydroxyapatite and celite columns, in the presence of cardiolipin.

The purified proteins displayed a molecular weight of 31.5 kDa (bovine and swine heart) and 32.5 kDa (rat liver). Functional studies, conducted both on intact mitochondria and proteoliposomes containing the protein <sup>[118]</sup>, showed that OGC catalyzes the 2-oxoglutarate/2-oxoglutarate and 2-oxoglutarate/malate exchange reactions, with a kinetic of pseudo-first order. This carrier has a high affinity for 2-oxoglutarate with a  $K_m$  of 65  $\mu$ M. For pH values comprised between 6 and 8, the transport is independent of pH, while it depends on temperature.

Kinetic studies showed a sequential transport mechanism, since the *carrier* simultaneously catalyzes the transport of a substrate molecule from the inside to the outside of the mitochondrion and of a second molecule in the opposite direction. During transport, it forms a ternary complex as described for other proteins belonging to the mitochondrial carrier family <sup>[4]</sup>, a group of transporters not only structurally related but also characterized by similar modes of operation.

The activity of this *carrier* is inhibited, both in the mitochondria and in proteoliposomes, in a specific and competitive manner, by the fialonic acid, the pyridoxal 5'-phosphate (PLP) and some specific reagents for sulfhydrylic groups, such as mersalyl and p-hydroxymercuribenzoate.

In bovine heart mitochondria the complete amino acid sequence of the OGC was deduced from the nucleotide sequence of the cDNA <sup>[119]</sup>. In human, bovine and rat, a single gene encodes the OGC. The human gene, SLC25A11, is located on chromosome 17p13.3. In bovine the gene consists of 6 exons and 5 introns, while in human are present 8 exons and 7 introns; the two proteins only differ from each other by 11 amino acids, located in the hydrophilic extra-membrane segment.

The human and bovine proteins are constituted by 314 amino acids. The sequences of the human and bovine mitochondrial 2-oxoglutarate carrier genes were determined from overlapping genomic clones generated by PCR. The coding and protein sequences of the human and bovine genes are 93% and 96.6% identical, respectively <sup>[119]</sup>.

The bovine protein shows an actual molecular weight of 34.172 kDa, and possesses the characteristic tripartite structure typical of all the mitochondrial family members <sup>[120]</sup>.

Based on its hydrophobic profile and immunochemical and enzymatic data, a secondary structural model was proposed, according to which OGC is organized into six highly hydrophobic segments forming transmembrane alpha-helices (Fig. 5.1).



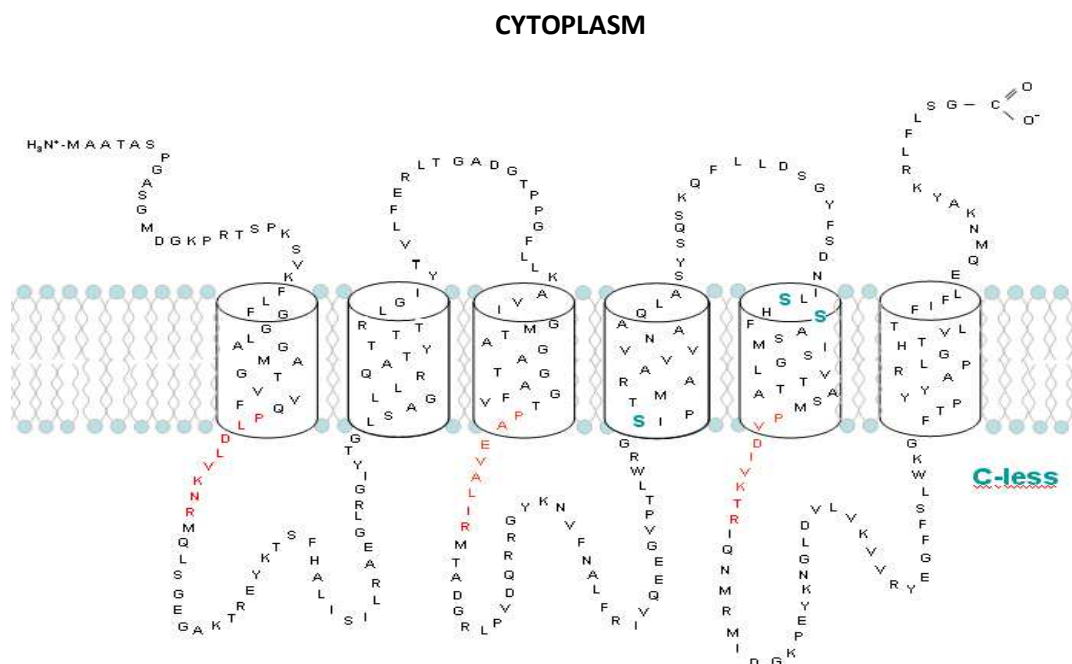


**Fig 5.1** Structure of OGC.

In red, the residues that constitute the characteristic sequence of all mitochondrial carriers

Topographical studies showed that the *carrier* contains three cysteines, in position 184, 221 and 224. Cysteine 184 is located in the fourth transmembrane segment, protruding in the mitochondrial matrix, and it is involved in the formation of a disulfide bridge between two monomers of the protein. The cysteines 221 and 224 are located in the fifth transmembrane segment and are joined together by an intramolecular disulfide bridge. Here, the role of the cysteines 184, 221 and 224 was investigated in order to gain new information about the structural rearrangements required for substrate translocation.

A number of symmetric residues are supposed to be important for transport mechanism. Some glycine and proline residues, found in odd- and even-numbered  $\alpha$ -helices were proposed to play a key structural role, considered essential in helical rearrangements, since they are required for opening and closing the carrier on the matrix or cytosolic side, during substrate translocation, triggering important conformational changes <sup>[60, 121]</sup>.

Furthermore, the complete Cys-scanning mutagenesis experiments performed on the 314 residues of the *B. taurus* SLC25A11\_OGC (BtOGC) showed that the mutation of these proline residues severely impaired 2-oxoglutarate translocation <sup>[29, 37, 38, 116, 121]</sup>.

So far the existence of a cytosolic salt bridge network, or cytosolic gate (c-gate), has only been hypothesized, but the conformational changes required for the transition from the c-state (when the internal carrier cavity is opened towards the cytosolic side and closed on the matrix side<sup>[18]</sup>) to the m-state (when the internal carrier cavity is opened towards the matrix side and closed on the cytosolic side) occurring during substrate translocation remain still unknown<sup>[29, 37, 38, 116, 121]</sup>. Previously the location of residues potentially involved in the formation of a c-gate was analyzed, revealing the presence of a group of charged residues proposed to constitute a new sequence motif [F/Y][D/E]XX[R/K] located at H2, H4 and H6 C terminus<sup>[60, 61, 121, 122]</sup>.

In this work, in order to investigate new structural rearrangements required for substrate translocation, site-directed mutagenesis was used to conservatively replace lysine 122 by arginine, since this residue is in the neighborhood of the predicted c-gate.

## 5.2 RESULTS

### 5.2.1 Expression, transport activity and kinetic analysis of the reconstituted K122R mutant

In this work, the roles of K122, located between proline/glycine residues of PG-level 1 [25, 60, 61] cysteine 184, located near the m-gate, cysteines 221 and 224, located near the c-gate, were analysed by site-directed mutagenesis, kinetic analysis and by the use of several sulfhydryl reagents, in order to shed light on the structural rearrangements required for 2-oxoglutarate translocation across BtOGC. K122 was firstly conservatively replaced by arginine and K122R mutated protein was expressed in *Escherichia coli*, its expression level was 85% as compared to that of the WT OGC (data not shown). The inclusion bodies containing the WT OGC and K122R mutant were disaggregated with sarcosyl and the solubilized proteins were reconstituted into liposomes, in order to measure initial transport rates of 2-oxoglutarate. The amount of reconstituted proteins varied between 18% and 31% of the added protein, according to the values usually found for other mitochondrial carrier proteins [24, 36]. The initial transport rate of K122R was 75% with respect to that of the WT OGC (Fig. 5.2). Kinetic constants were determined for the WT OGC and K122R mutant over a wide range of 2-oxoglutarate concentrations from a standard double-reciprocal set of experiments (see Fig. 5.3). The transport affinity ( $K_m$ ) for 2-oxoglutarate on the external membrane surface of the reconstituted WT OGC and K122R, measured by the forward exchange method, was determined to be  $0.2036 \pm 0.0105$  mM and  $0.2021 \pm 0.0101$  mM, respectively. The specific activities of the WT OGC and K122R ( $V_{max}$ ) were  $2883 \pm 128.1$  and  $1748 \pm 63.95$  nmol/min per mg protein, respectively. These activities were calculated by taking into account the amount of recombinant proteins recovered into proteoliposomes after reconstitution.



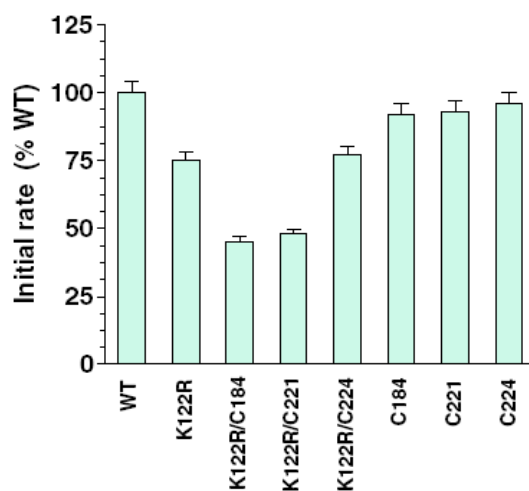


**Fig. 5.2 Initial uptake rate of 2-oxoglutarate by the WT OGC and OGC mutants.**

Proteoliposomes reconstituted with the WT OGC or OGC mutants were preloaded internally with 20 mM oxoglutarate and transport was started by the addition of 3 mM 2- oxo[1-<sup>14</sup>C]glutarate. Uptake rates of oxoglutarate/oxoglutarate exchange were measured at 30 s (in the initial linear range of substrate uptake). Results are expressed as a percentage of the WT OGC value, which was on average  $2699.77 \pm 114.24$  nmol/min per mg of protein. The means  $\pm$  SD of at least three independent experiments carried out in duplicate are shown.

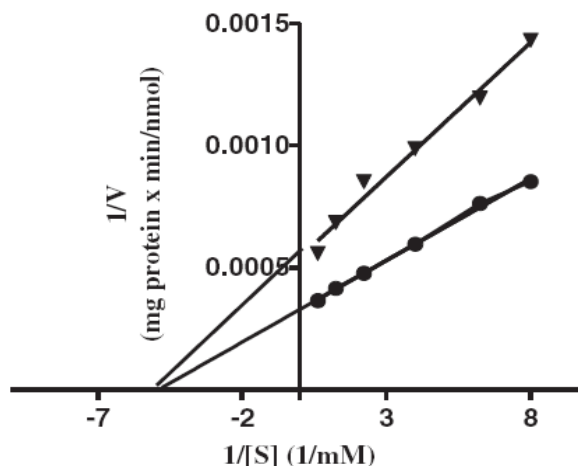


**Fig. 5.3 Lineweaver–Burk plots showing the dependence of transport rate on external oxoglutarate concentration for the WT OGC (●) and K122R mutant (▲).**

Liposomes reconstituted with the WT OGC or K122R mutant were loaded with 20 mM oxoglutarate. External 2-oxo[1-<sup>14</sup>C]glutarate was added at various concentrations. The exchange activity  $V$  is expressed in nmol/min per mg of protein. The kinetic constants  $V_{max}$  and  $K_m$  were determined from the radioactivity taken up by proteoliposomes after 30 s. The average  $V_{max}$  values of oxoglutarate uptake were  $2883 \pm 128.1$  and  $1748 \pm 63.95$  nmol/min per mg of protein for the WT OGC and K122R mutant, respectively. The half-saturation constant ( $K_m$ ) for oxoglutarate was  $0.2036 \pm 0.0105$  mM for the WT OGC and  $0.2021 \pm 0.0101$  mM for K122R mutant. Similar results were obtained in three independent experiments.

### 5.2.2 Influence of sulfhydryl reagents on the WT OGC and K122R transport activities

Since the WT OGC contains three native cysteine residues, the effects of several sulfhydryl reagents on the WT and K122R proteins were tested to investigate changes in the accessibility/reactivity of the cysteines in the WT or in the K122R background.

Firstly, the degree of influence of sulfhydryl reagents was assayed by using mersalyl, a well-known relatively membrane-impermeable mercurial reagent [29, 37, 38, 116]. It was observed that K122R initial transport rate was significantly inactivated by mersalyl as compared to the WT OGC. In particular, K122R residual activities were about 55%, 4% and 1%, and the WT OGC about 95%, 78% and 53% by 1  $\mu$ M, 10  $\mu$ M and 100  $\mu$ M mersalyl, respectively (Fig. 5.4). We extended our investigations to other relatively membrane impermeable cysteine-specific sulfhydryl reagents. In detail, the initial transport rates of the WT OGC and K122R proteins were evaluated after a pre-

incubation of 2 min with pCMBS (100  $\mu$ M), or 10 min with each one of the following reagents, used at 1 mM final concentration: MTSEA, MTSES and MTSET. The residual transport activity of the WT OGC was not significantly influenced by the treatment with pCMBS and the negatively charged MTSES (80% and 71%, respectively), on the contrary, it was inhibited by MTSEA and MTSET, both positively charged (29% and 36%, respectively). At variance with the WT OGC, K122R was significantly affected by pCMBS and MTSEA (33% and 5% respectively), whereas it showed a pattern of inhibition similar to that of the WT OGC in the presence of MTSES or MTSET (72% and 30% respectively) (Fig. 5.5).

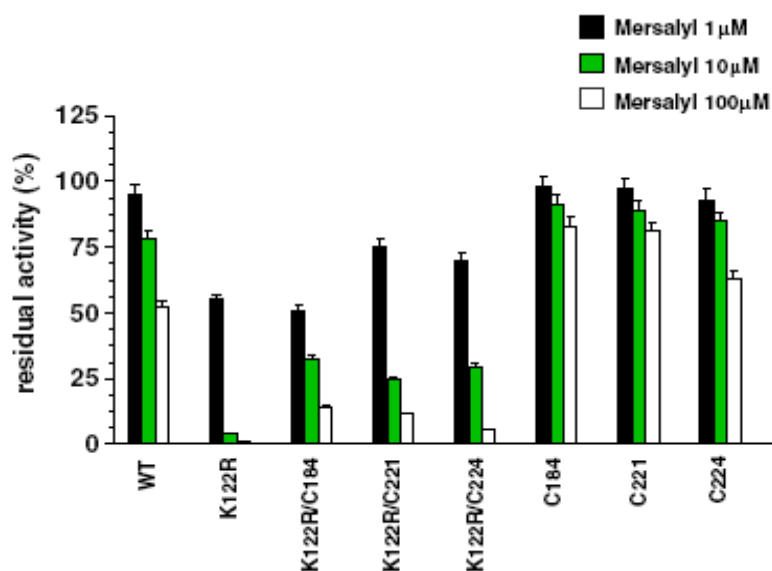


**Fig. 5.4 Effect of mersalyl on the rate of oxoglutarate transport in proteoliposomes reconstituted with the WT OGC or OGC mutants.**

Proteoliposomes were preincubated at 25  $^{\circ}$ C for 2 min with and without mersalyl, which was used at the concentrations 1  $\mu$ M (black bars), 10  $\mu$ M (green bars) and 100  $\mu$ M (white bars). After removal of unbound reagent by Sephadex G-75 chromatography, transport was started by adding 0.3 mM 2-oxo[1- $^{14}$ C]glutarate to proteoliposomes containing 20 mM 2-oxoglutarate and stopped after 30 s. Initial uptake rates are presented as a percentage of the rate measured in the absence of mersalyl. The data represent means  $\pm$  SD of at least three independent experiments carried out in duplicate.



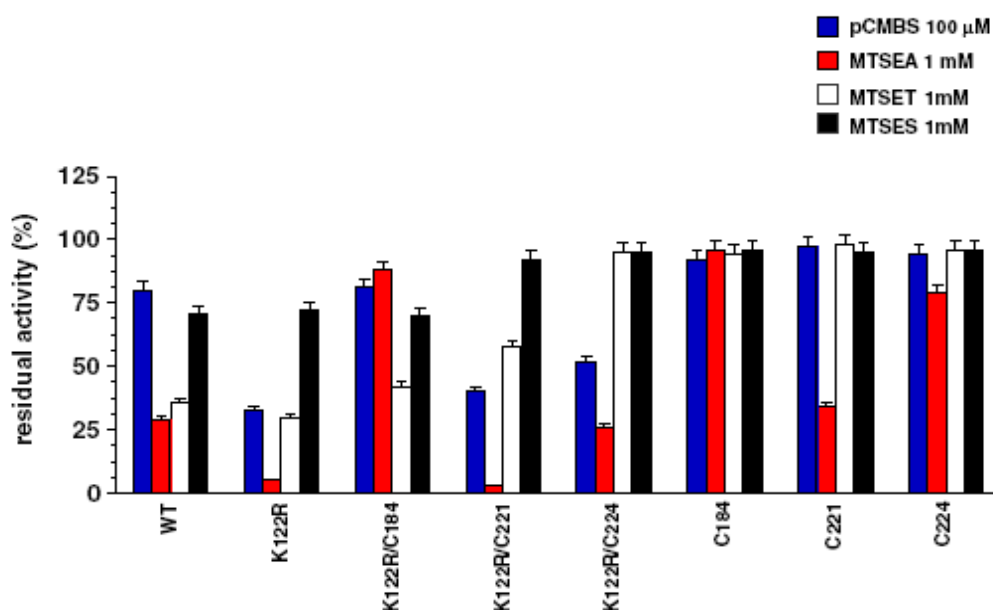


**Fig. 5.5 Effect of pCMBS, MTSEA, MTSET and MTSES on the rate of oxoglutarate uptake by the WT OGC or by OGC mutants.**

Proteoliposomes were pre-incubated at 25 °C for 2 min in the presence or absence of 100  $\mu$ M pCMBS (blue bars) or for 10 min in the presence or absence of 1 mM MTSEA (red bars), 1 mM MTSET (white bars) and 1 mM MTSES (black bars). The experimental details are described in the legend of Fig. 5.4.

### 5.2.3 Expression, transport activity and influence of sulfhydryl reagents on reconstituted C184, C221, C224, K122R/C184, K122R/C221 and K122R/C224 OGC mutants

As K122R displayed a major inhibitory effect by mersalyl, pCMBS and MTSEA, with respect to the WT OGC, it is conceivable that during substrate translocation changes of accessibility and/or reactivity involve cysteine residues located at the protein-membrane interface. We investigated their involvement by expressing three single-cysteine mutants, C184, C221 and C224 [28, 29] and by building three new single cysteine mutants, K122R/C184, K122R/C221 and K122R/C224; in these recombinant proteins only cysteine 184, 221 or 224, in combination with the mutation K122R is present, respectively. For all of the OGC mutants expression levels were not significantly different from those of the WT OGC (ranging between 76% and 94%), whereas the

yield of reconstituted proteins varied between 20% and 33% of the added protein. For all these mutants initial transport rates of 2-oxoglutarate, expressed as percentage of the value for the WT OGC, were significant (Fig. 5.2). The inhibitory effect of sulfhydryl reagents on the initial transport activity of OGC mutants was reported in Figs. 5.4 and 5.5, compared with the WT OGC residual transport activity rates. It is noteworthy that C184, C221 and C224 mutants were nearly unaffected by mersalyl, pCMBS, MTSET and MTSES. MTSEA appreciably inhibited C221, C224 was only weakly affected, whereas C184 was unaffected. Remarkably, mersalyl significantly inhibited K122R/C184, K122R/C221 and K122R/C224 proteins at a similar extent, even at concentration of 10  $\mu$ M; pCMBS appreciably inhibited K122R/C221 and K122R/C224, whereas K122R/C184 was poorly inhibited. MTSEA strongly inhibited K122R/C221 and to a lesser extent K122R/C224, whereas K122R/C184 was negligibly affected; MTSET and MTSES inhibited very weakly K122R/C224 and K122R/C221 mutants, whereas K122R/C184 displayed an inhibitory behavior similar to that of the WT OGC by each of these two reagents. In other experiments, the dependence of C221, C224, K122R/C221 and K122R/C224 inhibition on pCMBS and MTSEA concentrations was evaluated. After 2 min pre-incubation, half-maximal inhibition of oxoglutarate/oxoglutarate transport rate for K122R/C221 and K122R/C224 reconstituted mutants was achieved by using 80  $\mu$ M and 105  $\mu$ M pCMBS, respectively (data not shown). Under the same conditions, transport rates of C221 and C224 were virtually unaffected by 800  $\mu$ M pCMBS (data not shown). In further experiments, after 10 min pre-incubation half-maximal inhibitions of C221, C224, K122R/C221 and K122R/C224 transport rates were obtained using 520  $\mu$ M, 3 mM, 8  $\mu$ M and 500  $\mu$ M MTSEA, respectively (data not shown).

#### **5.2.4 Influence of substrate on the inhibition of C224, K122R/C224, C221 and K122R/C221 mutants by MTSEA**

To investigate the effect of substrate on MTSEA inhibition of C224 and K122R/C224, their proteoliposomes were pre-incubated with 3 mM or 500  $\mu$ M MTSEA, respectively, in the presence or absence of 0.2 or 1 mM 2-oxoglutarate (Fig. 5.6). Interestingly, when the substrate was present during the incubation of the proteoliposomes with this sulfhydryl reagent, it significantly enhanced the extent of inhibition, which was

dependent on 2-oxoglutarate concentration for both these mutants, although the effect was more marked in K122R/C224 (Fig. 5.6). In detail, C224 and K122R/C224 residual activities were about 49%, 38%, 18% and 48%, 27%, 8% in the absence or presence of 0.2 or 1 mM 2-oxoglutarate, respectively.

Influence of substrate on the inhibition of C221 and K122R/C221 mutants by 520  $\mu$ M and 8  $\mu$ M MTSEA was also investigated (Fig. 5.6). In K122R/C221 the extent of inhibition was meaningfully enhanced by the presence of 2-oxoglutarate, conversely C221 was poorly influenced. In detail, C221 and K122R/C221 residual activities were about 50%, 43%, 38% and 48%, 28%, 15% in the absence or presence of 0.2 or 1 mM 2-oxoglutarate, respectively. Further experiments were performed in similar conditions, using in place of 2-oxoglutarate some substrates not transported by BtOGC, as glutarate or ADP, which did not affect the extent of inhibition (data not shown).

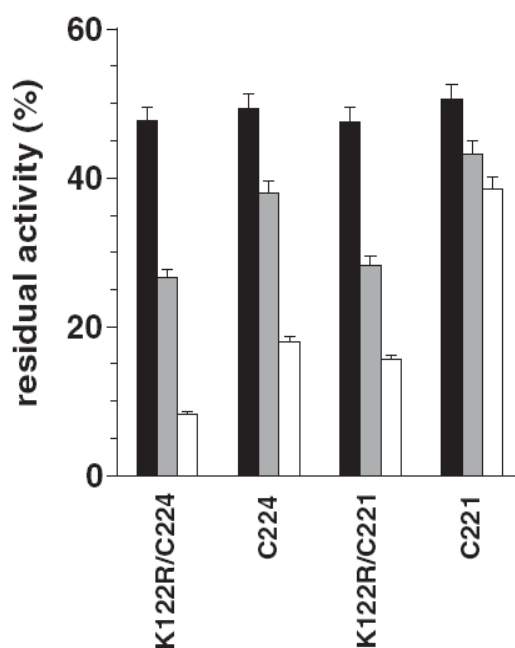


**Fig. 5.6 Influence of substrate on the inhibition of K122R/C224, C224, K122R/C221 and C221 reconstituted mutants by MTSEA.**

Proteoliposomes preloaded with 20mM 2-oxoglutarate were pre-incubated for 10 min with 500  $\mu$ M (K122R/C224), 3 mM (C224), 8  $\mu$ M (K122R/C221) and 520  $\mu$ M (C221) MTSEA, in the absence (black bars) or presence of 0.2mM (grey bars) or 1 mM (white bars) 2-oxoglutarate. After removal of unbound reagent and external substrate by Sephadex G-75 chromatography, transport was initiated by the addition of 1 mM 2-oxo[1- $^{14}$ C]glutarate and terminated after 30 s. Results are expressed as residual activity percentage with respect to the control values without inhibitor. The data represent means  $\pm$  SD of four independent experiments carried out in duplicate.



### 5.2.5 Molecular modeling studies of SLC25A11\_OGC

The 3D model of the WT OGC, K122R and the three triple mutants K122R/C184, K122R/C221 and K122R/C224, in the presence or absence of sulfhydryl specific reagents, allowed investigating through *in silico* simulations the importance of the aforementioned residues in substrate binding and translocation. In particular, local 3D structure rearrangements were probed by estimating the accessibility of each triple OGC mutant to oxoglutarate in the presence or absence of MTSEA. In order to investigate the influence of the OGC mutations on the substrate binding site, docking analyses were performed using 2-oxoglutarate as ligand. It was found that this substrate binds to the WT OGC by interacting with residues R90, R190, R288, A191, L289 at the level of the MC common substrate binding site (see Fig. 5.7A) <sup>[61, 122]</sup>, with A134, T234, V194, T293, T187, Y285, M188 at the level of the substrate-binding area <sup>[61]</sup>, with E141 and K244 at the level of the matrix gate <sup>[61, 122]</sup> and with Q248 at the level of the c-gate area <sup>[61]</sup>. All of the cited residues are within 5 Å from the 2-oxoglutarate substrate.

In these simulations K122, positioned at the same level of cysteine 224 and located on transmembrane helix 3 (between proline/glycine residues of PG-level 1 <sup>[61, 122]</sup> and the residues of the c-gate) was firstly mutated in arginine (Fig. 5.7B). Docking analyses showed that 2-oxoglutarate can enter carrier cavity and bind to the residues located at the level of the proposed common substrate binding site in the presence of both lysine and arginine at position 122 (Fig. 5.7), according to transport assays that did not show any difference in the affinity of 2-oxoglutarate for OGC binding site (both WT OGC and K122R mutant showed very similar  $K_m$  for 2-oxoglutarate, see kinetics section and Fig. 5.3). Nevertheless, transport assays showed that the  $V_{max}$  value of K122R mutant was almost one half of that of the WT OGC (see kinetics section). Furthermore, the presence of sulfhydryl reagents employed to investigate the role of cysteine residues within BtOGC revealed that the triple mutants K122R/C221 and K122R/C224 were more sensitive to mersalyl, MTSEA and pCMBS than K122R/C184. Docking of 2-oxoglutarate within the triple mutants in the presence or absence of MTSEA revealed that serine replacement of the cysteine residues did not affect the substrate binding, since 2-oxoglutarate continued to bind residues of the substrate binding area (Fig. 5.7C–D). Nevertheless, it was observed that when MTSEA was added to cysteine 184, in K122R/C184 mutant, the docked 2-oxoglutarate showed some interactions also with MTSEA functional groups (Fig. 5.7C).

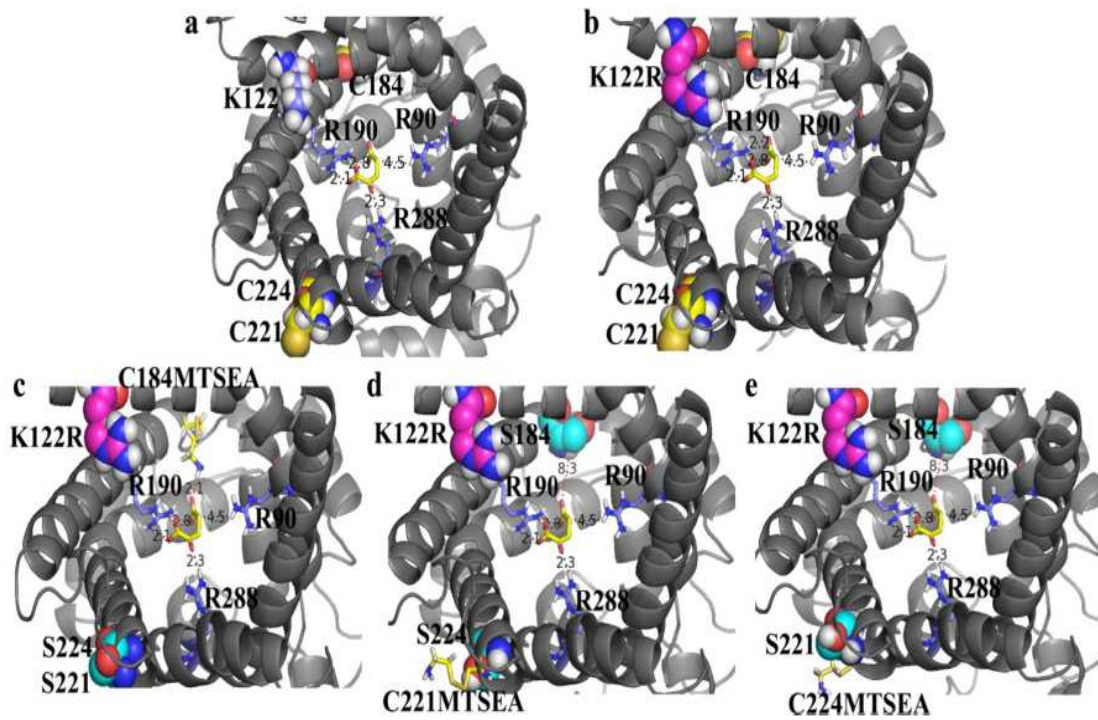


**Fig. 5.7. Docking of 2-oxoglutarate into the cavity of the WT OGC and OGC mutants.**

The OGC carrier is reported in grey cartoon representation with a view into the cavity from the cytosolic side. Panel a shows the WT OGC, panel b shows K122R mutant, whereas in panels c–e K122R/C184, K122R/C221 and K122R/C224 mutants are reported. In each panel 2-oxoglutarate is displayed in yellow sticks, cysteine residues are presented in yellow spheres, while R90, R190 and R288 in blue sticks. In panel a, K122 is reported in blue spheres. In panels b–e, K122R is reported in violet spheres. In panels c–e, serines used to replace the native cysteines are displayed in cyan sticks and MTSEA bound to cysteine residues is reported in yellow sticks. Putative H-bonds are labeled and represented by black dashed lines.

Other distances are labeled and represented by red dashed lines for comparative purposes.

### 5.3 DISCUSSION

The oxoglutarate transporter has been object of research for many years. Our knowledge on its structural and functional properties has been extended; however, the specific mechanism of substrate translocation is not yet entirely understood. In particular, the substrate-induced conformational changes and the structural rearrangements required for substrate translocation remain to be clarified.

Previous studies carried on BtOGC showed the involvement of lysine in position 122 (K122) in substrate-induced conformational changes, indeed in the presence of 2-oxoglutarate the accessibility and/or reactivity of K122C mutant (where lysine 122 was replaced by cysteine) was strongly reduced <sup>[25]</sup>. Furthermore, OGC appeared to be dysfunctional after modification of K122C with sulfhydryl reagents <sup>[29]</sup>. This modification was believed to interfere with the formation of the hypothesized salt-bridge network of the cytosolic gate, during the transport cycle <sup>[18, 38]</sup>. Since K122 is located in the first cytosolic loop hosting residues not essential for substrate binding, its side chain protrudes towards OGC central axis, interacting most likely with the residues of the c-gate, when the carrier goes from the c- to the m-conformation.

In this work, K122 was replaced by an arginine (K122R). This mutation has small effect on initial transport rate, most likely because of the chemical similarity between lysine and arginine side chains. Furthermore, this replacement does not interfere with 2-oxoglutarate binding site, because in transport assays the WT OGC and K122R mutant showed similar  $K_m$  values. However, K122R  $V_{max}$  value was almost one half of the WT OGC  $V_{max}$  value. The decreased  $V_{max}$  could be due to the more hindering arginine side chain at position 122, which could make more difficult conformational changes required for the formation of the m-state during substrate translocation. The effect of several sulfhydryl reagents on K122R was tested. Mersalyl, pCMBS and MTSEA showed a more efficient inhibition compared to the WT OGC, supporting the hypothesis that the presence of the bulky arginine side chain in position 122 might modify the accessibility and/or reactivity of the native cysteines in this carrier. The WT OGC hosts three cysteine residues that can be targeted by sulfhydryl reagents: cysteines 221 and 224, located on transmembrane helix 5, close to the c-gate <sup>[61, 122]</sup>, and cysteine 184, located at the N-terminal of transmembrane helix 4, close to the m-gate <sup>[61, 122]</sup>. The single-cysteine mutants C184, C221 and C224, constructed using the WT OGC



background, were employed in transport assays in the presence or absence of sulfhydryl reagent, to test their effect on each single cysteine residue. All mutants exhibited a remarkable initial transport rate, differing from previous studies carried on rat OGC<sup>[123]</sup>. Mersalyl, pCMBS, MTSES and MTSET showed nearly no effects on mutants. MTSEA inhibited significantly C221, and to a lesser extent C224, implying that cysteines 221 and 224 can be targeted by this reagent. On the other hand, the lack of inhibitory effect on C184 by MTSEA, can not be due to the inaccessibility of cysteine 184, since a previous paper demonstrated that this cysteine was targeted by several sulfhydryl reagents, including the fluorescent N-(1-pyrenyl)maleimide<sup>[124]</sup>.

To test the influence of K122R mutation on the reactivity of OGC cysteines, three triple mutants having a single cysteine residue combined with K122R mutation were prepared and characterized. All of these mutants retained a relatively good initial transport rate. K122R/C221 and K122R/C224 transport activities were more affected than those of K122/C184 mutant and the WT OGC by mersalyl, pCMBS or MTSEA. In K122R/C221 and K122R/C224 mutants the reactivity of cysteines 221 and 224 is probably increased, because of the presence of the arginine side chain at position 122, which could be able to reorient sulfhydryl reagents carrying a partial positive charge (mersalyl, MTSEA and, at a lower extent, pCMBS), favoring their interactions with cysteines 221 and 224. The guanidinium group, present in the arginine side chain and able to delocalize the positive charge, might cause a major electrostatic repulsion that could promote a more effective reorientation of the reagents carrying a partial positive charge.

It is expected that, due to local conformational changes, during substrate translocation cysteines 221 and 224 can face OGC carrier cavity. It could then be speculated that the binding of mersalyl, MTSEA and, at a lower extent, pCMBS to cysteines 221 and 224 does not affect 2-oxoglutarate binding; by the way, sulfhydryl modification of cysteines 221 and 224 might cause a steric hindrance able to affect the c-gate formation, impairing conformational changes occurring during the transition from the c-state to the m-state. The presence of 2-oxoglutarate is able to significantly increase the degree of inhibition of K122R/C221, K122R/C224 and C224 activity by MTSEA, highlighting that cysteines 221 and 224 are involved in substrate-induced conformational changes. Moreover, the effect of 2-oxoglutarate is dependent on its concentration and it is specific, since glutarate (a chemically related anion) or ADP had no influence. C221

mutant showed less evident and significant effects in the bond of MTSEA to cysteine 221 than those observed in C224 and K122R/C221 mutants. It is feasible to hypothesize that the mutation K122R amplifies the inhibitory effects observed on K122R/C221 mutant compared to those observed in the WT background, suggesting that the arginine side chain reorients the substrate through the carrier cavity towards cysteine residues of transmembrane helix 5. On the other hand, the more bulky MTSET and mostly the negatively charged MTSES inhibit at a very low extent C221, K122R/C221, C224 and K122R/C224 mutants. Considering that OGC carrier is unidirectionally inserted in proteoliposomes, with an orientation opposite that found in mitochondria <sup>[125]</sup>, it could be speculated that these reagents have more difficulties to reach cysteines 221 and 224, as they have to pass through almost the entire carrier cavity. The inhibition of K122R/C184 mutant clearly shows that MTSET is able to target cysteine 184 in K122R background. It is also observed that MTSET was able to inhibit the WT OGC and K122R mutant. It should be noticed that cysteine 184 is adjacent to the second/last glycine residue of the second part of the sequence motif and the region containing cysteine 184 is less packed suggesting that it may be involved in conformational rearrangements during substrate transport <sup>[126]</sup>. The minor influence of the negatively charged MTSES and pCMBS on cysteine 184, in K122R/C184 mutant, could also depend on repulsive interactions with the negatively charged residues of the sequence motif. MTSES and pCMBS could also get in touch with positively charged residues belonging to the sequence motif. The binding of the smaller positively charged MTSEA to cysteine 184 could scarcely influence K122R/C184 activity, because of its smaller size, which could make difficult to create the same interactions achievable in the presence of MTSET.

In conclusion, the measure of the kinetic parameters (i.e.  $K_m$  and  $V_{max}$ ) of K122R mutant demonstrates that the residue in position 122 doesn't take part to the substrate binding but, considering the less stable OGC c-gate, it is expected that the presence of the charged/hindering arginine side chain at position 122 may affect the formation of the OGC c-gate, while cysteine 184 could play a role in triggering conformational changes suitable to form a functional m-gate. Transport experiments using different sulfhydryl reagents (in the presence or absence of substrate) of reconstituted BtOGC mutants together with molecular modeling studies let us hypothesize further substrate-induced conformational changes at the protein-membrane interface, involving cysteines

221 and 224, located close to the c-gate. However, the crystallized structure of a mitochondrial carrier in m-conformation will be necessary to definitively highlight interactions responsible for the formation of a c-gate.



---

## ABBREVIATIONS

---

|       |                                 |
|-------|---------------------------------|
| ADP   | Adenosine diphosphate           |
| ALA   | Aminolevulinic acid             |
| ALAS2 | Aminolevulinate synthase 2      |
| AP4   | Adenosine 5'-tetraphosphate     |
| APS   | Adenosine 5'-phosphosulfate     |
| ATP   | Adenosine-5'-triphosphate       |
| BAT   | Bathophenanthroline             |
| BKA   | Bongkrekiic acid                |
| BMA   | Butylmalonate                   |
| BrCP  | Bromocresol purple              |
| BTA   | 1,2,3-Benzenetricarboxylate     |
| CAT   | Carboxyatractyloside            |
| CCN   | $\alpha$ -Cyanocinnamate        |
| CoA   | Coenzyme A                      |
| COASY | Coenzyme A synthase             |
| CSA   | Congenital sideroblastic anemia |
| Cyt   | Cytochrome                      |
| DPCK  | Dephospho-coenzyme A kinase     |
| dPCoA | Dephospho-coenzymeA             |
| FAO   | Fatty acid oxidation            |
| GDC   | Graves' Disease <i>Carrier</i>  |
| GLY   | Glycine                         |

|        |                                                          |
|--------|----------------------------------------------------------|
| GlyC   | Glycine carrier                                          |
| IMM    | Inner mitochondrial membrane                             |
| MCF    | Mitochondrial carrier family                             |
| MCs    | Mitochondrial carriers                                   |
| MER    | Mersalyl                                                 |
| mtDNA  | mitochondrial DNA                                        |
| MTSEA  | 2-Aminoethyl methanethiosulfonate hydrobromide           |
| MTSES  | Sodium(2-sulfonatoethyl)-methanethiosulfonate            |
| MTSET  | [2-(trimethylammonium)ethyl]methanethiosulfonate bromide |
| NBIA   | Neurodegeneration with brain iron accumulation           |
| NEM    | N-ethylmaleimide                                         |
| OGC    | Oxoglutarate carrier                                     |
| OMM    | Outer mitochondrial membrane                             |
| OXPHOS | Oxidative phosphorylation                                |
| Pan    | Pantothenate                                             |
| PANK   | Pantothenate kinase                                      |
| PAP    | Adenosine 3',5'-diphosphate                              |
| PAPS   | 3'- Phosphoadenosine-5'-phosphosulfate                   |
| pCMBS  | p-(chloromercuri)benzenesulfonic acid                    |
| PCR    | Polymerase chain reaction                                |
| pHMB   | p-Hydroxymercuribenzoate                                 |
| PhSu   | Phenylsuccinate                                          |
| PLP    | Pyridoxal-5'-phosphate                                   |
| PPAT   | 4'-Phosphopantetheine adenylyltransferase                |
| PPCDC  | 4'-Phosphopantothenoilcysteine decarboxylase             |

|             |                                          |
|-------------|------------------------------------------|
| PPCS        | 4'-Phosphopantothenoylecysteine synthase |
| SM          | Synthetic minimal medium                 |
| TAN         | Tannic acid                              |
| ThMP        | Thiamine monophosphate                   |
| ThPP        | Thiamine pyrophosphate                   |
| WT          | Wild-type                                |
| YP          | Rich medium                              |
| 4'-P-Pan    | 4'-Phosphopantothenate                   |
| 4'-P-PanCys | 4'-Phospho-N-pantothenoylecysteine       |
| 4'-P-Panthe | Pantetheine 4'-phosphate                 |



---

## REFERENCES

---

- [1] Cardellini, P., Ciani, F., Ciarcia, G., Cirotto, C., Desantis, S., Dini, L., Fasulo, S., Franceschini, V., Labate, M., Laforgia, V., Longo, M., Mauceri, A.R., Serra, G., Tagliafierro, G. e Vallarano, M. (2004) *Citologia & Istologia* (Idelson Gnocchi eds), 122-123.
- [2] Rosati, P. and Colombo, R. (1997) *La cellula*, (Edi-Ermes eds), 200-222.
- [3] Anderson, S., A. T. Bankier, et al. (1981). *Sequence and organization of the human mitochondrial genome*. Nature 290(5806): 457-465.
- [4] Palmieri, F. (2004) *The mitochondrial transporter family (SLC25): physiological and pathological implications*. Pflugers Arch. 447:689-709.
- [5] Palmieri, F., (2013) *The mitochondrial transporter family SLC25: identification, properties and physiopathology*. Mol. Aspects Med. 34, 465-484.
- [6] Walker, J. E. and Runswick, M. J. (1993). *The Mitochondrial Transport Protein Superfamily*. J. Bioenerg. Biomembr. 25, 435-446.
- [7] Lodish, H., Berk, A., Zipursky, S.L., Matsudaira, P., Baltimore, D., Darnell, J. (2002) *Biologia molecolare della cellula, II edizione italiana condotta sulla IV edizione americana*. Zanichelli.
- [8] Dolce, V., Iacobazzi, V., Palmieri, F., Walker, J.E. (1994) *The sequences of human and bovine genes of the phosphate carrier from mitochondria contain evidence of alternatively spliced forms*. Biol. Chem. 269 (14):10451-60.
- [9] Huizing, M., Ruitenbeek, W., van den Heuvel, L.P., Dolce V., Iacobazzi V., Smeitink J. A. M., Palmieri F., Trijbels J. M. F. (1998) *Human Mitochondrial Transmembrane Metabolite Carriers: Tissue Distribution and Its Implication for Mitochondrial Disorders*. J Bioenerg Biomembr 30: 277.
- [10] Joseph JW, Jensen MV, Ilkayeva O, Palmieri F, Alárcon C, Rhodes CJ, Newgard CB. (2006) *The mitochondrial citrate/isocitrate carrier plays a regulatory role in glucose-stimulated insulin secretion*. J Biol Chem. Nov 24;281(47):35624-32.

- [11] Aquila, H., Link, T.A., and Klingenberg, H., (1985) *The uncoupling protein from brown fat mitochondria is related to the mitochondrial ADP/ATP carrier. Analysis of sequence homologies and of folding of the protein in the membrane.* EMBO J 4 : 2369-2376.
- [12] Bouillaud, F., Weissenbach, J., and Riquier, D., (1986) *Complete cDNA-derived amino acid sequence of rat brown uncoupling proteins.* J. Biol. Chem. 261: 1487-1490.
- [13] De Marcos Lousa, C., Trézéguet, V., Dianoux, A.C., Brandolin, G., Lauquin, G.J.M. (2002) *The human mitochondrial ADP/ATP carriers: kinetic properties and biogenesis of wild-type and mutant proteins in the yeast S. cerevisiae.* Biochemistry 41:14412–14420.
- [14] Dolce, V., Scarcia, P., Iacopetta, D., Palmieri, F. (2004) *A fourth ADP / ATP carrier isoform in man: identification, bacterial expression, functional characterization and tissue distribution.* FEBS Lett. 579 N°3: 633-637.
- [15] Heazlewood JL, Whelan J, Millar AH. (2003) *The products of the mitochondrial orf25 and orfB genes are FO components in the plant F1FO ATP synthase.* FEBS Lett. 10;540(1-3):201-5.
- [16] Palmieri, F., Agrimi, G., Blanco, E., Castegna, A., Di Noia, M. A., Iacobazzi, V., Lasorsa, F. M., Marobbio, C. M., Palmieri, L., Scarcia, P., Todisco, S., Vozza, A. & Walker, J. (2006). *Identification of mitochondrial carriers in Saccharomyces cerevisiae by transport assay of reconstituted recombinant proteins.* Biochim Biophys Acta, 1757, 1249-62.
- [17] Picault, N., Hodges, M., Palmieri, L. & Palmieri, F. (2004). *The growing family of mitochondrial carriers in Arabidopsis.* Trends Plant Sci, 9, 138-46.
- [18] Pebay-Peyroula, E., Dahout-Gonzalez, C., Kahn, R., Trezeguet, V., Lauquin, G.J., Brandolin, G. (2003) *Structure of mitochondrial ADP/ATP carrier in complex with carboxyatractyloside.* Nature 426 (6962): 39-44.
- [19] Maloney, P.C. (1990) *Membrane topology of the melibiose carrier of Escherichia coli.* Res. Microbiol. 141: 374-383.

- [20] Palmieri, F., (2008) *Diseases caused by defects of mitochondrial carriers: a review*. *Biochimica et Biophysica Acta* 1777: 564–578.
- [21] Iacopetta D., Madeo M., Tasco G., Carrisi C., Curcio R., Martello E., Casadio R., Capobianco L., Dolce V., (2011) *A novel subfamily of mitochondrial dicarboxylate carriers from *Drosophila melanogaster*: biochemical and computational studies*, *Biochim. Biophys. Acta* 1807 251–261.
- [22] Damiano, F., Alemanno, S., Gnoni, G., and Siculella, L. (2010) *Translational control of the sterol-regulatory transcription factor SREBP-1 mRNA in response to serum starvation or ER stress is mediated by an internal ribosome entry site*. *Biochem. J.* 429, 603-612.
- [23] Rigracciolo, D. C., Scarpelli, A., Lappano, R., Pisano, A., Santolla, M. F., De Marco, P., Cirillo, F., Cappello, A. R., Dolce, V., Belfiore, A., Maggiolini, M., and De Francesco, E. M. (2015) *Copper activates HIF-1 $\alpha$ /GPER/VEGF signalling in cancer cells*. *Oncotarget.* 6, 34158-34177.
- [24] Carrisi, C., Madeo, M., Morciano, P., Dolce, V., Cenci, G., Cappello, A. R., Mazzeo, G., Iacopetta, D., and Capobianco, L. (2008) *Identification of the *Drosophila melanogaster* mitochondrial citrate carrier: bacterial expression, reconstitution, functional characterization and developmental distribution*. *J. Biochem.* 144, 389-392.
- [25] Morozzo Della Rocca B., Miniero D.V., Tasco G., Dolce V., Falconi M., Ludovico A., Cappello A.R., Sanchez P., Stipani I., Casadio R., Desideri A., Palmieri F., (2005) *Substrate-induced conformational changes of the mitochondrial oxoglutarate carrier: a spectroscopic and molecular modelling study*. *Mol. Membr. Biol.* 22 443–452.
- [26] Ho S.N., Hunt H.D., Horton R.M., Pullen J.K., Pease L.R., (1989) *Site-directed mutagenesis by overlap extension using the polymerase chain reaction*. *Gene* 77 51–59.
- [27] Runswick M.J., Walker J.E., Bisaccia F., Iacobazzi V., Palmieri F., (1990) *Sequence of the bovine 2-oxoglutarate/malate carrier protein: structural relationship to other mitochondrial transport proteins*. *Biochemistry* 29 11033–11040.
- [28] Stipani V., Cappello A.R., Daddabbo L., Natuzzi D., Miniero D.V., Stipani I., Palmieri F., (2001) *The mitochondrial oxoglutarate carrier: cysteine-scanning mutagenesis of transmembrane domain IV and sensitivity of Cys mutants to sulfhydryl reagents*. *Biochemistry* 40 15805–15810.



- [29] Cappello A.R., Miniero D.V., Curcio R., Ludovico A., Daddabbo L., Stipani I., Robinson A.J., Kunji E.R., Palmieri F., (2007) *Functional and structural role of amino acid residues in the odd-numbered transmembrane alpha-helices of the bovine mitochondrial oxoglutarate carrier*. J. Mol. Biol. 369 400–412.
- [30] Carrisi C., Antonucci D., Lunetti P., Migoni D., Girelli C.R., Dolce V., Fanizzi F.P., Benedetti M., Capobianco L., (2014) *Transport of platinum bonded nucleotides into proteoliposomes, mediated by Drosophila melanogaster thiamine pyrophosphate carrier protein (DmTpc1)*. J. Inorg. Biochem. 130 28–31.
- [31] Fiermonte G., Walker J.E., Palmieri F., (1993) *Abundant bacterial expression and reconstitution of an intrinsic membrane transport protein from bovine mitochondria*. The Biochemical journal, 294 (Pt1):293-299.
- [32] Ersoy Tunali, N., Marobbio, C. M. T., Tiryakioğlu, N. O., Punzi, G., Saygılı, S. K., Onal, H., Palmieri, F. (2014) *A novel mutation in the SLC25A15 gene in a Turkish patient with HHH syndrome: functional analysis of the mutant protein*. Mol. Genet. Metab. 112, 25-29.
- [33] Madeo, M., Carrisi, C., Iacopetta, D., Capobianco, L., Cappello, A. R., Bucci, C., Palmieri, F., Mazzeo, G., Montalto, A., and Dolce, V. (2009) *Abundant expression and purification of biologically active mitochondrial citrate carrier in baculovirus-infected insect cells*. J. Bioenerg. Biomembr. 41, 289-297.
- [34] Palmieri F., Indiveri C., Bisaccia F., Iacobazzi V., (1995) *Mitochondrial metabolite carrier proteins: purification, reconstitution, and transport studies*. Methods Enzymol. 260 349–369.
- [35] Lunetti, P., Cappello, A. R., Marsano, R. M., Pierri, C. L., Carrisi, C., Martello, E., Caggese, C., Dolce, V., and Capobianco, L. (2013) *Mitochondrial glutamate carriers from Drosophila melanogaster: biochemical, evolutionary and modeling studies*. Biochim. Biophys. Acta. 1827, 1245-1255.
- [36] Iacopetta, D., Carrisi, C., De Filippis, G., Calcagnile, V. M., Cappello, A. R., Chimento, A., Curcio, R., Santoro, A., Voza, A., Dolce, V., Palmieri, F., and Capobianco, L. (2010) *The biochemical properties of the mitochondrial thiamine pyrophosphate carrier from Drosophila melanogaster*. FEBS J. 277, 1172-1181.

- [37] Cappello A.R., Curcio R., Miniero D. V., Stipani I., Robinson A.J., Kunji E.R., Palmieri F., (2006) *Functional and structural role of amino acid residues in the even numbered transmembrane alpha-helices of the bovine mitochondrial oxoglutarate carrier*. J. Mol. Biol. 363 51–62.
- [38] Miniero D.V., Cappello A.R., Curcio R., Ludovico A., Daddabbo L., Stipani I., Robinson A.J., Kunji E.R., Palmieri F., (2011) *Functional and structural role of amino acid residues in the matrix alpha-helices, termini and cytosolic loops of the bovine mitochondrial oxoglutarate carrier*. Biochim. Biophys. Acta 1807 302–310.
- [39] Fiermonte G., Dolce V., Palmieri F., (1998) *Expression in Escherichia coli, functional characterization, and tissue distribution of isoforms A and B of the phosphate carrier from bovine mitochondria*. J. Biol. Chem. 273 22782–22787.
- [40] Daum, G., Bohni, P. C., and Schatz, G. (1982) *Import of proteins into mitochondria. Cytochrome b2 and cytochrome c peroxidase are located in the intermembrane space of yeast mitochondria*. J. Biol. Chem. 257, 13028-13033.
- [41] Ferramosca, A., and Zara, V. (2013) *Biogenesis of mitochondrial carrier proteins: Molecular mechanisms of import into mitochondria*. Biochim. Biophys. Acta. 1833, 494-502.
- [42] Pringle, J. R., Adams, A. E., Drubin, D. G., and Haarer, B. K. (1991) *Immunofluorescence methods for yeast*. Methods Enzymol. 194, 565-602.
- [43] Iacopetta, D., Lappano, R., Cappello, A. R., Madeo, M., De Francesco, E. M., Santoro, A., Curcio, R., Capobianco, L., Pezzi, V., Maggiolini, M., and Dolce, V. (2010) *SLC37A1 gene expression is up-regulated by epidermal growth factor in breast cancer cells*. Breast Cancer. Res. Treat. 122, 755-764.
- [44] De Caroli, M., Lenucci, M.S., Manualdi, F., D'alessandro, G., De Lorenzo, G., and Piro, G. (2015) *Molecular dissection of Phaseolus vulgaris polygalacturonase-inhibiting protein 2 reveals the presence of hold/release domains affecting protein trafficking toward the cell wall*. Front. Plant Sci. 6:660.
- [45] Villas-Bôas, S. G., Højer-Pedersen, J., Akesson, M., Smedsgaard, J., and Nielsen, J. (2005) *Global metabolite analysis of yeast: evaluation of sample preparation methods*. Yeast 22, 1155- 1169.

- [46] De Benedetto, G. E., and Fanigliulo, M. (2009) *A new CE-ESI-MS method for the detection of stable hemoglobin acetaldehyde adducts, potential biomarkers of alcohol abuse*. Electrophoresis. 30, 1798-1807.
- [47] Materazzi, S., Napoli, A., Risoluti, R., Finamore, J., and D'Arienzo, S. (2014) *Characterization of thermally induced mechanisms by mass spectrometry-evolved gas analysis (EGA-MS): A study of divalent cobalt and zinc biomimetic complexes with N-heterocyclic dicarboxylic ligands*. Int. J. Mass Spectrom. 365-366, 372-376.
- [48] De Benedetto, G. E., Fico, D., Margapoti, E., Pennetta, A., Cassiano, A., and Minerva, B. (2013) *The study of the mural painting in the 12th century monastery of Santa Maria delle Cerrate (Puglia-Italy): characterization of materials and techniques used*. J. Raman Spectrosc. 44, 899- 904.
- [49] Kranen, R. W., van Kuppevelt, T. H., Goedhart, H. A., Veerkamp, C. H., Lambooy, E., and Veerkamp, J. H. (1999) *Hemoglobin and myoglobin content in muscles of broiler chickens*. Poult. Sci. 78, 467-476.
- [50] Sinclair, P. R., Gorman, N., and Jacobs, J. M. (2001) *Measurement of heme concentration*. Curr. Protoc. Toxicol. Chapter 8:Unit 8.3.
- [51] Benard, G., Faustin, B., Passerieux, E., Galinier, A., Rocher, C., Bellance, N., Delage, J. P., Casteilla, L., Letellier, T., and Rossignol, R. (2006) *Physiological diversity of mitochondrial oxidative phosphorylation*. Am. J. Physiol. Cell Physiol. 291, 1172-1182.
- [52] Stendardi, A., Focarelli, R., Piomboni, P., Palumberi, D., Serafini, F., Ferramosca, A., and Zara, V. (2011) *Evaluation of mitochondrial respiratory efficiency during in vitro capacitation of human spermatozoa*. Int. J. Androl. 34, 247-255.
- [53] Conte, A., Papa, B., Ferramosca, A., and Zara, V. (2015) *The dimerization of the yeast cytochrome bc1 complex is an early event and is independent of Rip1*. Biochim. Biophys. Acta. 1853, 987-995.
- [54] Pierri C.L., Parisi G., Porcelli V., (2010) *Computational approaches for protein function prediction: a combined strategy from multiple sequence alignment to molecular docking-based virtual screening*. Biochim. Biophys. Acta 1804 1695–1712.
- [55] Sánchez R., Šali A., (2000) *Comparative protein structure modeling. Introduction and practical examples with modeler*. Methods Mol. Biol. 143 97–129.



- [56] Vriend G., (1990) *WHAT IF: a molecular modeling and drug design program*. J. Mol. Graph. 8 52–56.
- [57] Laurie A.T.R., Jackson R.M., (2005) *Q-SiteFinder: an energy-based method for the prediction of protein-ligand binding sites*. Bioinformatics 21 1908–1916.
- [58] Morris G.M., Huey R., Lindstrom W., Sanner M.F., Belew R.K., Goodsell D.S., Olson A.J., (2009) *AutoDock4 and AutoDockTools4: automated docking with selective receptor flexibility*. J. Comput. Chem. 30 2785–2791.
- [59] Persson B., (2000) *Bioinformatics in protein analysis*. EXS 88 215–231.
- [60] Palmieri F., Pierri C.L., (2009) *Structure and function of mitochondrial carriers — role of the transmembrane helix P and G residues in the gating and transport mechanism*, FEBS Lett. 584 1931–1939.
- [61] Pierri C.L., Palmieri F., De Grassi A., (2014) *Single-nucleotide evolution quantifies the importance of each site along the structure of mitochondrial carriers*. Cell. Mol. Life Sci. 71 349–364.
- [62] Kunji E.R.S., Robinson A.J., (2006) *The conserved substrate binding site of mitochondrial carriers*. Biochim. Biophys. Acta 1757 1237–1248.
- [63] Tamura K., Stecher G., Peterson D., Filipinski A., Kumar S., (2013) *MEGA6: Molecular Evolutionary Genetics Analysis version 6*. Mol. Biol. Evol. 30 2725–2729.
- [64] Guindon S., Dufayard J. F., Lefort V., Anisimova M., Hordijk W., Gascuel O., (2010) *New algorithms and methods to estimate maximum-likelihood phylogenies: assessing the performance of PhyML 3.0*. Syst. Biol. 59 307–321.
- [65] Anisimova M., Gil M., Dufayard J. F., Dessimoz C., Gascuel O., (2011) *Survey of branch support methods demonstrates accuracy, power, and robustness of fast likelihood based approximation schemes*. Syst. Biol. 60 685–699
- [66] Haitina T, Lindblom J, Renström T, Fredriksson R. (2006) *Fourteen novel human members of mitochondrial solute carrier family 25 (SLC25) widely expressed in the central nervous system*. Genomics. 88 (6):779-90.
- [67] Guernsey D.L., Jiang H., Campagna D.R., Evans S.C., Ferguson M., Kellogg M.D., Lachance M., Matsuoka M., Nightingale M., Rideout A., Saint-Amant L., Schmidt P.J., Orr A., Bottomley S.S., Fleming M.D., Ludman M., Dyack

- S., Fernandez C.V., Samuels M.E., (2009) *Mutations in mitochondrial carrier family gene SLC25A38 cause nonsyndromic autosomal recessive congenital sideroblastic anemia*. Nat Genet. 41(6):651-3.
- [68] Kannengiesser C, Sanchez M, Sweeney M, Hetet G, Kerr B, Moran E, Fuster Soler JL, Maloum K, Matthes T, Oudot C, Lascaux A, Pondarré C, Sevilla Navarro J, Vidyatilake S, Beaumont C, Grandchamp B, May A. (2011) *Missense SLC25A38 variations play an important role in autosomal recessive inherited sideroblastic anemia*. Haematologica. 96(6):808-13.
- [69] Ponka, P., Prchal, J. T. (2010) *Hereditary and acquired sideroblastic anemias in Williams Hematology* (Kaushansky, K., Beutler, E., Seligsohn, U., Lichtman, M. A., Kipps, T. J., and Prchal, J. T. eds.), 8th Ed., McGraw Hill, New York. pp. 865-881.
- [70] Ducamp S, Schneider-Yin X, de Rooij F, Clayton J, Fratz EJ, Rudd A, Ostapowicz G, Varigos G, Lefebvre T, Deybach JC, Gouya L, Wilson P, Ferreira GC, Minder EI, Puy H. (2013) *Molecular and functional analysis of the C-terminal region of human erythroid-specific 5-aminolevulinic synthase associated with X-linked dominant protoporphyria (XLDPP)*. Hum Mol Genet. 1;22(7):1280-8.
- [71] Chiabrando, D., Mercurio, S., Tolosano, E. (2014) *Heme and erythropoiesis: more than a structural role*. Haematologica. 99(6):973-83.
- [72] Ajioka, R. S., Phillips, J. D., and Kushner, J. P. (2006) *Biosynthesis of heme in mammals*. Biochim Biophys Acta. 1763(7):723-36.
- [73] Fernández-Murray, J. P., Prykhozhiy, S. V., Dufay, J. N., Steele, S. L., Gaston, D., Nasrallah, G. K., Coombs, A. J., Liwski, R. S., Fernandez, C. V., Berman, J. N., McMaster, C. R. (2016) *Glycine and folate ameliorate models of congenital sideroblastic anemia*. PLoS Genet. doi: 10.1371/journal.pgen.1005783.
- [74] Agrimi, G., Di Noia, M. A., Marobbio, C. M., Fiermonte, G., Lasorsa, F. M., Palmieri, F., (2004) *Identification of the human mitochondrial S-adenosylmethionine transporter: bacterial expression, reconstitution, functional characterization and tissue distribution*. Biochem. J. 379, 183-190.
- [75] Dolce, V., Cappello, A. R., Capobianco, L. (2014) *Mitochondrial tricarboxylate and dicarboxylate-tricarboxylate carriers: from animals to plants*. IUBMB Life. 66, 462-471.

- [76] Palmieri, L., Vozza, A., Hönlinger, A., Dietmeier, K., Palmisano, A., Zara, V., Palmieri, F. (1999) *The mitochondrial dicarboxylate carrier is essential for the growth of Saccharomyces cerevisiae on ethanol or acetate as the sole carbon source*. Mol. Microbiol. 31, 569-577.
- [77] Palmieri, L., Rottensteiner, H., Girzalsky, W., Scarcia, P., Palmieri, F., Erdmann, R. (2001) *Identification and functional reconstitution of the yeast peroxisomal adenine nucleotide transporter*. EMBO J. 20, 5049-5059.
- [78] Kim, H. J., Khalimonchuk, O., Smith, P. M., Winge, D. R. (2012) *Structure, function, and assembly of heme centers in mitochondrial respiratory complexes*. Biochim. Biophys. Acta. 1823, 1604-1616.
- [79] Zara, V., Conte, L., and Trumpower, B. L. (2007) *Identification and characterization of cytochrome bc1 subcomplexes in mitochondria from yeast with single and double deletions of genes encoding cytochrome bc1 subunits*. FEBS J. 274, 4526-4539.
- [80] Lombardi A., Silvestri E., Moreno M., de Lange P., Farina P., Goglia F., Lanni A. (2002) *Muscle mitochondrial free-fatty-acid content and membrane potential sensitivity in different thyroid states: involvement of uncoupling protein-3 and adenine nucleotide translocase*. FEBS Lett. 532, 12-16.
- [81] Zara V., Conte L., Trumpower B. L. (2009) *Biogenesis of the yeast cytochrome bc1 complex*. Biochim. Biophys. Acta. 1793, 89-96.
- [82] Monschau N., Stahmann K. P., Sahm H., McNeil, J. B., Bognar, A. L. (1997) *Identification of Saccharomyces cerevisiae GLY1 as a threonine aldolase: a key enzyme in glycine biosynthesis*. FEMS Microbiol. Lett. 150, 55-60.
- [83] Schlösser T., Gätgens C., Weber U., Stahmann K. P. (2004) *Alanine:glyoxylate aminotransferase of Saccharomyces cerevisiae-encoding gene AGX1 and metabolic significance*. Yeast. 21, 63-73.
- [84] Lee J. C., Tsoi A., Kornfeld G. D., Dawes I. W. (2013) *Cellular responses to L-serine in Saccharomyces cerevisiae: roles of general amino acid control, compartmentalization, and aspartate synthesis*. FEMS Yeast Res. 13, 618-634.



- [85] Kastanos E. K., Woldman Y. Y., Appling D. R. (1997) *Role of mitochondrial and cytoplasmic serine hydroxymethyltransferase isozymes in de novo purine synthesis in Saccharomyces cerevisiae*. *Biochemistry*. 36, 14956-14964.
- [86] Tibbetts A.S., Appling D.R., (2010) *Compartmentalization of Mammalian folate-mediated one-carbon metabolism*. *Annu Rev Nutr*. 21;30:57-81.
- [87] Benavides J., Garcia M. L., Lopez-Lahoya J., Ugarte M., Valdivieso F., (1980) *Glycine transport in rat brain and liver mitochondria*. *Biochim. Biophys. Acta*. 598, 588-594.
- [88] Palmieri F., Monné M. (2016) *Discoveries, metabolic roles and diseases of mitochondrial carriers: A review*. *Biochim. Biophys. Acta*. doi: 10.1016/j.bbamcr.2016.03.007.
- [89] Trotter P. J., Adamson A. L., Ghrist A. C., Rowe L., Scott L. R., Sherman M. P., Stites N. C., Sun Y., Tawiah-Boateng M. A., Tibbetts A. S., Wadington M. C., West A. C. (2005) *Mitochondrial transporters involved in oleic acid utilization and glutamate metabolism in yeast*. *Arch. Biochem. Biophys*. 442, 21-32.
- [90] Dallabona C., Marsano R. M., Arzuffi P., Ghezzi D., Mancini P., Zeviani M., Ferrero I., Donnini C. (2010) *Sym1, the yeast ortholog of the MPV17 human disease protein, is a stressinduced bioenergetic and morphogenetic mitochondrial modulator*. *Hum. Mol. Genet*. 19, 1098-1107.
- [91] Smith P. M., Fox J. L., Winge D. R. (2012) *Biogenesis of the cytochrome bcl complex and role of assembly factors*. *Biochim. Biophys. Acta*. 1817, 276-286.
- [92] Leonardi R., Zhang Y. M., Rock C.O., Jackowski S., (2005) *Coenzyme A: back in action* *Prog. Lipid Res.*, 44 pp. 125–153
- [93] Choudhry A.E., Mandichak T.L., Broskey J.P., Egolf R.W., Kinsland C., Begley T.P., Seefeld M.A., Ku T.W., Brown J.R., Zalacain M., Ratnam K., (2003) *Inhibitors of Pantothenate Kinase: Novel Antibiotics for Staphylococcal Infections*. *Antimicrobil Agents and Chemotherapy* 47 (6), 2051-2055.
- [94] Prohl C., Pelzer W., Diekert K., Kmita H., Bedekovics T., Kispal G., Lill R., (2001) *The yeast mitochondrial carrier Leu5p and its human homologue Graves' disease protein are required for accumulation of coenzyme A in the matrix*. *Mol Cell Biol*. 21(4):1089-97.

- [95] Fiermonte G., Paradies E., Todisco S., Marobbio C.M.T., Palmieri F., (2009) *A novel member of solute carrier family 25 (SLC25A42) is a transporter of coenzyme A and adenosine 3',5'-diphosphate in human mitochondria*, J. Biol. Chem. 284 18152–18159.
- [96] Zhyvoloup A., Nemazanyy I., Panasyuk G., Valovka T., Fenton T., Rebholz H., Wang M.L., Foxon R., Lyzogubov V., Usenko V., Kyyamova R., Gorbenko O., Matsuka G., Filonenko V., Gout I.T., (2003) *Subcellular localization and regulation of coenzyme A synthase*, J. Biol. Chem. 278 50316–50321.
- [97] Zarrilli R., Oates E. L., McBride O. W., Lerman M. I., Chan J. Y., Santisteban P., Ursini M. V., Notkins A. L., Kohn L. D. (1989) *Sequence and chromosomal assignment of a novel cDNA identified by immunoscreening of a thyroid expression library: similarity to a family of mitochondrial solute carrier proteins*. Molec. Endocr. 3: 1498-1508.
- [98] Rossi E., Zarrilli R., Zuffardi O., (1993) *Regional assignment of the gene coding for a human Graves' disease autoantigen to 10q21.3-q22.1*. Hum. Genet. 90: 653-654.
- [99] Nelson D. R., Felix C. M., Swanson J. M., (1998) *Highly conserved charge-pair networks in the mitochondrial carrier family*. J. Mol. Biol. 277:285–308.
- [100] Dusi S., Valletta L., Haack T.B., Tsuchiya Y., Venco P., Pasqualato S., Goffrini P., Tigano M., Demchenko N., Wieland T., Schwarzmayer T., Strom T.M., Invernizzi F., Garavaglia B., Gregory A., Sanford L., Hamada J., Bettencourt C., Houlden H., Chiapparini L., Zorzi G., Kurian M.A., Nardocci N., Prokisch H., Hayflick S., Gout I., Tiranti V., (2014) *Exome sequence reveals mutations in CoA synthase as a cause of neurodegeneration with brain iron accumulation*. Am J Hum Genet. 2;94(1):11-22.
- [101] Shamseldin H.E., Smith L.L., Kentab A., Alkhalidi H., Summers B., Alsedairy H., Xiong Y., Gupta V.A., Alkuraya F.S., (2016) *Mutation of the mitochondrial carrier SLC25A42 causes a novel form of mitochondrial myopathy in humans*. Hum Genet. 135(1):21-30.
- [102] Begley T.P., Kinsland C., Strauss E., (2001) *The biosynthesis of coenzyme A in bacteria*, Vitam. Horm. 61 157–171.

- [103] Fiermonte G., De Leonardis F., Palmieri L., Palmieri F., (2004) *Identification of the mitochondrial ATP-Mg/Pi transporter*. Bacterial expression, reconstitution, functional characterization, and tissue distribution, *J. Biol. Chem.* 279 30722–30730.
- [104] Todisco S., Di Noia M.A., Castegna A., Lasorsa F.M., Paradies E., Palmieri F., (2014) *The Saccharomyces cerevisiae gene YPR011c encodes a mitochondrial transporter of adenosine 5'-phosphosulfate and 3'-phospho-adenosine 5'-phosphosulfate*. *Biochim. Biophys. Acta* 1837 326–334.
- [105] Zallot R., Agrimi G., Lerma-Ortiz C., Teresinski H.J., Frelin O., Ellens K.W., Castegna A., Russo A., de Crecy-Lagard V., Mullen R.T., Palmieri F., Hanson A.D., (2013) *Identification of mitochondrial coenzyme A transporters from maize and Arabidopsis*. *Plant Physiol.* 162 581–588.
- [106] Madigan S.J., Edeen P., Esnayra J., McKeown M., (1996) *att, a target for regulation by tra2 in the testes of Drosophila melanogaster, encodes alternative RNAs and alternative proteins*. *Mol. Cell. Biol.* 16 4222–4230.
- [107] Klingenberg M., (1989) *Molecular aspects of the adenine nucleotide carrier from mitochondria*. *Arch. Biochem. Biophys.* 270 1–14.
- [108] Palmieri F., Pierri C.L., De Grassi A., Nunes-Nesi A., Fernie A.R., (2011) *Evolution, structure and function of mitochondrial carriers: a review with new insights*. *Plant J.* 66 161–181.
- [109] Robinson A.J., Kunji E.R.S., (2006) *Mitochondrial carriers in the cytoplasmic state have a common substrate binding site*. *Proc. Natl. Acad. Sci. U. S. A.* 103 2617–2622.
- [110] Rhee H.W., Zou P., Udeshi N.D, Martell J.D., Mootha V.K., Carr S.A., Ting A.Y., (2013) *Proteomic mapping of mitochondria in living cells via spatially restricted enzymatic tagging*. *Science* 339 1328–1331.
- [111] Skrede S., Halvorsen O., (1983) *Mitochondrial pantetheinophosphate adenyltransferase and dephospho-CoA kinase*. *Eur. J. Biochem.* 131 57–63.
- [112] Bosveld F., Rana A., van der Wouden P.E., Lemstra W., Ritsema M., Kampinga H.H., Sibon O.C., (2008) *De novo CoA biosynthesis is required to maintain DNA integrity during development of the Drosophila nervous system*. *Hum. Mol. Genet.* 17 2058–2069.

- [113] Zhou B., Westaway S.K., Levinson B., Johnson M.A., Gitschier J., Hayflick S.J., (2001) *A novel pantothenate kinase gene (PANK2) is defective in Hallervorden-Spatz syndrome*. Nat. Genet. 28 345–349.
- [114] Wu Z., Li C., Lv S., Zhou B., (2009) *Pantothenate kinase-associated neurodegeneration: insights from a Drosophila model*. Hum. Mol. Genet. 18 3659–3672.
- [115] Srinivasan B., Baratashvili M., van der Zwaag M., Kanon B., Colombelli C., Lambrechts R.A., Schaap O., Nollen E.A., Podgorsek A., Kosec G., Petkovic H., Hayflick S., Tiranti V., Reijngoud D.J., Grzeschik N.A., Sibon O.C., (2015) *Extracellular 4'-phosphopantetheine is a source for intracellular coenzyme A synthesis*. Nat. Chem. Biol. 11 784–792.
- [116] Monné M., Miniero D.V., Iacobazzi V., Bisaccia F., Fiermonte G., (2013) *The mitochondrial oxoglutarate carrier: from identification to mechanism*. J. Bioenerg. Biomembr. 45 1–13.
- [117] Palmieri F., Bisaccia F., Capobianco L., Dolce V., Fiermonte G., Iacobazzi V., Zara V., (1993) *Transmembrane topology, genes, and biogenesis of the mitochondrial phosphate and oxoglutarate carriers*. J. Bioenerg. Biomembr. 25 493–501.
- [118] Wallin E., Von Heijne G., (1998) *Genome-wide analysis of integral membrane proteins from eubacterial, archaean, and eukaryotic organisms*. Prot. Sci., 7, 1029–1038.
- [119] Iacobazzi V., Palmieri F., Runswick M. J., Walker J. E., (1992) *Sequences of the human and bovine genes for the mitochondrial 2-oxoglutarate carrier*. DNA Seq. 3: 79–88.
- [120] Koulintchenko M., Konstantinov Y., Dietrich A., (2003) *Plant mitochondria actively import DNA via the permeability transition pore complex*. EMBO J. 22:1245–1254.
- [121] Monné M., Palmieri F., Kunji E.R., (2013) *The substrate specificity of mitochondrial carriers: mutagenesis revisited*, Mol. Membr. Biol. 30 149–159.
- [122] Robinson A.J., Overy C., Kunji E.R., (2008) *The mechanism of transport by mitochondrial carriers based on analysis of symmetry*, Proc. Natl. Acad. Sci. U. S. A. 105 17766–17771.



- [123] Xu F., Putt D.A., Matherly L.H., Lash L.H., (2005) *Modulation of expression of rat mitochondrial 2-oxoglutarate carrier in NRK-52E cells alters mitochondrial transport and accumulation of glutathione and susceptibility to chemically induced apoptosis*. J. Pharmacol. Exp. Ther. 316 1175–1186.
- [124] Capobianco L., Bisaccia F., Mazzeo M., Palmieri F., (1996) *The mitochondrial oxoglutarate carrier: sulfhydryl reagents bind to cysteine-184, and this interaction is enhanced by substrate binding*. Biochemistry 35 8974–8980.
- [125] Bisaccia F., Capobianco L., Brandolin G., Palmieri F., (1994) *Transmembrane topography of the mitochondrial oxoglutarate carrier assessed by peptide-specific antibodies and enzymatic cleavage*. Biochemistry 33 3705–3713.
- [126] Morozzo Della Rocca B., Lauria G., Venerini F., Palmieri L., Polizio F., Capobianco L., Stipani V., Pedersen J., Cappello A.R., Desideri A., Palmieri F., (2003) *The mitochondrial oxoglutarate carrier: structural and dynamic properties of transmembrane segment IV studied by site-directed spin labeling*. Biochemistry 42 5493–5499.